

Laboratory Evaluation of Fabrics for Reducing Reflection Cracking

1983

Texas Transportation Institute

Laboratory Evaluation of Fabrics
for
Reducing Reflection Cracking

by

Joe W. Button
Associate Research Engineer

Jon E. Epps
Research Engineer

Robert L. Lytton
Research Engineer

Interim Report RF 3424-3

Prepared for

Mirafi Inc.

by

Texas Transportation Institute
Texas A&M University
College Station, Texas

January, 1983

Prologue

Said the pavement to the fabric
"Go 'way, nothing is lacking,"
The fabric replied,
"Swallow your pride,
I'll better your ride,
I'm here to keep you from cracking."

EXECUTIVE SUMMARY

Increased emphasis on rehabilitation of existing pavements has developed a particular interest in pavement overlay systems that will retard reflection cracking. Fabrics in combination with asphalt concrete overlays is one method that offers promise in reducing or delaying reflection cracking.

Laboratory experiments were conducted to establish the mechanisms responsible for the performance of fabrics as effective reflection crack arrestors and determine fabric properties which provide the desired field performance. The laboratory testing program includes testing of fabrics and fabric-mixture systems to determine the following:

1. Asphalt content of fabrics at saturation,
2. Temperature - shrinkage characteristics of fabrics,
3. Adhesive strength between pavement and fabric,
4. Shear strength of old pavement-fabric-new overlay interface,
5. Flexural fatigue properties of fabric-mixture system,
6. Resistance to thermal reflection cracking (overlay tester) and
7. Tensile properties of fabric-mixture system.

Some of the tests used to describe the above parameters were developed in the course of this research.

Several properties of the fabrics were determined by Mirafi Inc and are included herein. Fabric properties measured include grab strength, grab elongation, Mullen burst, free shrinkage, and shrinkage force. Fabric properties were compared to laboratory test results and some significant correlations were found.

Asphalt content of fabrics at saturation was determined by soaking the fabric in hot asphalt cement, placing it between two absorbent papers, then pressing out the excess asphalt using a hot iron. Asphalt contents at saturation ranged from 0.03 to 0.33 gallons per square yard (0.00013 to 0.0015 m³/m²). With this knowledge about the fabric and similar information about the pavement surface, Equation i may be used to obtain pavement tack coat quantities:

$$Q_d = 0.08 + Q_s + Q_c \quad (\text{Equation i})$$

where

Q_d = design tack quantity, gal/yd²

Q_s = fabric asphalt saturation content, gal/yd²

Q_c = correction based on asphalt demand of old surface, gal/yd²

0.08 is a correlative factor based on field experience for overlays with no fabric.

Linear shrinkage was determined by soaking the fabrics in hot asphalt then simply measuring the change in dimensions. The temperature of 250°F appears to be critical, above which significant shrinkage is exhibited in most fabrics.

The construction cracking test was devised to determine if fabric shrinkage could cause early cracking in a new overlay. In the presence of wrinkles or cuts in certain fabrics, cracks may appear in a thin overlay within less than one hour. Techniques to minimize these adverse effects are given herein.

Peel strength, a measure of adhesive strength between a fabric and a tacked pavement surface, was quantified. Adequate adhesion between the

fabric and the old pavement surface is important during construction to prevent the fabric from "rolling up" or "wrinkling" under construction equipment. Surface characteristics of a fabric as well as quantity and grade of asphalt cement tack can affect peel strength. To date, an acceptable level of shear strength cannot be established since there is no correlation between laboratory measurements and field requirements.

Interface shear strength was measured by using a test method developed to simulate the braking action of a wheel on a pavement. The apparatus induced shear stresses within a test specimen at the fabric-pavement interface. From a performance standpoint, it is desirable to have adequate shear strength at the old pavement-fabric interface to prevent slippage failures. Test results indicate fabrics will not compound overlay slippage problems.

Fatigue cracking of pavements is caused by repetitive wheel loads and will appear as alligator cracks in the wheel path. Flexural fatigue characteristics of asphalt concrete containing fabrics were compared with a similar mixture containing no fabric. Test results indicate that when a fabric is placed within a specimen to withstand a portion of the tensile load fatigue performance can be improved. Those fabrics capable of holding more asphalt give best fatigue results.

Resistance to thermal reflection cracking was determined using the "overlay tester". This machine was designed to simulate the cyclic displacements within a pavement due to periodic thermal variations. Laboratory test data indicates all the fabrics studied will reduce thermal reflection cracking of asphaltic concrete.

Tensile properties of the fabric-mixture system were determined from

uniaxial tensile tests. Results of these tests can be used to define the material's stress-strain behavior and predict thermal cracking. Indications are that the use of fabrics will improve tensile strength and strain at failure of asphalt concrete.

Increased tack coat quantity appears to enhance performance for most of these laboratory tests. The reason for this correlation is unclear at this time and should be studied from a more fundamental basis.

Existing field data is summarized and briefly discussed which includes systems other than fabrics used to retard reflection cracking. The basic conclusions include the following: (1) fabrics perform well in mild climates (2) fabrics are most effective in arresting alligator-type cracking (3) performance of fabrics is questionable when placed over thermally cracked pavements and (4) for flexible pavements with alligator cracking a fabric with one inch of asphalt concrete will perform about equivalent to two inches of asphalt concrete overlay. However, because of the sketchy nature of existing data, more field performance information will be required prior to stating these conclusions with confidence.

Economics of several alternative methods used to reduce reflection cracking are considered. First costs and life cycle analysis techniques are used to compare several different rehabilitation strategies including (1) new asphalt concrete (2) recycled asphalt concrete (3) chip seal coat (4) heater-scarification (5) asphalt -rubber interlayer and (6) fabric interlayer. Major competition for fabrics has been identified, however, relative performance needs to be firmly established for various pavement conditions.

Finite element theory and fracture mechanics are applied to the over-

lay test and direct tension test results. Fracture properties of asphalt concrete can be altered substantially by the inclusion of fabrics. From this analysis, it appears that best performance may be obtained by placing a level-up course on the old pavement prior to the placement of the fabric and the overlay.

Generally, laboratory investigations of fabrics incorporated into asphalt concrete specimens have shown improvements in tensile properties, increased fatigue performance and a reduction in crack propagation rate and there is evidence to indicate fabrics will not compound overlay slippage problems. A review of several existing field studies of methods used to reduce reflection cracking reveals fabrics to be a competitive product and further that fabrics will reduce pavement maintenance and extend service life.

TABLE OF CONTENTS

	Page
EXECUTIVE SUMMARY	iii
TABLE OF CONTENTS	viii
INTRODUCTION	1
MATERIALS	4
DESCRIPTION OF TESTS AND SPECIMEN FABRICATION	13
Saturation Test	13
Fabric Shrinkage (Construction Cracking Test)	14
Peel Strength	16
Interface Shear Strength	18
Flexural Fatigue	21
Resistance to Thermal Reflection Cracking	25
Direct Tension Tests	29
TEST RESULTS	31
SYSTEMS TO REDUCE REFLECTION CRACKING (Field Experience)	82
ECONOMIC CONSIDERATIONS	89
GENERAL CONCLUSIONS	98
REFERENCES	99
BIBLIOGRAPHY	103
APPENDIX A - Cooling Time for Asphalt Mats	105
APPENDIX B - Peel Strength Test Data	107
APPENDIX C - Shear Strength Test Data	110
APPENDIX D - Flexural Fatigue Test Data	115
APPENDIX E - Thermal Reflection Cracking Test Data	130
APPENDIX F - Application of Fracture Mechanics to Pavement Reflection Cracking	136
APPENDIX G - Direct Tension Test Data	160

LIST OF FIGURES

- Figure 1. Rounded Gravel Aggregates Showing Size and Shape of Particle
- Figure 2. Crushed Limestone Aggregate Showing Size and Shape of Particles
- Figure 3. ASTM D-1663 - Aggregate Gradation 5A Specification and Project Gradation Design
- Figure 4. Apparatus Used to Determine Likelihood of Construction Cracking
- Figure 5. Test Specimen in Position for Peel Strength Test
- Figure 6. Schematic of Shear Test Apparatus
- Figure 7. Load Distribution and Fabric Location in Flexural Fatigue Test
- Figure 8. Schematic of Overlay Tester
- Figure 9. Typical Recordings of Load versus Deformation at Various Phases During a Test
- Figure 10. Direct Tension Test Apparatus
- Figure 11. Relationship Between Fabric Saturation and Fabric Weight
- Figure 12. Temperature Stability of Fabrics in 250°F Asphalt Cement
- Figure 13. Temperature Stability of Fabrics in 300°F Asphalt Cement
- Figure 14. Relationship Between Fabric Free Shrinkage and Fabric-Asphalt Linear Shrinkage
- Figure 15. Relationship Between Fabric Shrinkage Force and Fabric-Asphalt Linear Shrinkage
- Figure 16. Peel Strength of Fabrics on Portland Cement Concrete at a Peel Rate of 5 inches/minute
- Figure 17. Peel Rate of Fabrics on Portland Cement Concrete at a Peel Rate of 20 inches/minute

- Figure 18. Peel Strength of Fabrics on Asphalt Concrete at a Peel Rate of 5 inches/minute @ 122°F (50°C)
- Figure 19. Peel Strength of Fabrics on Asphalt Concrete at a Peel Rate of 20 inches/minute
- Figure 20. Overlay Shear Test Results with Mixtures using Fabric A
- Figure 21. Overlay Shear Test Results with Mixtures using Fabric D
- Figure 22. Overlay Shear Test Results with Mixtures using Fabric E
- Figure 23. Overlay Shear Test Results with Mixtures using Fabric F
- Figure 24. Overlay Shear Test Results with Mixtures using Fabric G
- Figure 25. Shear Strength as a Function of Tack Coat Quantity at 103°F (40°C)
- Figure 26. Stress versus Load Applications to Failure for Control Specimens
- Figure 27. Strain versus Load Applications to Failure for Control Specimens
- Figure 28. Stress versus Load Applications to Failure for Specimens Containing Fabric G at Optimum Asphalt Content
- Figure 29. Strain versus Load Applications to Failure for Specimens Containing Fabric G at Optimum Asphalt Content
- Figure 30. Mean No. of Load Cycles to Failure from Flexural Fatigue Test. (Only those specimens tested at or near 100 psi)
- Figure 31. Initial Stiffness Modulus (200th Cycle) From Flexural Fatigue Test
- Figure 32. Relationship Between Specimens Stiffness Modulus and Number of Load Applications to Failure
- Figure 33. Relationship Between Optimum Tack Coat and Number of Cycles to Failure
- Figure 34. Mean Number of Cycles to Failure from Overlay Tests (Specimens about one year older than all others)
- Figure 35. Effects of Air Void Content on Overlay Life
- Figure 36. Load Supported by Specimens Containing Different Fabrics
- Figure 37. Load Supported by Specimens Containing Fabric G
- Figure 38. Normalized Average Tensile Strength of Test Specimens

- Figure 39. Normalized Average Ultimate Tensile Strain of Test Specimens
- Figure 40. Average Initial Tangent Modulus of Tensile Test Specimens
- Figure 41. Simplified Relationship Between Equal Annual Cost and First Cost
- Figure A-1. Time for Mat to Cool to 225 F vs. Mat Thickness for Lines of Constant Mix and Base Temperatures.
- Figure A-2. Time for Mat to Cool to 200 F vs. Mat Thickness for Lines of Constant Mix and Base Temperatures.
- Figure A-3. Time for Mat to Cool to 175 F vs. Mat Thickness for Lines of Constant Mix and Base Temperatures.
- Figure A-4. Time for Mat to Cool to 175 F vs. Mat Thickness for Lines of Constant Mix and Base Temperatures.
- Figure C-1. Airport Shear Test Specimens after Testing with Fabric A (Tack Coat Rate Increases from Left to Right-Low, Optimum, and High).
- Figure D-1. Strain versus Load Applications to Failure for Specimens Containing Fabric A
- Figure D-2. Strain versus Load Applications to Failure for Specimens Containing Fabric D
- Figure D-3. Strain versus Load Applications to Failure for Specimens Containing Fabric E
- Figure D-4. Strain versus Load Applications to Failure for Specimens Containing Fabric F
- Figure D-5. Strain versus Load Applications to Failure for Specimens Containing Fabric G
- Figure D-6. Initial Bending Strain (200th Cycle) from Flexural Fatigue Test
- Figure D-7. Comparison of Total Input Energy for Flexural Fatigue Test
- Figure E-1. Crack Height versus Number of Cycles for Control Specimens
- Figure E-2. Crack Height versus Number of Cycles for Specimens with Fabric A
- Figure E-3. Crack Height versus Number of Cycles for Specimens with Fabric D

- Figure E-4. Crack Height versus Number of Cycles for Specimens with Fabric D
- Figure E-5. Crack Height versus Number of Cycles for Specimens with Fabric F
- Figure E-6. Crack Height versus Number of Cycles for Specimens with Fabric G and Low Tack Coat
- Figure E-7. Crack Height versus Number of Cycles for Specimens with Fabric G and Optimum Tack
- Figure E-8. Crack Height versus Number of Cycles for Specimens with Fabric G and Optimum Tack (Old Specimens)
- Figure E-9. Crack Height versus Number of Cycles for Specimens with Fabric G and High Tack Coat
- Figure E-10. Crack Height versus Number of Cycles for Specimens with Fabric H
- Figure F-1. Crack Length as a Function of Number of Tension Cycles for Control Specimens
- Figure F-2. Crack Length as a Function of Number of Tension Cycles for Specimens Containing Fabric G with Optimum Tack
- Figure F-3. Relationship Between Initial Crack Growth and Initial Stress Intensity Factor
- Figure F-4. Relationship Between Rate of Crack Growth and Final Stress Intensity Factor
- Figure F-5. Relationship Between n and $\log A$, Initial and Final
- Figure F-6. Typical Recording of Load Versus Crack Opening for Two Successive Load Cycles
- Figure F-7. Relationship Between Energy and Number of Tension Cycles for Control Specimens
- Figure F-8. Relationship Between Energy and Number of Tension Cycles for Fabric G-Optimum Tack
- Figure G-1. Relationship Between Tensile Strength and Air Voids
- Figure G-2. Relationship Between Tensile Strain at Failure and Air Voids

LIST OF TABLES

Table 1.	Summary of Asphalt Cements
Table 2.	Physical Properties of Aggregates
Table 3.	Mixture Properties at Optimum Asphalt Content
Table 4.	Fabric Properties
Table 5.	Fabric Saturation Quantities and Recommended Tack Coat Quantities
Table 6.	Construction Cracking Test Results
Table 7.	Linear Shrinkage Test
Table 8.	Simple Statistics of Flexural Fatigue Data
Table 9.	Results from "Overlay" Test Specimens
Table 10.	Statistical Summary of Direct Tension Test Results
Table 11.	Summary of State Field Trials
Table 12.	Fabric Manufacturers
Table 13.	Typical Costs for Rehabilitation Alternatives Suitable for Reducing or Eliminating Reflection Cracking
Table 14.	Rehabilitation Alternatives Defined
Table 15.	Rehabilitation Alternatives Cost Schedules *
Table 16.	Cost of Rehabilitation Alternatives *
Table 17.	Representative Costs for Maintenance and Rehabilitation Activities
Table B-1.	Individual and Mean Peel Strength Test Results at 122°F (50°C)
Table B-2.	Coefficients of Variation of Peel Strength Measurements
Table C-1.	Results of Shear Strength Tests
Table C-2.	Physical Properties of Shear Test Specimens
Table D-1.	Test Results from Fatigue Specimens Fabricated by Two Techniques

Table D-2.	Beam Fatigue Data
Table F-1.	Initial and Final Elastic Moduli from the Direct Tension Tests
Table F-2.	Calculations of Stress Intensity Factors, K_i and K_f , for Fabric G at Optimum Tack Rate
Table F-3.	Crack Growth Constants for Different Fabric
Table F-4.	Crack Growth Rate Per Cycle for Fabric G with Optimum Tack Rate
Table F-5.	Fracture Properties of Asphalt Concrete With and Without Fabric
Table F-6.	Tensile Work Coefficients
Table F-7.	Fracture Toughness Properties
Table G-1.	Direct Tension Test Results on Individual Test Specimens
Table G-2.	Physical Properties of Direct Tension Specimens and Test Results

INTRODUCTION

The major portion of highway pavement expenditures in the United States during the next 20 years will be for reconstruction, rehabilitation and maintenance of our existing facilities rather than construction of new facilities. This emphasis on reconstruction, rehabilitation and maintenance has increased research and development efforts aimed at pavement overlay systems that will eliminate, reduce or delay cracks from reflecting from the old pavement through the new overlay. The use of fabrics in combination with asphalt concrete overlays is one of several promising systems for reducing or delaying reflection cracks.

In an attempt to further define the performance of fabrics as effective reflection crack arrestors, a cooperative research program was initiated between Mirafi Inc and Texas A&M University in the fall of 1976. The objectives of the research program are given below:

1. Establish the mechanisms responsible for the performance of fabrics as effective reflection crack arrestors,
2. Define conditions (subgrade conditions, existing type of pavement, overlay thickness, environmental conditions) under which Mirafi is an effective crack arrestor,
3. Determine fabric properties which provide the desired field performance under a variety of conditions and
4. Define and delineate satisfactory field installation procedures for utilizing Mirafi as part of an overlay system to reduce or prevent reflection cracking.

Initial research efforts were aimed at objective No. 4 and resulted in the publication of a report titled "Mirafi Fabric Tack Coat Requirements

for Asphalt Overlays" (1). This report provides the engineer with a method for selecting the type and amount of tack coat to use in the field. The design method is based on laboratory and field results developed to a large extent under contract with Celanese.

The second major research effort was concerned with special field problems including early cracking of overlays placed on fabrics and an investigation of potential slippage problems of airfield pavement overlays made with fabrics. Laboratory tests were developed to help identify parameters which contribute to early cracking of fabric overlays. Fabric shrinkage tests were conducted by both Mirafi Inc and Texas A&M University and a "construction crack test" was developed. Results from these tests illustrate the importance of using "low" shrinkage force fabrics and the importance of proper construction techniques to reduce fabric wrinkles.

The investigation of potential slippage problems included the development of a special "airport shear" test to determine the shear strength of the interface between the fabric and the old asphalt concrete and the new asphalt concrete overlay. Computer programs were also utilized to calculate the magnitude of the shear stress at the interface. Results of this study have been published in a report titled "Asphalt Overlays with Mirafi Fabric - The Slippage Question" (2).

Objectives 1, 2 and 3 have been met in part by a combination of laboratory testing and field evaluation. Results of the laboratory testing program are contained in this report together with a summary of the field performance of fabric test sections placed in several states. Field performance information has been summarized on over 15 experimental projects throughout the United States. The laboratory testing program

includes testing of fabrics to determine the following properties:

1. Asphalt content at saturation,
2. Temperature shrinkage characteristics,
3. Adhesion strength between the pavement and fabric,
4. Shear strength of old pavement-fabric-new overlay interface,
5. Tensile strength of fabric-mixture system,
6. Flexural fatigue properties of fabric-mixture system and
7. Resistance to reflection cracking (overlay tester).

Properties of the asphalts, aggregates, asphalt concrete mixtures and fabrics will be summarized prior to the presentation of test results.

MATERIALS

The asphalt cements and aggregates utilized to fabricate asphalt concrete test specimens are currently used as laboratory standards in the Texas A&M University materials testing laboratory (3). Standard mixture properties for various asphalt-aggregate combinations are reported in Reference 3. Fabric properties were supplied by Mirafi Inc. Detailed properties are discussed below.

Asphalt Cements

Three asphalt cements were utilized in this study. All asphalts were obtained from the American Petrofina refinery located near Mt. Pleasant, Texas. The properties of the viscosity graded asphalt cements are shown on Table 1. The AC-10 asphalt cement was utilized for all asphalt concrete mixtures while the AC-5, AC-10 and AC-20 asphalt cement were utilized in tests to determine adhesion strength between the pavement and the fabric. The asphalts utilized are laboratory standard asphalts at the Texas A&M University materials laboratory.

Aggregates

A subgrounded, siliceous gravel and a crushed limestone are utilized as laboratory standard aggregates at the Texas A&M University materials laboratory.

The subgrounded, siliceous gravel was obtained from a Gifford-Hill plant located near the Brazos River at College Station, Texas. The crushed limestone was obtained from the White's Mines quarry located near Brownwood, Texas.

TABLE 1. Summary of Asphalt Cements.

Grade of Asphalt	AC-5	AC-10	AC-20
Viscosity @ 77°F (25°C), poise	2.8×10^5	5.8×10^5	3.0×10^6
Viscosity @ 140°F (60°C), poise	468	1576	1989
Viscosity @ 275°F (135°C), poise	2.34	3.76	4.19
Penetration @ 39.2°F (4°C), dmm	82	26	18
Penetration @ 77°F (25°C), dmm	189	118	63
Penetration Ratio, %	43	22	29
R & B Softening Pt, °F (°C)	104 (40)	107 (41.7)	120 (48.9)
Specific Gravity @ 60°F (16°C)	1.017	1.020	1.034
Flash Point (COC), °F (°C)	580 (304.4)	615 (323.9)	578 (303.3)
Solubility in $C_2H_3Cl_3$, %	99.8	99.9	99.9
Spot Test	Negative	Negative	Negative
Thin-Film Oven Test, Residue Properties			
Viscosity @ 140°F (60°C), poise	1135	3054	5151
Penetration @ 77°F (25°C), dmm	103	68	38
Ductility @ 77°F (25°C), cm	150	150	150

Standard sieves (ASTM E-11) were used to separate the aggregates into fractions sized from 3/4 inch to minus No. 200 mesh. Photographs of the sized gravel and limestone are shown on Figures 1 and 2. Prior to mixing with asphalt, the various aggregate sized were recombined according to the ASTM D 3515-77 5A grading specification. The aggregate gradation as well as the upper and lower limits of the specifications are shown in Figure 3. Standard tests were conducted to determine various physical properties of these aggregates such as specific gravity, absorption capacity, abrasion resistance, and unit weight. One additional test (4) was conducted to estimate the optimum asphalt content. Physical properties of the gravel and limestone aggregates are shown on Table 2.

Mixtures

Mixtures of these aggregates and the AC-10 asphalt cement were prepared at various quantities of asphalt cement and tested using Marshall and Hveem stability tests to determine the optimum asphalt contents. (Details of these tests can be found in Reference 3). Based on these tests, optimum asphalt contents were selected. Properties of the mixtures at optimum asphalt content are given on Table 3. The limestone mixture was utilized to evaluate the shear strength of the fabric-old pavement-overlay interface while the gravel mixture was used for all other mixtures utilized in the study.

Fabrics

Eight fabrics, labeled A, B, C, D, E, F, G and H, supplied by Mirafi Inc have been tested. Basic properties of these fabrics are shown on Table 4. Fabric properties were determined in the Mirafi Inc laboratory.

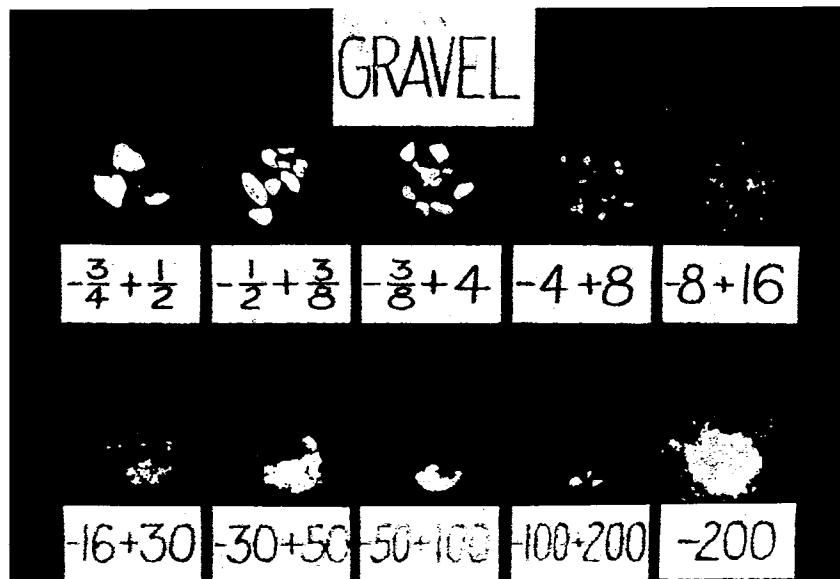


Figure 1. Rounded Gravel Aggregate Showing Size and Shape of Particles.

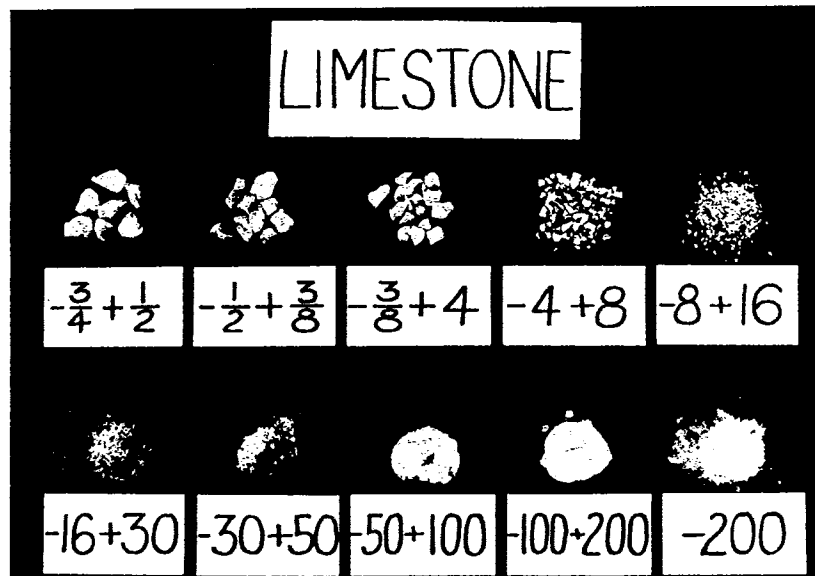


Figure 2. Crushed Limestone Aggregate Showing Size and Shape of Particles.

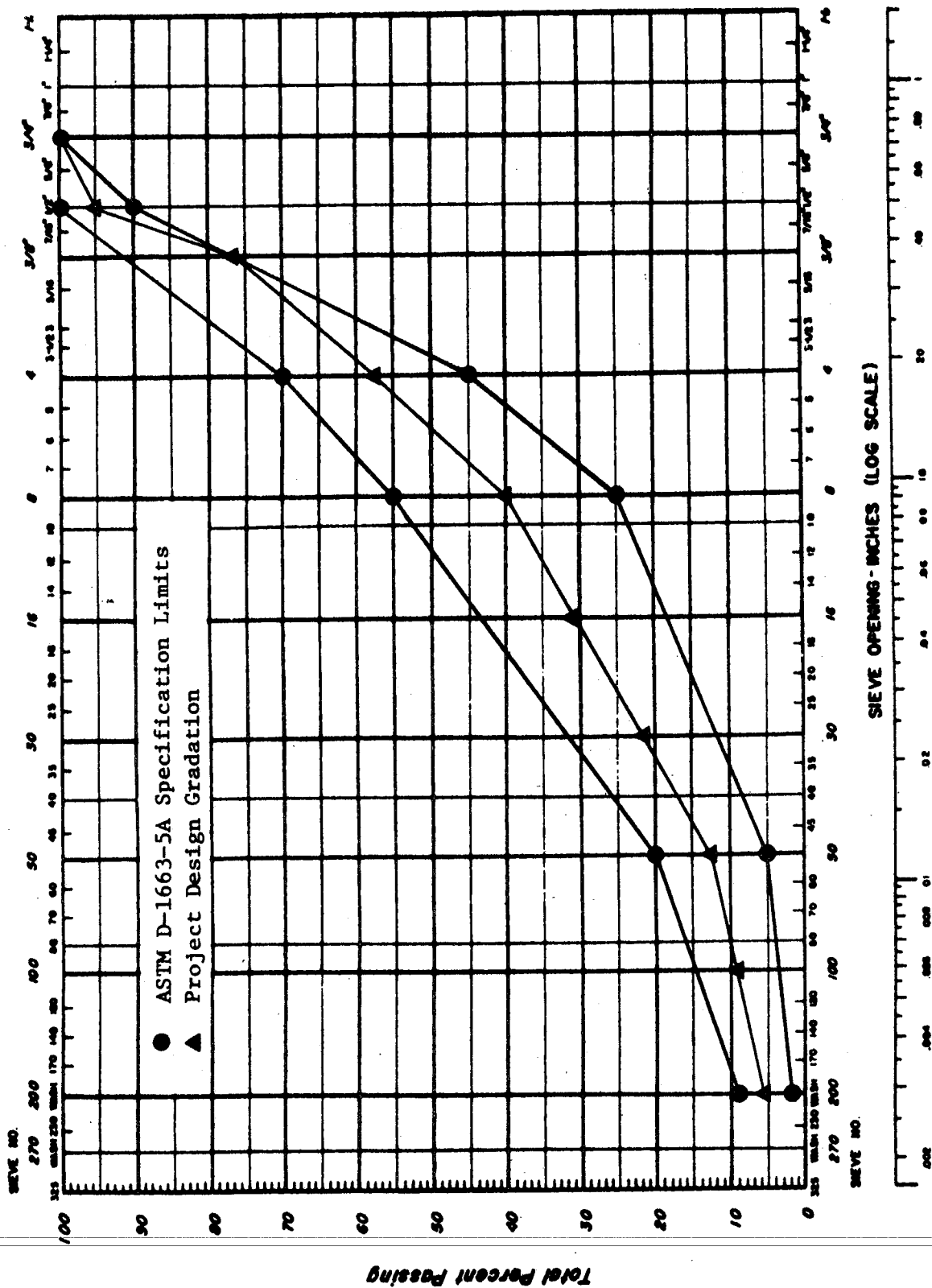


FIGURE 3. ASTM D-1663 - Aggregate Gradation 5A Specification and Project Gradation Design.

TABLE 2. Physical Properties of Aggregates.

Physical Property	Test Designation	Aggregate Grading	Test Gravel	Results Limestone
Bulk Specific Gravity	ASTM C 127 AASHTO T 85	Coarse Material*	2.621	2.663
Bulk Specific Gravity (SSD)			2.640	2.678
Apparent Specific Gravity			2.672	2.700
Absorption, percent			0.72	0.7
Bulk Specific Gravity	ASTM C 218 AASHTO T 84	Fine Material**	2.551	2.537
Bulk Specific Gravity (SSD)			2.597	2.597
Apparent Specific Gravity			2.675	2.702
Absorption, percent			1.8	2.2
Bulk Specific Gravity	ASTM C 127 & C 128 AASHTO T 84 & T 85	Project Design Gradation	2.580	2.589
Apparent Specific Gravity			2.671	2.701
Absorption, percent			1.3	1.56
Abrasion Resistance, percent loss	ASTM C 131 AASHTO T 96	Grading C	19	23
Compacted Unit Weight pcf	ASTM C 29 AASHTO T 19	Project Design Gradation	129	122
Surface Capacity, percent by wt. dry aggregate	Centifuge Kerosene Equivalent	Fine Material***	3.0	4.1
Surface Capacity, percent oil retained by wt. agg.	Oil Equivalent	-3/8 inch to + No. 4	1.8	2.3
Estimated Optimum Asphalt Content, percent by wt. dry aggregate	C.K.E. and Oil Equivalent	Project Design Gradation	4.7	5.5

*Material retained on No. 4 sieve from Project Design Gradation.

**Material passing No. 4 sieve from Project Design Gradation.

TABLE 3. Mixture Properties at Optimum Asphalt Content.

Property	Rounded Gravel	Crushed Limestone
Design Asphalt Content percent by wt. aggregate	3.8	4.5
Marshall Specimens		
Unit Weight, pcf (gm/cc)	152(2.44)	153(2.45)
Air Void Content,	2.1	3.0
VMA, percent	9.1	10.5
VMA Filled w/Asphalt, percent	80	78
Marshall Stability, lbs(N)	1270(5650)	2740(12,200)
Marshall Flow, .01 in.(mm)	7(1.8)	11(2.8)
Hveem Specimens		
Unit Weight, pcf (gm/cc)	151(2.42)	154(2.47)
Air Void Content, percent	2.9	2.5
VMA, percent	9.7	9.1
VMA Filled w/Asphalt, percent	76	81
Hveem Stability, percent	25	54
Resilient Modulus, psi(kPa)	570,000(3.9x10 ⁶)	590,000(4.1x10 ⁶)
Elastic Modulus, @ Failure *, psi (kPa)	39,000(0.27x10 ⁶)	26,000(0.18x10 ⁶)

*From Splitting Tensile Test.

TABLE 4. Fabric Properties**

Fabric Property	A	B	C	D	E	F	G	H
Grab Strength*, lbs (N)	177 x 265 (790 x 1180)	----	216 x 183 (960 x 810)	99 x 114 (440 x 510)	217 x 201 270 x 890	120 x 131 (530 x 580)	121 x 119 (540 x 530)	116 x 165 (520 x 730)
Grab Elongation*, percent	24 x 30	----	36 x 22	68 x 85	71 x 80	54 x 45	132 x 132	82 x 70
Mullen Burst, psi (kPa)	286(2.0)	----	415(2.9)	211(1.5)	301(2.1)	234(1.6)	102(0.70)	116(0.80)
Weight, oz/yd ² (gm/m ²)	5.2(176)	12.7(430)	4.7(160)	3.7(125)	6.2(210)	4.2(142)	3.9(132)	4.1(140)
Free Shrinkage*, percent at 300°F	21 x 10	42 x 38	----	8.8 x ---	----	6.0 x 5.8	9.2 x 9.0	22 x 21
Shrinkage Force*, gm @ 300°F	332 x 260	1303 x 202	101 x 153	142 x 52	8 x 16	1 x 10	109 x 159	137 x 168

* First value is fabric property in length direction, second value in width direction.

** Compiled by Mirafi Inc.

DESCRIPTION OF TESTS AND SPECIMEN FABRICATION

Evaluation of field performance consumes considerable time and is difficult to control. Therefore, laboratory apparatus were designed and developed to mechanistically evaluate fabrics in a logical sequence of tests. These new test methods were developed to simulate field loading conditions and hence are capable of evaluating overlay systems on a relative basis. First, fabrics were evaluated to see if they could withstand temperatures encountered in hot mix pavement construction; if so, the appropriate quantity of asphalt tack was determined. The specimens were fabricated and tested in controlled atmospheres to define the effects of fabrics in overlay slippage, and to separately evaluate the performance of fabrics in the reduction of fatigue and thermal cracking.

The test results are presented in this logical sequence which is not considered to be the order of importance.

Saturation Test

Three test methods have been investigated for prediction of fabric saturation (1). The test method selected for use involves the soaking of a piece of fabric 8 x 8-inches, (200 x 200 mm) in AC-10 asphalt cement at 250°F for 1 minute. The saturated fabric is allowed to cool and then pressed with a hot iron between two absorbent papers to remove the excess asphalt. This method produces a uniformly appearing saturated fabric without an excess of asphalt cement on any area of the fabric.

Fabric asphalt saturation content is one parameter that is utilized to determine field tack coat quantities for adequate adhesion between pavement layers. The tack coat quantity may be obtained from the equation

shown below:

$$Q_d = 0.08 + Q_s \pm Q_c$$

(Equation 1)

where:

Q_d = design tack coat quantity, gallons per square yard,

Q_s = fabric asphalt saturation content, gallons per square yard.

Q_c = correction to tack coat quantity based on asphalt demand of old surface, gallons per square yard.

The quantity, 0.08 gallons per square yard is based on field experience for overlays with no fabric. This equation, developed earlier in this research program (1), was utilized to determine asphalt tack coat quantities for laboratory testing purposes. A value of +0.02 was selected for Q_c based on the surface conditions of the laboratory samples.

Fabric Shrinkage

Two laboratory techniques were developed to identify the effect of temperature on fabric length change and stability.

Construction Cracking Test. The construction cracking test involves the placement of a hot asphalt concrete mixture over a fabric which has been placed in a rectangular mold. This laboratory test was developed to identify possible causes of cracking associated with the hot asphalt concrete during the early life (within 1 day) of the overlay. The fabric properties of free shrinkage and shrinkage force (Table 4) are indicators of temperature-associated cracking probability when fabrics are utilized in overlay systems.

Two rectangular molds, 48-inches (1220 mm) long by 5 1/2-inches (140 mm) wide, were fabricated from wood (Figure 4). One mold was fabricated with a 1/8-inch (32 mm) transverse crack in the bottom near

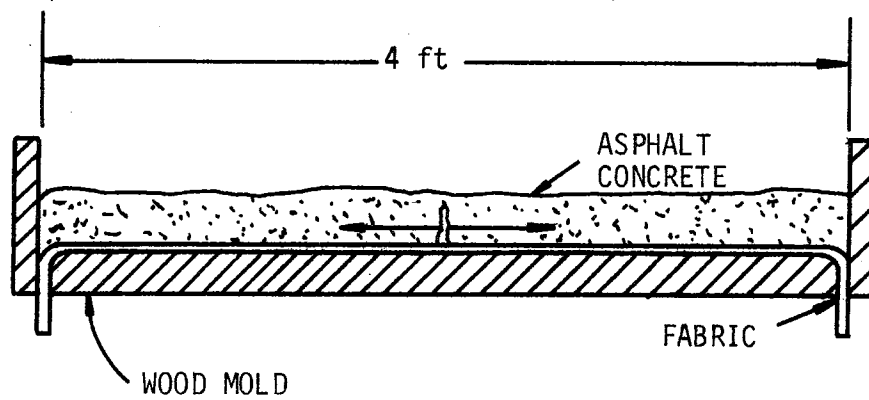


FIGURE 4. Apparatus Used to Determine Likelihood of Construction Cracking .

the center of the other mold contained no crack. An appropriate quantity of tack was placed in the bottom of the molds, depending on the requirements of the fabric. Fabric was placed over the tack coat in one of three different orientations: (1) control samples - either no fabric or smooth fabric with no wrinkles (2) one 3/8-inch (10 mm) fabric wrinkle near the center of the mold (wrinkle down in crack when using mold with crack) (3) fabric cut transversely near the center of the mold. In all cases the fabric was 5 1/2-inches (140 mm) wide and longer than the mold so that it could be securely fastened to each end of the mold (Figure 4). Hot mix asphalt concrete was placed in the mold over the fabric and compacted using a hand tamper with a 5 x 6-inch tamping face. The compacted asphalt concrete, which ranged in thickness from 3/4-inch to 1 1/2-inch was observed periodically to check for cracking. If cracks did appear in the overlay, it was usually within 15 minutes after placement and compaction. In some tests smaller cracks appeared after more than an hour of time elapsed.

Linear Shrinkage Test. This test involves soaking of the fabric in asphalt cement to simulate the application of the fabric to the hot tack coat and/or simulate the fabric saturation by tack coat immediately after placement of a hot asphalt concrete overlay. Four pieces of each fabric with dimensions of 4 x 4 inches (100 x 100 mm) were submerged in 250°F (121°C) and 300°F (149°C) asphalt cement. One of the four pieces of fabric was removed after elapsed times of 1, 5, 15, and 30 minutes and allowed to cool then measured along the run of the fabric to determine the effects of heat on length change as a function of time and temperature.

Peel Strength Tests

Adequate adhesion between the fabric and the old pavement is important

during construction in order to prevent the fabric from "rolling up" and/or "wrinkling" under construction equipment. Two types of tests have been developed to define the adhesion between the old pavement and the fabric. Details of both test methods can be found in Reference 1 together with test results on Fabric G in which different types of asphalt were utilized as tack coats and tests were conducted over a range of temperatures, tack coat quantities and test rates.

Fabric tests described herein consist of only the 180 degree peel test concrete surfaces. The surface texture of the asphalt concrete surface as measured by the Silicon Putty Method (6) was 0.022 cubic inches per square inch ($0.56 \frac{\text{mm}^3}{\text{in}^2}$). The portland cement concrete surface texture was $0.024 \text{ in}^3/\text{in}^2$ ($0.61 \frac{\text{mm}^3}{\text{mm}^2}$). The asphalt concrete was obtained from a city street in College Station, Texas. The portland cement concrete specimens were cast and the surfaces prepared in the laboratory. The test surfaces were 10 inches (250 mm) in length and 2 inches (50.8 mm) in width. A predetermined quantity of asphalt cement (depending on fabric requirements) at 250°F (121°C) was applied as a tack coat to each test surface.

The quantity of asphalt cement tack applied was varied around the optimum required for each fabric. Low tack was one-half the optimum and high tack was twice the optimum. Optimum tack coat was determined using Equation 1. For tests with high tack coats and hence thicker asphalt films, masking tape was affixed to the sides of the test specimens to provide a lip that prevented the asphalt from flowing off the test surface. While the asphalt cement was hot, a 10-inch (25 mm) strip of fabric about 25 inches (635 mm) in length was applied. The fabric was seated by covering it with waxed paper, placing a foam rubber cushion on top, and applying a 15 lb load for one minute.

The test specimens were fastened in a specially prepared frame, on the Instron Universal Testing Machine, with the loose end of the fabric downward. The loose end of the fabric was turned upward and clamped in the grips of the testing machine (Figure 5). This configuration facilitated a 180 degree peel test. All tests were conducted at constant displacement rates of either 5 or 20 inches per minute (137 and 508 mm/min) at a temperature of 122°F (50°C).

Interface Shear Strength

Adequate shear strength must be attained or pavement slippage failures will occur (2). Slippage failures, typically crescent shaped, are associated with high shear stress areas of a pavement and are most likely to occur during braking or turning operations when ambient temperatures are high.

A test method was developed which stimulates the braking action of a wheel on an overlaid pavement and used to determine the shear strength of the interfaces at the old pavement-fabric-new overlay. Tests were conducted at 68, 104, and 140°F (20, 40, 60°C, respectively) at a deformation rate of approximately 13 inches per second (330 mm/sec) with the apparatus shown in Figure 6 (2). A static vertical load of 400 pounds (1780 N) was applied to the 3x3x2-inch (75x75x50 mm) samples (67 psi or 460 kPa vertical pressure). Specimens at 140°F would not support the vertical load and were thus tested with no appreciable vertical load.

Samples for testing were fabricated in the laboratory with the laboratory standard limestone aggregate and 4.5 percent asphalt cement (AC-10). Twenty-four 3x3x14-inch (75x75x375 mm) asphalt concrete beams were compacted in three 1-inch (25 mm) layers at 250°F (121°C). Following compaction of the first two layers, the incomplete specimen was allowed to cool to less than

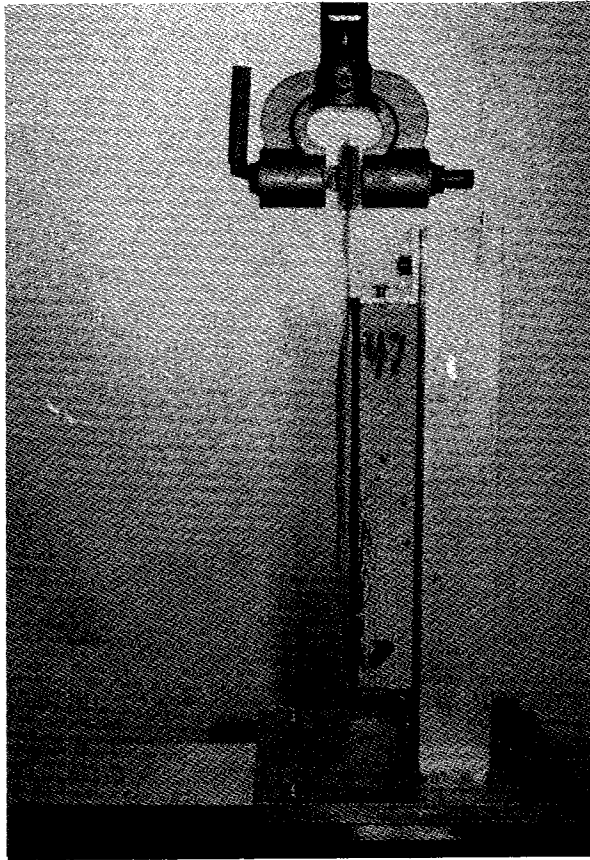


FIGURE 5. Test Specimen in Position for Peel Strength Test.

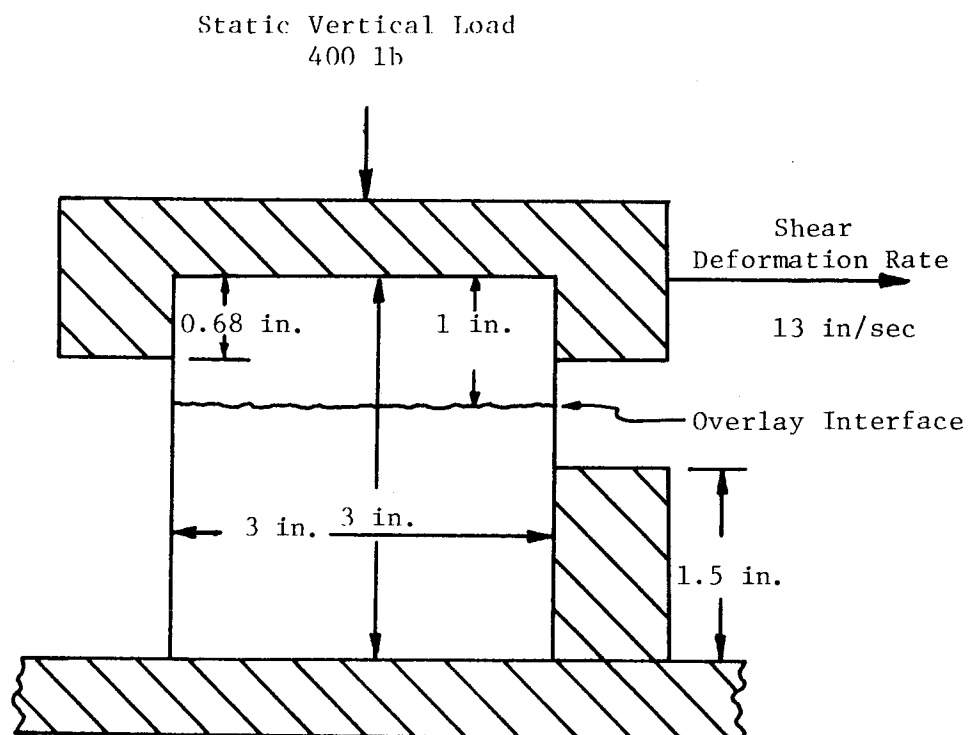


FIGURE 6. Schematic of Shear Test Apparatus .

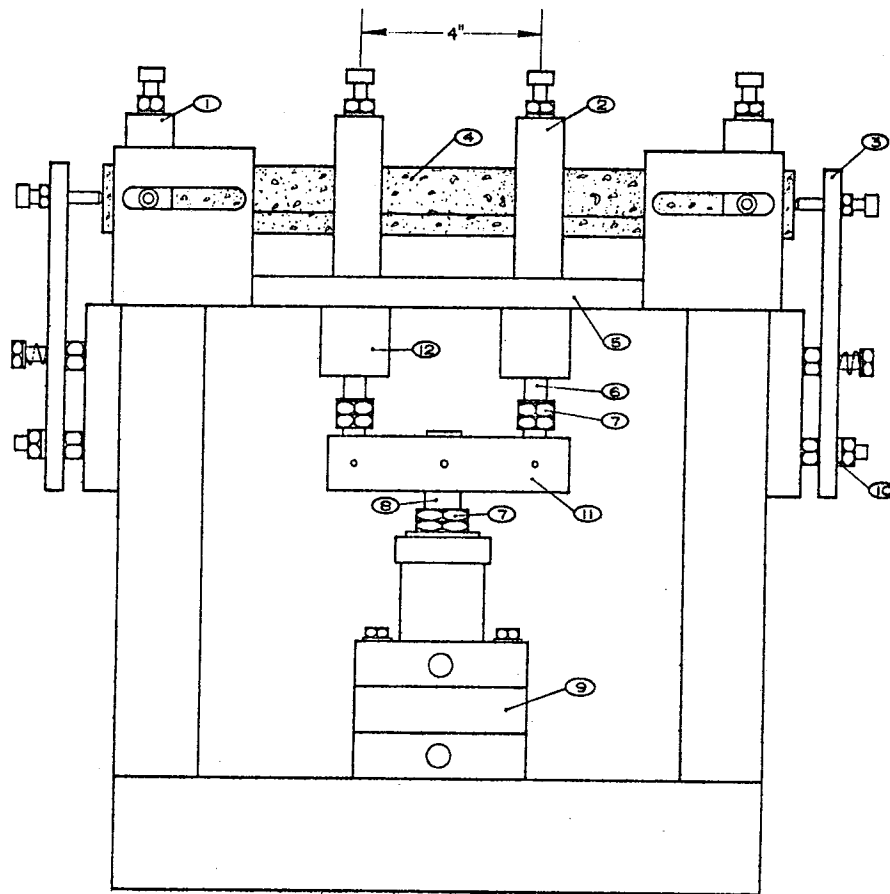
100°F (38°C). Then the appropriate quantity of tack coat (depending on individual fabric requirements) was applied evenly to the upper surface, a 3x15-inch piece of fabric was applied over the tack coat, and the third one-inch layer of asphalt concrete was compacted. The beams were then sawed transversely to yield 3x3x2-inch shear test specimens.

Flexural Fatigue

Beam fatigue tests were performed to provide information for prediction of the fatigue life of pavements. Fatigue cracking of pavements is caused by repeated wheel loads and will appear as cracks in the wheel path. These cracks will have a pattern similar to "chicken wire" or "alligator skins".

Computer models are available to predict pavement fatigue life. Required input includes elastic properties of the pavement materials and stress versus fatigue life or strain versus fatigue life relationships which can be obtained from laboratory beam fatigue tests.

Flexural fatigue characteristics of asphalt concrete mixtures with and without fabric were determined with the test equipment shown in Figure 7. This equipment is a larger scale model of a device originally developed by Deacon (8). Loads are applied at the third points of the beam, four inches on center, with one inch wide steel blocks. The applied load is measured by a load transducer and continuously recorded on an oscillographic recorder. Specimen deflection is measured at the center using a linear variable differential transformer (LVDT) and also recorded on the two channel oscillographic recorder. The machine is operated in the load control mode with a half-sine wave form at a frequency of 100 cycles per minute (1.67 Hz) and a load duration of 0.1 seconds. The test specimens are oriented such that the fabric is subjected to tensile stress



Key:

- | | | |
|-------------------|----------------|--------------------------------------|
| 1. Reaction clamp | 5. Base plate | 9. Double-acting, Bellofram cylinder |
| 2. Load clamp | 6. Loading rod | 10. Rubber washer |
| 3. Restrainer | 7. Stop nut | 11. Load bar |
| 4. Specimen | 8. Piston rod | 12. Thomson ball bushing |

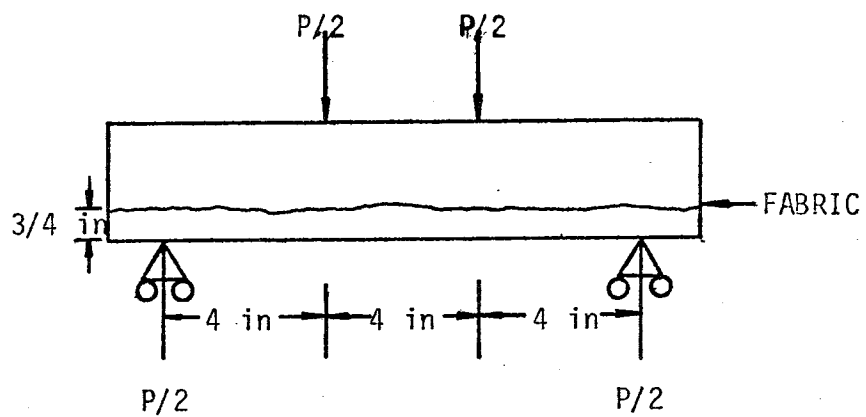


FIGURE 7. Load Distribution and Fabric Location in Flexural Fatigue Test.

during the loading phase. A reverse load is applied at the end of each load cycle to insure that the specimen will return to its original at-rest position after each cycle. It is necessary to periodically tighten the specimen loading and holding clamps as a result of plastic flow of the asphalt concrete. Upon rupture of the specimen, limit switches shut off the testing machine, and a cycle counter indicates the number of cycles to complete rupture.

Specimen Fabrication Techniques. Two methods of beam fabrication were investigated. Both methods were attempts to realistically simulate pavement overlay operations with fabrics. The first beam fabrication method utilized the following technique:

1. Compaction of a 3 x 3 15-inch (76 x 76 x 30-mm) asphalt concrete beam,
2. Extruding the beam from the mold and allowing the beam to cool,
3. Sawing and retaining the top and bottom 3/4-inch (19-mm) of the beam.
4. Artificially weathering the outer surface (unsawed face) with soapy water and a stiff brush,
5. Applying an appropriate quantity of asphalt cement tack coat,
6. Placing a 3 x 15-inch (76 x 380-mm) piece of fabric on the tacked beam surface,
7. Placing the 3/4-inch prepared beam into the beam mold, and
8. Compacting two 1 1/8-inch (29-mm) layers of asphalt concrete over the fabric.

This method of beam fabrication was time consuming and produced samples with non-uniform asphalt absorption into the fabric.

The second beam fabrication method utilized the following technique:

1. Compaction of a 3/4-inch (19-mm) layer of asphalt concrete
2. Applying a 3 x 15-9-inch (76 x 380-mm) of presoaked fabric
3. Compacting two 1 1/8-inch (29-mm) layers of asphalt concrete

over the fabric.

The presoaked fabric was obtained by placing the fabric in an AC-10 asphalt at 250°F (121°C) for 1 minute. The fabric was then repeatedly pressed between absorbent paper until the design asphalt content (as determined from Equation 1) was obtained. The second method of fabrication produced uniform asphalt absorption into the fabric and was less time consuming.

The asphalt concrete mixture utilized in the fatigue study was made with the laboratory standard subrounded gravel and 3.8 percent AC-10 asphalt cement. The asphalt cement and aggregate were mixed at 300°F (150°C) and molded at 250°F (121°C). A Soil-Test Model CN-425 kneading compactor with a 3 x 4-inch (7.6 x 10.2 cm) tamping foot was utilized to apply 35 tamps on the first two layers and 70 tamps on the third layer of asphalt concrete at a foot pressure of 1,300 pounds (5,800 N). After placing the three layers of asphalt concrete a leveling load of 12,000 pounds (5.3×10^4 N) was applied for 1 minute. Following extrusion from the mold, the beams were allowed to cool to room temperature. The specific gravity of each sample was determined gravimetrically in air and water and the air void content was computed. Results are contained on Table D1, Appendix D.

A review of data presented on Table D1 indicates the beams molded using the first technique were slightly stiffer than the beams molded using the second technique (presoaked fabric) while the air void contents of the beams was nearly identical for both techniques. Examination of the

coefficient of variation of the fatigue life indicates that a more uniform result was obtained when the molding procedure used the fabric presoak technique. However, additional data would have to be developed to make this statement with a high degree of confidence. From an ease of fabrication standpoint and from a uniformity standpoint the second method discussed using presoaked fabric was utilized.

As stated above all beams with fabric were fabricated utilizing the second method discussed. Control samples which contained no fabric were prepared by compacting three equal layers. The first two layers were subjected to 35 tamps and third layer was subjected to 70 tamps of the kneading compactor with 110 psi (760 Pa) foot pressure. A leveling load of 12,000 lbs (5.3×10^4 N) or 1,000 psi (6.9 kPa) was applied. All samples were aged for a period of at least two weeks at room temperature. All tests were conducted at a temperature of 68°F (20°C).

Resistance to Thermal Reflection Cracking

The "overlay tester" (Figure 8), developed at Texas A&M University, is essentially a displacement controlled fatigue testing machine designed to initially produce a small crack (due to tension) in a test specimen and then continue to induce repetitive longitudinal displacements at the base of the crack which causes the crack to propagate upward through the specimen. This process is intended to simulate the cyclic stressing of a pavement due to periodic thermal variation. Results obtained with this apparatus should prove very useful in predicting pavement service life extension effected by systems purported to reduce reflection cracking.

The construction materials as well as the fabrication procedures for the specimens tested in this experiment were identical to those used in

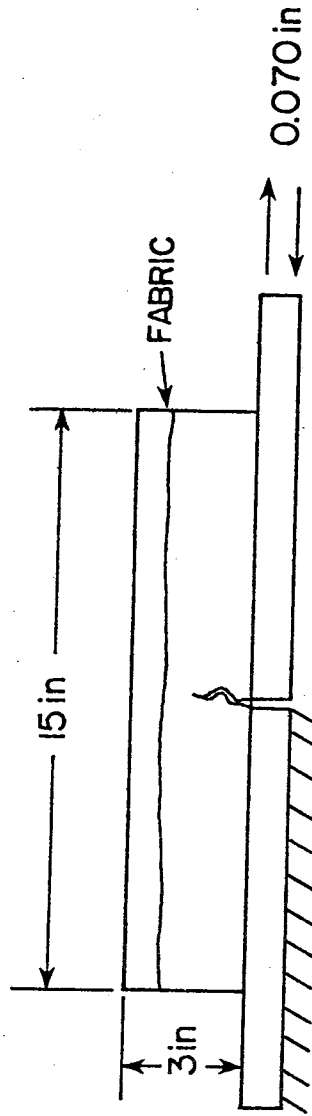


FIGURE 8. Schematic of Overlay Tester.

the preparation of the 3x3x15-inch (7.6 x 7.6 x 38 cm) beams tested in flexural fatigue. Siliceous gravel with a 3.8 percent AC-10 asphalt and presoaked fabric was utilized in the fabrication of all these specimens. All test specimens with fabric were made using only the optimum tack rate except those containing Fabric G which utilized three tack rates (one-half optimum, optimum and twice optimum). Control samples contained no fabric and were prepared by compacting three equal layers.

After allowing the test specimens to age at room temperature for at least two weeks, each specimen was epoxied to two rigid plates; one fixed, the other regulated to oscillate at a constant displacement of 0.070-inches and at a rate of 6 cycles per minute. The initial movement was outward which caused tensile stresses at the center of the specimen. All these tests were conducted at 77°F (25°C). Load was measured by a strain gage load transducer and displacement of the moving plate was monitored by a linear variable differential transformer (LVDT). Load as a function of displacement was recorded on an X-Y recorder. An example of recorded data is given in Figure 9. The length of the crack was periodically measured on each side of the specimen. The average of the two measurements was used as the crack length corresponding to the given number of cycles. The machine was allowed to oscillate until complete specimen failure, that is, until the crack propagated completely through the beam specimen. Ideally, complete failure would be defined as the cycle at which the load approached zero, however, with those specimens containing fabric, a measurable load was supported by the fabric even after the asphalt concrete specimen was completely cracked.

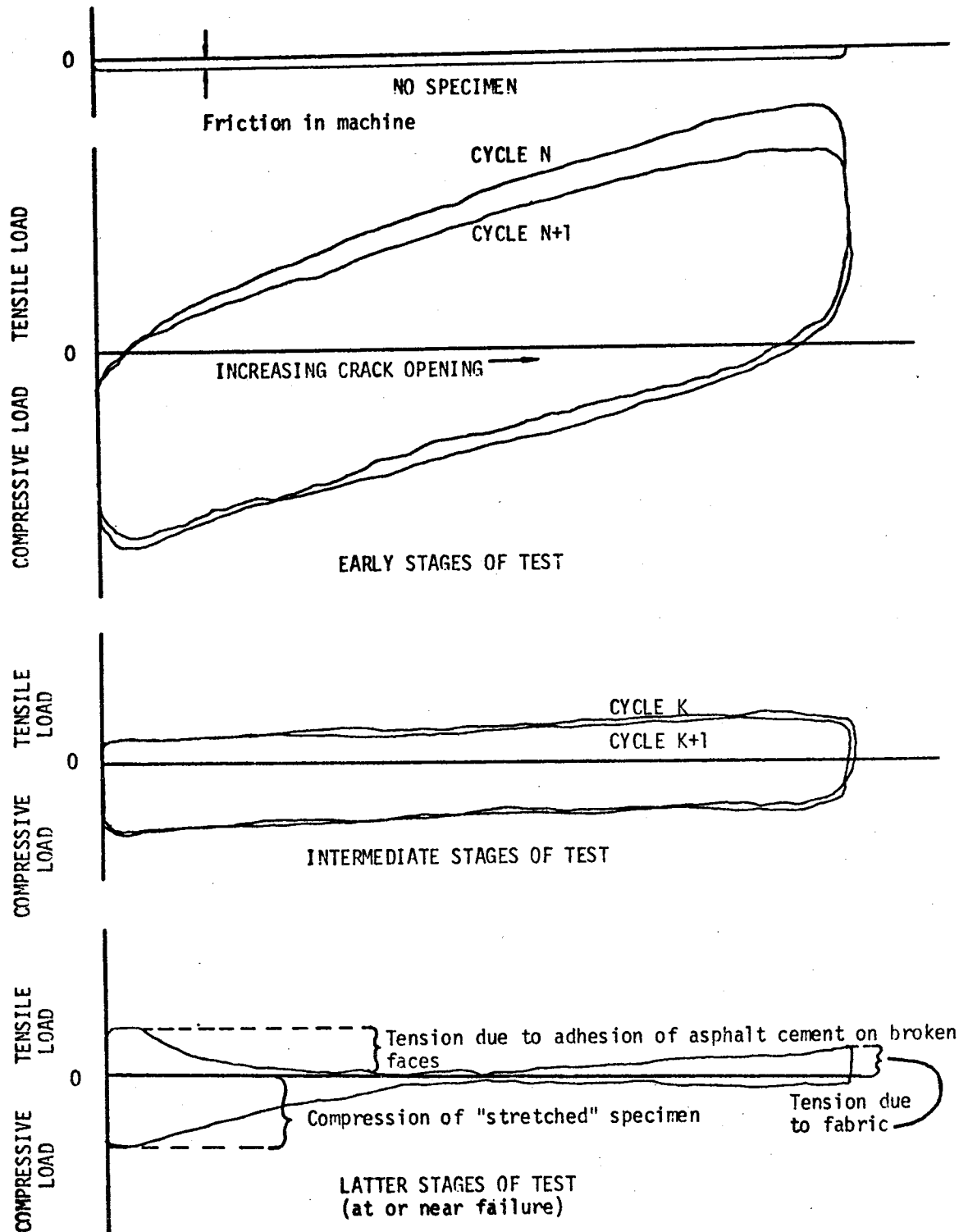


FIGURE 9. Typical Recordings of Load versus Deformation at Various Phases During a Test.

Direct Tension Tests

Results of tensile tests can be used to define a material's stress-strain behavior to failure, predict thermal cracking as well as provide needed information for crack prediction models based on fracture mechanics theory (Appendix F).

In an effort to determine the effects of fabric on the tensile properties of asphalt concrete, uniaxial tensile tests (Figure 10) were conducted on specimens containing fabrics as well as control specimens at a constant displacement rate of 2 inches per minute (5.1 cm/min) and a temperature of 68°F (20°C).

All specimens were prepared with the laboratory standard gravel and asphalt cement (AC-10) mixed at 300°F (150°C) and molded at 250°F (121°C). The first step was to mold a 2 x 3 x 15-inch (50 x 75 x 375 mm) beam using the modified soil-test model CN-425 kneading compactor with a 3 x 4-inch (75 x 100 mm) tamping foot applying 35 tamps on each of the two 1-inch layers. After the first one inch layer was compacted, the appropriate quantity of asphalt cement tack coat was uniformly distributed over the top surface, a 3 x 15-inch (75 x 375 mm) piece of fabric was applied, and lastly, a second one inch layer was compacted. Following extrusion from the mold, the beams were allowed to cool to room temperature. The specific gravity of each specimen was determined gravimetrically in air and water, and the air void content was computed. Each of the six beams made with different fabrics were cut in half longitudinally, then each half was sawed into three pieces to ultimately produce test specimens approximately 1.5 x 1.5 x 5-inches (38 x 38 x 135-mm) with a strip of fabric near the center.

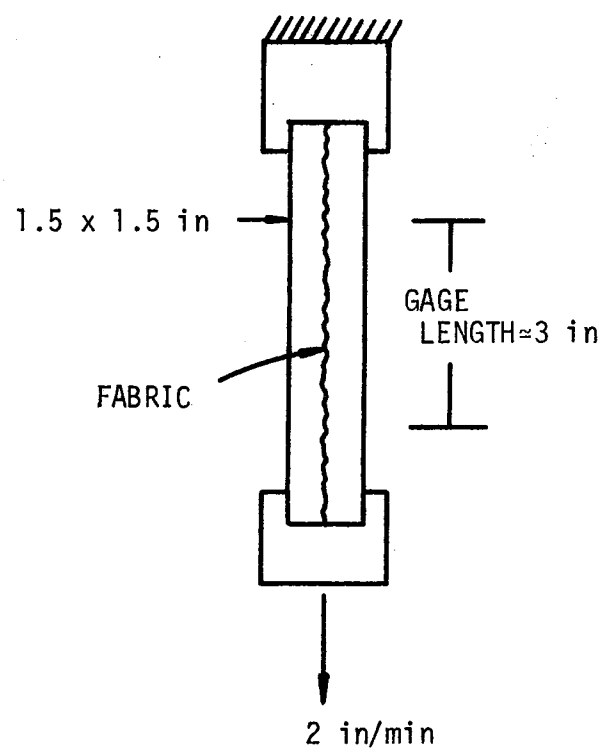


FIGURE 10. Direct Tension Test Apparatus.

TEST RESULTS

Laboratory test results are presented below. The relative laboratory performance of different fabric variants (types of fabrics) are evident from these tests. It is difficult, if not impossible, to directly predict field performance from these test results; however, the laboratory tests that were developed attempt to realistically simulate field loading conditions. The relative performance of fabrics in the field is in all probability correlatable to their relative laboratory performance.

Fabric Saturation

Fabric saturation contents are shown in Table 5. Asphalt saturation contents range from a low of 0.03 gallons per square yard ($1.3 \times 10^{-4} \text{ m}^3/\text{m}^2$) (Fabric F) to a high of 0.33 gallons per square yard ($1.5 \times 10^{-3} \text{ m}^3/\text{m}^2$) (Fabric E). Estimates of required tack coat quantities for each fabric on a surface texture of $0.20 \text{ in}^3/\text{in}^2$ ($0.5 \text{ cm}^3/\text{cm}^2$) (1) are included in the table. These quantities were utilized as the design asphalt content for the test specimens prepared in this laboratory testing program.

Figure 11 has been prepared to illustrate that a simple relationship does not exist between fabric weight and saturation asphalt content. Each fabric should be tested to determine its asphalt saturation content. The type of fiber (polypropylene, polyester, nylon, etc.), fabric structure, etc. must be considered to determine a fabrics asphalt retention. Fabric weight alone does not correlate well with fabric saturation.

Fabric Shrinkage

Two tests were developed and performed to determine the effects of hot mix asphalt overlay temperatures on fabric dimensions.

TABLE 5. Fabric Saturation Quantities and Recommended Tack Coat Quantities.

Fabric	Saturation Content, gallons per square yard of Fabric ($\text{m}^3/\text{m}^2 \times 10^{-4}$)	Asphalt Tack Coat Quantity, gallons per square yard, ($\text{m}^3/\text{m}^2 \times 10^{-4}$)
A	0.04 (1.8)	0.14 (6.3)
B*	0.02 (0.9)	0.12 (5.4)
C	0.04 (1.8)	0.14 (6.3)
D	0.13 (5.9)	0.23 (10.4)
E	0.33 (14.9)	0.40 (18.1)
F	0.03 (1.4)	0.13 (5.9)
G	0.10 (4.5)	0.20 (9.1)
H	0.15 (6.8)	0.25 (11.3)

*This fabric is manufactured with about .09 gallons per square yard of impregnated asphalt. The quantity shown is the amount of additional asphalt cement required to saturate the fabric.

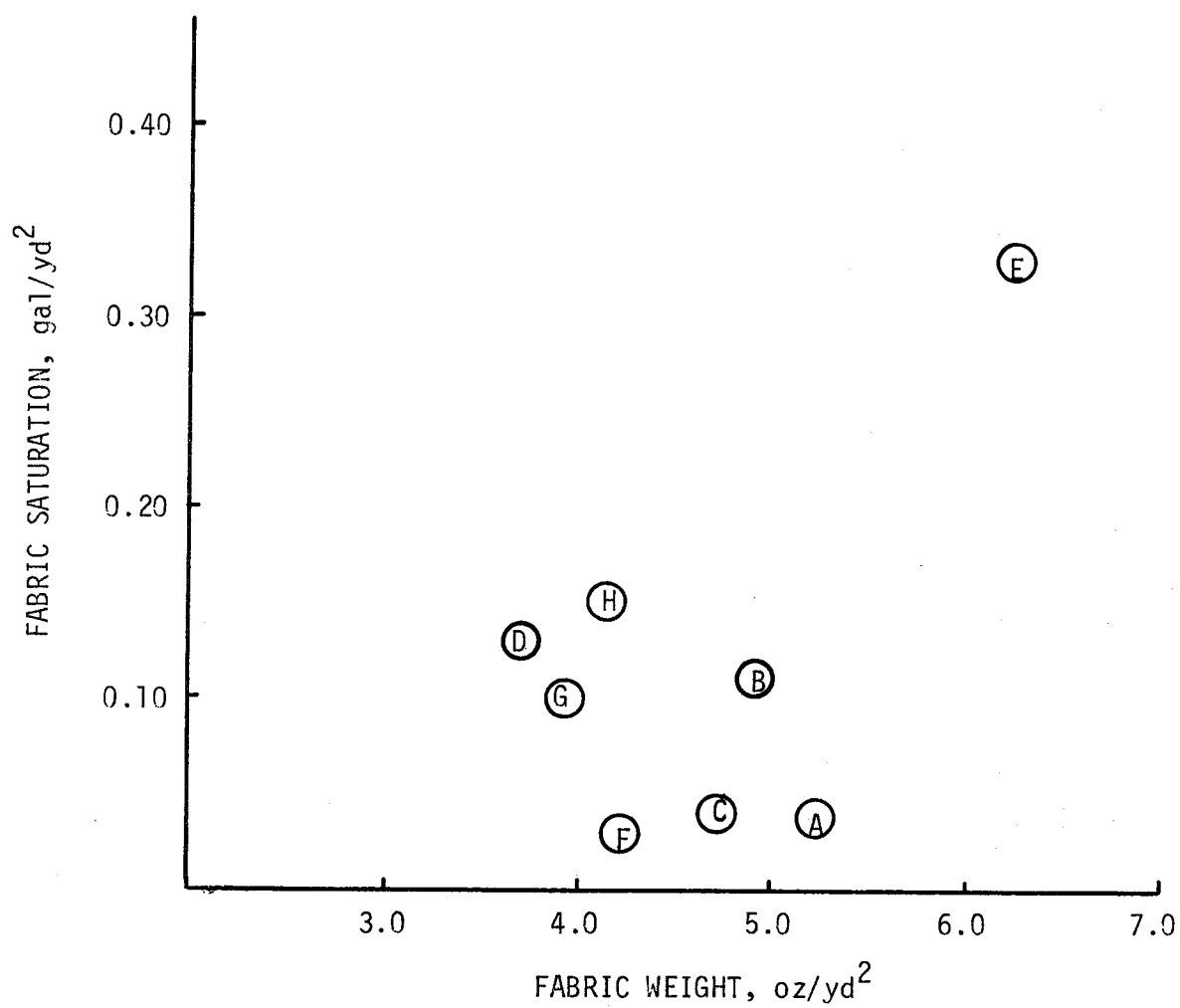


FIGURE 11. Relationship Between Fabric Saturation and Fabric Weight.

Construction Cracking Test. The test results using the four foot mold are given in Table 6 for fabrics B, E, F, and G. No shrinkage cracks appeared in any of the tests conducted using a two foot mold which was used initially. However, cracks did appear in certain similar tests using the four foot mold. This indicates the shrinkage forces that accumulated over a one foot length of fabric on each side of the wrinkle were not sufficient to cause cracking in the hot overlay. Furthermore, the shrinkage forces in some fabrics are capable of acting from a distance greater than one foot to produce cracking in a hot asphalt overlay.

Fabrics E and F, which exhibited very little shrinkage in the temperature stability test, did not produce cracks in this test. And conversely, Fabric B, which exhibited excessive shrinkage in the temperature stability test, produced the largest cracks and was the only fabric tested that produced a crack in the 1 1/2-inch (38 mm) overlay. In the temperature stability test, Fabric G exhibited comparatively little shrinkage but shrank over a relatively long time period; similarly, in this test it produced small cracks in the thin overlays and more than hour elapsed before they appeared. These test results also correlated quite well with the shrinkage forces generated by the fabrics at 300°F (Table 4). Those fabrics exhibiting low shrinkage forces (Fabrics E and F) did not cause cracking in the overlay. The fabric exhibiting a relatively high shrinkage force (Fabric B) did cause cracking. Fabric G with a moderate shrinkage force caused small cracks to form.

Although the number of tests were not sufficient to make positive statements, the following conjectures are made based on test observations:

- (1) There was no noticeable difference in crack propagation between tests using emulsion and asphalt cement tack coats.

TABLE 6. Construction Cracking Test Results.

FABRIC	TYPE SURFACE	OVERLAY THICKNESS, INCHES	TYPE TEST	OPTIMUM TACK COAT		FABRIC SHRINKAGE FORCE @ 300°F, gm
				CRS-2	AC-5	
B	Wood	3/4 1 1/2 3/4	C+W C+W CUT		CRACK CRACK LARGE CRACK	1303
E	Wood	3/4 1 1/2 1 1/2 3/4	W W C+W CUT	No No No	No	8
F	Wood	3/4 3/4 3/4 3/4	C+W C+W W CUT	No	No No No	1
G	Wood	1 1/2 3/4 1 1/2 3/4	W C+W C+W CUT	SMALL CRACKS No	No SMALL CRACKS	109
Control	Wood	3/4 3/4 3/4	C (No Fab) C (Smooth) No CRACK No Fabric		No No No	NA

(2) The cut fabric allowed slightly more cracking than the wrinkle alone or the wrinkle in the crack. (3) The thicker overlay was less likely to crack due to fabric shrinkage. (4) Fabrics with free shrinkage in excess of about 7% may cause construction cracks. (5) Fabrics with shrinkage forces in excess of about 100 grams may cause construction cracks. (6) Fabric-asphalt cement systems with linear shrinkages greater than 5 percent after soaking in 300°F asphalt for 30 minutes may cause construction cracking.

Linear Shrinkage Test. These tests were conducted on fabrics A, B, C, D, E, F, and G. The results are given in Table 7 and plotted in Figures 12 and 13. Based on several observations a reasonable estimate of the precision of this data is ± 5 percent.

As expected, the higher temperature caused more fabric shrinkage. The lowest test temperature (250°F) appears to be located near a critical temperature, that is, below this temperature very little shrinkage occurs, but above this temperature significant shrinkage occurs in most of the fabrics. Fabrics E, F, and G, with linear shrinkage values of 5 percent or less after fifteen minutes, have the lowest temperature susceptibility. Fabric B, the most temperature susceptible fabric tested, as well as C and G apparently would have continued to shrink after 30 minutes exposure to the hot asphalt cement. Most of the other fabrics reached a maximum shrinkage after 30 minutes exposure.

Fabrics A and C which have negligible shrinkage when exposed to 250°F asphalt cement have significant shrinkage characteristics when exposed to 300°F asphalt cement. Fabrics E and G show little change in shrinkage between 250 and 300°F exposure conditions.

Figures 14 and 15 have been prepared to investigate the relationship

TABLE 7. Linear Shrinkage Test.

FABRIC TYPE	ASPHALT TEMPERATURE, °F (°C)	ELAPSED TIME, MIN.	LINEAR SHRINKAGE, PERCENT
A	250 (120)	1	0
		5	0
		15	0
		30	0
	300 (150)	1	8
		5	10
		15	15
		30	15
B	250 (120)	1	2
		5	3
		15	5
		30	8
	300 (150)	1	8
		5	13
		15	20
		30	23
C	250 (120)	1	0
		5	0
		15	0
		30	0
	300 (150)	1	3
		5	10
		15	13
		30	15
D	250 (120)	1	5
		5	8
		15	8
		30	8
	300 (150)	1	8
		5	10
		15	13
		30	13

TABLE 7. Continued.

FABRIC TYPE	ASPHALT TEMPERATURE, °F (°C)	ELAPSED TIME, MIN.	LINEAR SHRINKAGE, PERCENT
E	250 (120)	1	2
		5	3
		15	3
		30	3
	300 (150)	1	0
		5	0
		15	3
		30	3
F	250 (120)	1	0
		5	0
		15	0
		30	0
	300 (150)	1	3
		5	3
		15	3
		30	3
G	250 (120)	1	0
		5	0
		15	1
		30	2
	300 (150)	1	5
		5	5
		15	5
		30	6

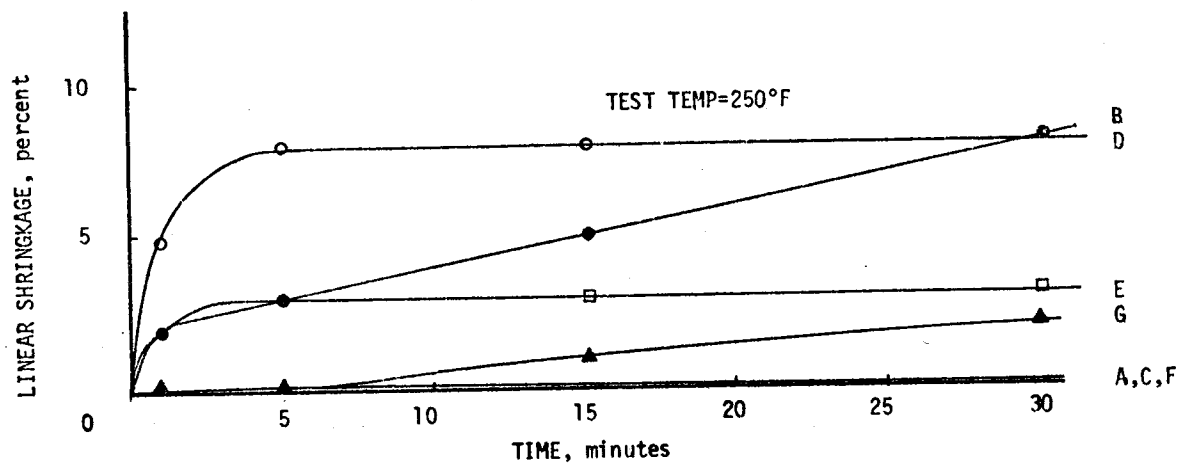


FIGURE 12. Temperature Stability of Fabrics in 250°F Asphalt Cement.

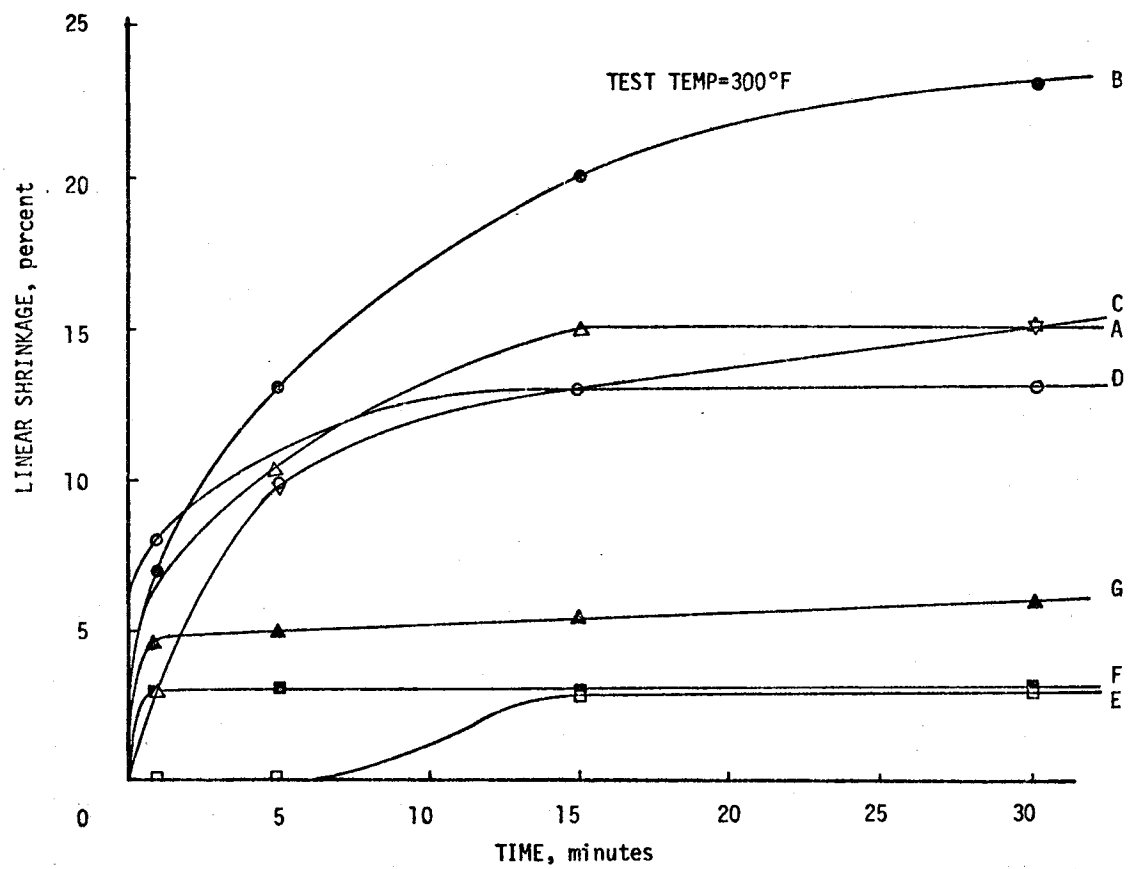


FIGURE 13. Temperature Stability of Fabrics in 300°F Asphalt Cement.

between fabric test properties of free shrinkage and shrinkage force and the fabric-asphalt property of linear shrinkage. Although only limited data are available, a correlation between fabric free shrinkage and fabric-asphalt linear shrinkage does appear to exist (Figure 14). An apparent correlation also exists between fabric shrinkage force and fabric-asphalt linear shrinkage (Figure 15).

Significance of Test Results. It is fairly common knowledge that heat (250°F or more) will cause varying degrees of shrinkage in most currently available fabrics. This shrinkage may be advantageous at least temporarily, as the "post-tensioned" fabric would improve the tensile properties of the system, particularly at low strains. The temporary nature of these benefits are due to stress relaxation in the viscoelastic system.

When wrinkles (or cuts without adequate overlap) are present in a fabric during an overlay operation, tensile forces caused by fabric shrinkage can produce a significant displacement of the fabric normal to the wrinkle or cut. Shrinkage occurs while the asphalt concrete overlay is hot and without appreciable tensile strength; thus, the motion of the fabric displaces the hot overlay resulting in a crack in the new overlay along the wrinkle or cut.

Assume an asphalt concrete has no appreciable tensile strength at temperatures above 175°F. Depending on ambient temperature, base temperature and wind velocity, one-inch mat of hot mix asphalt concrete placed at 300°F (120°C) may require up to 7 minutes to cool to 175°F (80°C) whereas a 3-inch mat under similar conditions may require up to 37 minutes (5) (See Figures A1 through A4, Appendix A). Based on observations of laboratory experiments, this is adequate time for certain high shrinkage and high shrinkage-force fabrics to damage an overlay.

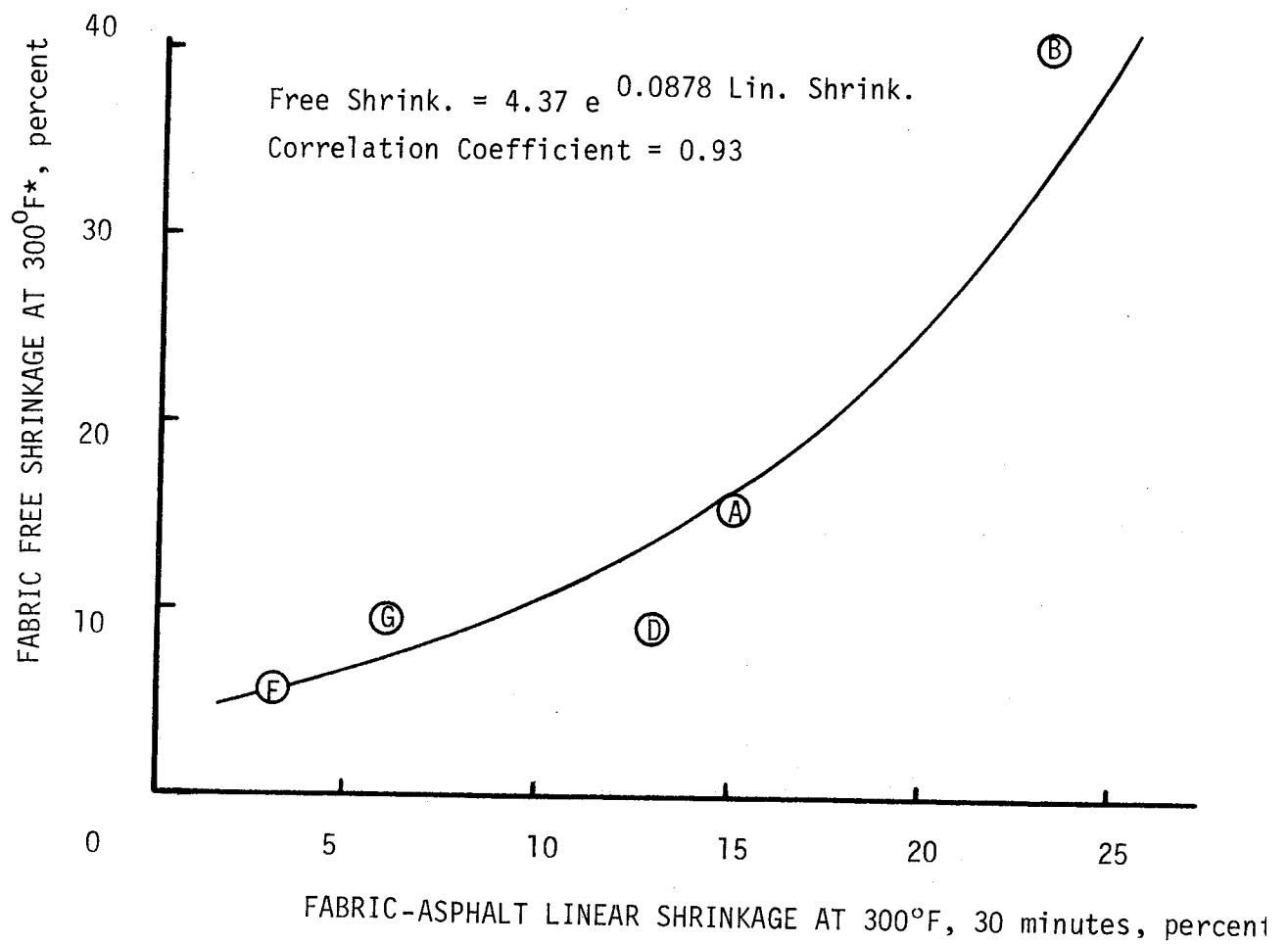
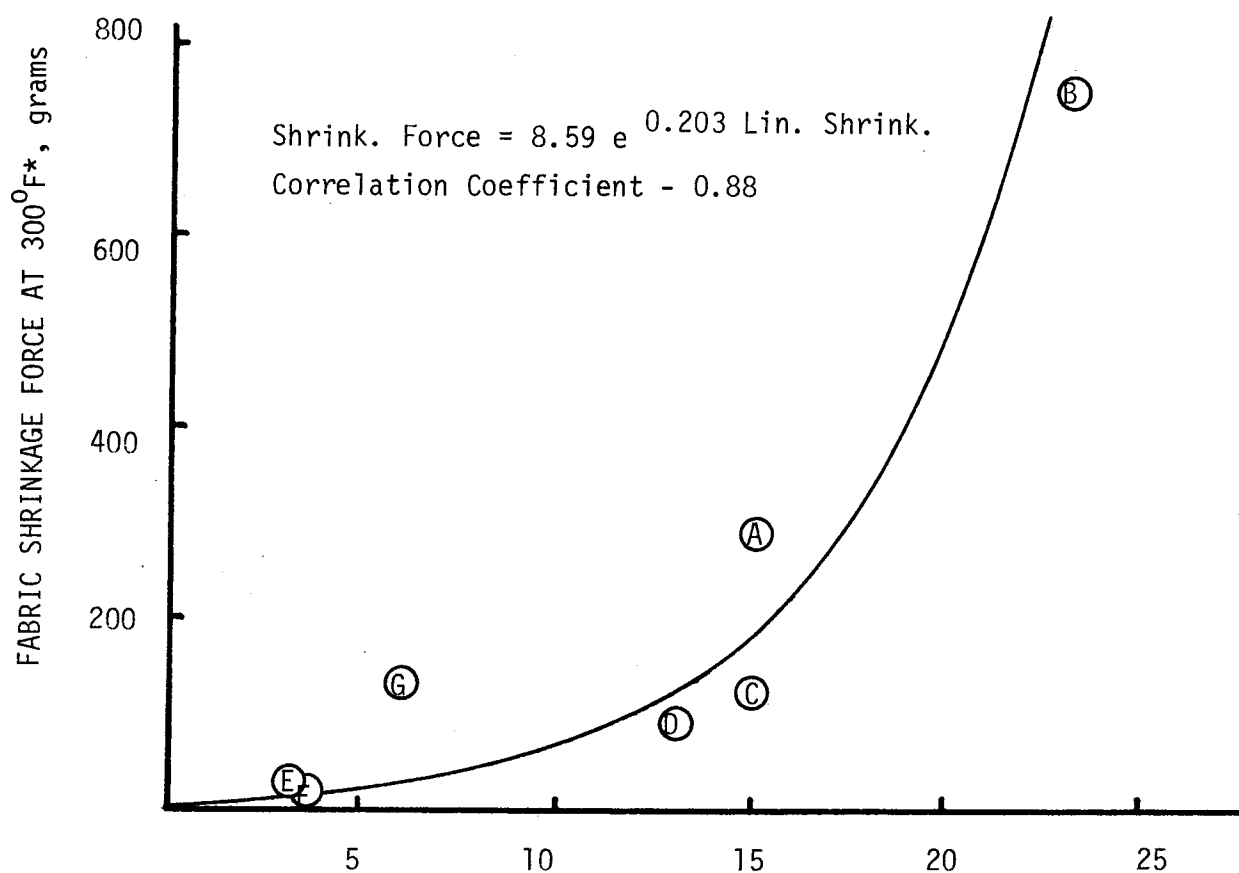


FIGURE 14. Relationship Between Fabric Free Shrinkage and Fabric-Asphalt Linear Shrinkage.

*Average of Two Directional Value.



FABRIC-ASPHALT LINEAR SHRINKAGE AT 300°F, 30 minutes, percent

FIGURE 15. Relationship Between Fabric Shrinkage Force and Fabric-Asphalt Linear Shrinkage.

*Average of Two Directional Value.

Conclusions

1. Shrinkage of fabric adjacent to the underside of an overlay impart stresses to the overlay.
2. Shrinkage of a fabric with wrinkles can cause immediate cracking of overlay due to opposing (tensile) forces on either side of the wrinkle.
3. Heat is a detrimental factor: The hotter the overlay material the greater the shrinkage of "fabrics", therefore, the greater the stresses or likelihood of cracking. There is apparently a relationship between fabric shrinkage force, temperature, and probability of cracking an overlay at a fabric wrinkle or joint.
4. When large cracks are present in the "old" pavement there may be a lack of compaction in the overlay along the crack because of the lack of support under the overlay. If a wrinkle is present along this crack, then the low tensile strength of the overlay along the crack compounds the overlay cracking problem.
5. Fabrics with low shrinkage force minimize problems with construction cracking.

Recommendations. The following field construction practices are recommended especially when a low shrinkage force fabric is not used.

1. Minimize wrinkles and/or cuts in fabric during overlay construction and provide adequate overlap at joints.
2. Roll fabric to insure intimate contact with "old" pavement.
3. Do not greatly exceed optimum tack coat requirements as this affords a lubricating action to allow fabric movement.

Note: Tack coats below optimum may be detrimental to shear strength at the pavement-overlay interface and fatigue life.

4. Control overlay laydown temperature toward lower end of specification.
5. Delay rolling as long as possible to afford compaction after most fabric shrinkage has occurred.
6. Fill cracks in "old" pavement larger than about 0.2-inch prior to application of fabric.

Peel Strength Test

From a construction standpoint it is important to have sufficient peel strength to prevent the fabric from rolling up and/or wrinkling under construction equipment. Thus a relatively high adhesive strength is preferred. It is not desirable to obtain the desired peel strength by increasing tack coat quantity beyond that obtained from Equation 1 as this asphalt tack may migrate or bleed through the asphalt concrete overlay and cause hazardous wet weather driving conditions.

Individual and mean values of peel strength are presented in Appendix B. Figures 16 through 19 graphically illustrate the relationship between tack coat quantity, rate of deformation and type of surface on peel strength.

Under all conditions, Fabrics A and D yielded higher peel strengths than the other fabrics tested. There is not a common fabric property to which this phenomenon can be attributed. Fabrics on the portland cement concrete surface consistently gave higher peel strengths than those on the asphalt concrete surfaces. Microtexture, surface porosity and aggregate surface characteristics could account for this observed difference.

At the percent time an acceptable level of peel strength cannot be firmly established. A correlation between laboratory peel strength and

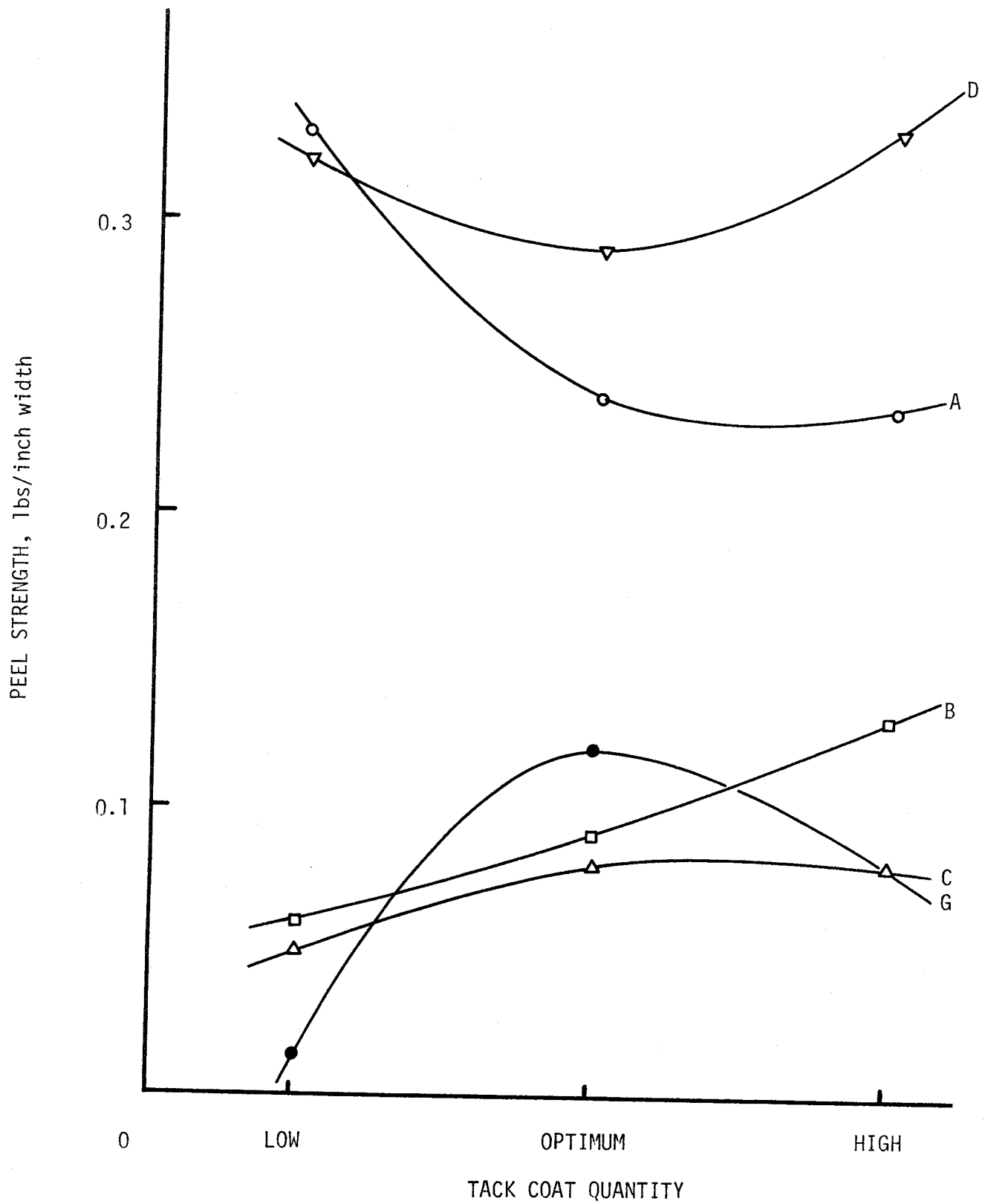


FIGURE 16. Peel Strength of Fabrics on Portland Cement Concrete at a Peel Rate of 5 inches/minute.

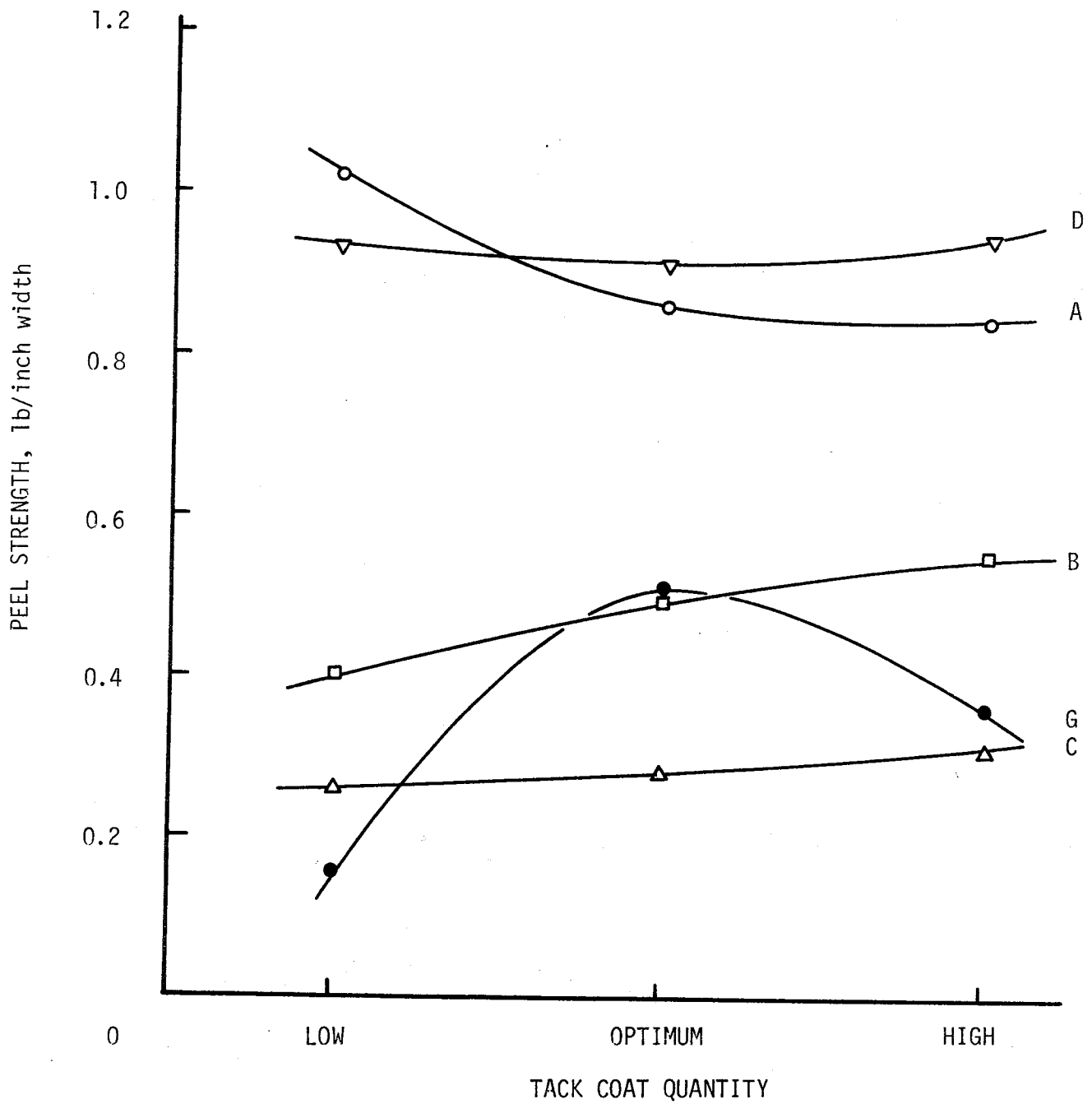


FIGURE 17. Peel Rate of Fabrics on Portland Cement Concrete at a Peel Rate of 20 inches/minute.

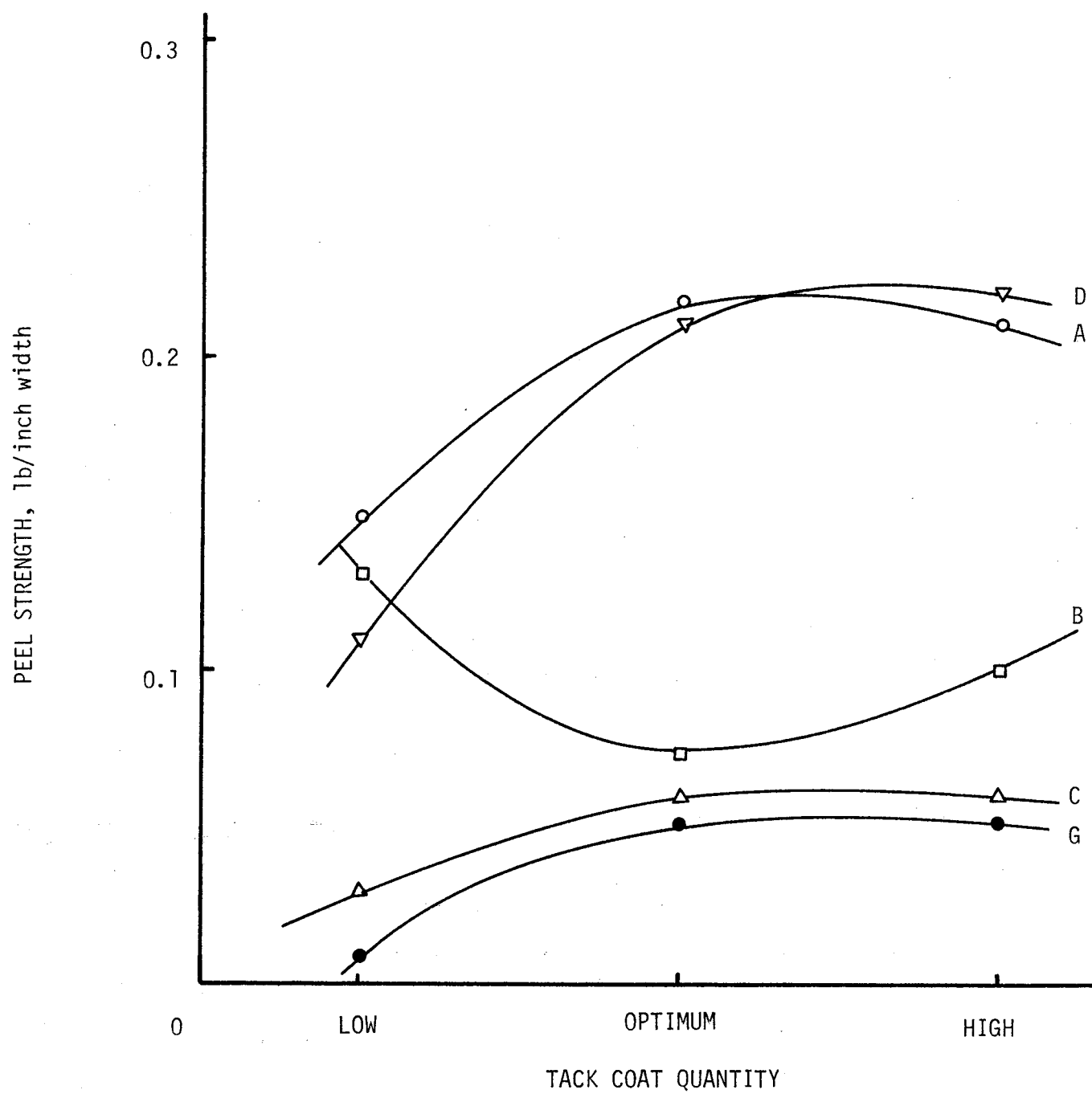


FIGURE 18. Peel Strength of Fabrics on Asphalt Concrete at a Peel Rate of 5 inches/minute @122°F (50°C).

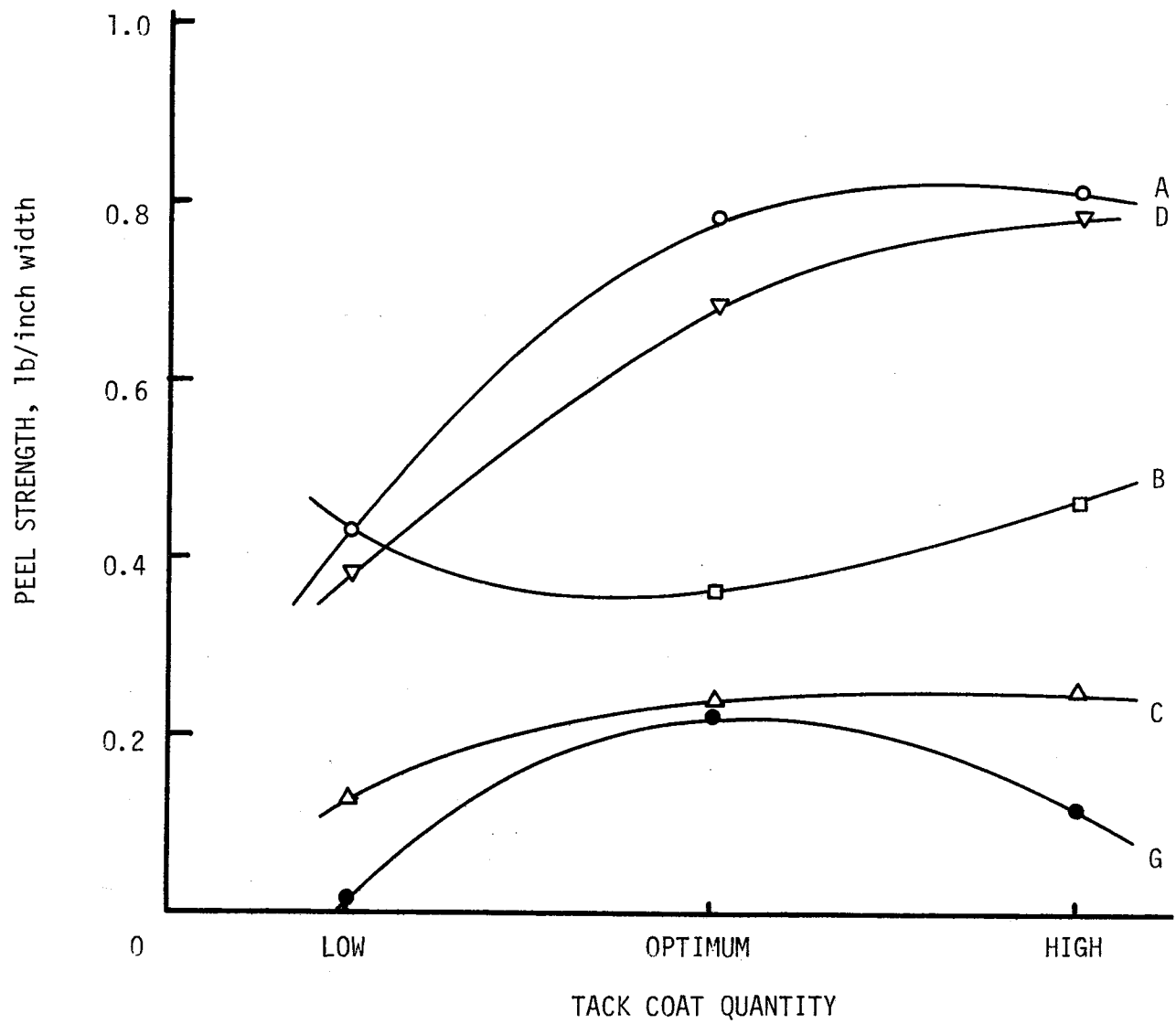


FIGURE 19. Peel Strength of Fabrics on Asphalt Concrete at a Peel Rate of 20 inches/minute.

field project construction performance needs to be established. As a minimum a peel strength of 0.01 lbs. per inch (0.00178 N/mm) of fabric width is recommended. The peel strength should be determined at the expected "old surface" pavement temperature, at optimum tack coat and preferable on a surface that duplicates as nearly as possible that pavement surface upon which the fabric is to be placed. It should be noted that the above criteria are meaningful only when tests are performed using the same testing techniques upon which the criteria is based.

Interface Shear Strength

Individual and mean values of interface shear strength for Fabrics A, D, E, F and G are presented in Appendix C. Figures 20 through 24 illustrate the influence of test temperature on shear strength. Figure 25 illustrates the effect of tack coat quantity on shear strength for the fabrics tested. Optimum tack coat was established by use of Equation 1. Low tack coat is one-half the optimum value while high tack coat is twice the optimum value.

Curves associated with Control-1 samples indicate strengths for typical old pavement-new overlay interfaces. Five hundredths of a gallon per square yard of AC-10 asphalt cement was used as the interface tack coat. Curves associated with Control-2 indicate mixture shear strength (i.e. no construction interface in the plane of shear). As expected the shear strength of the mixture is in excess of the interface shear strength. At the calculated optimum tack coat and low temperatures the shear strength of those samples without a fabric at the interface (Control-1) is usually in excess of those samples with fabric at this interface. At

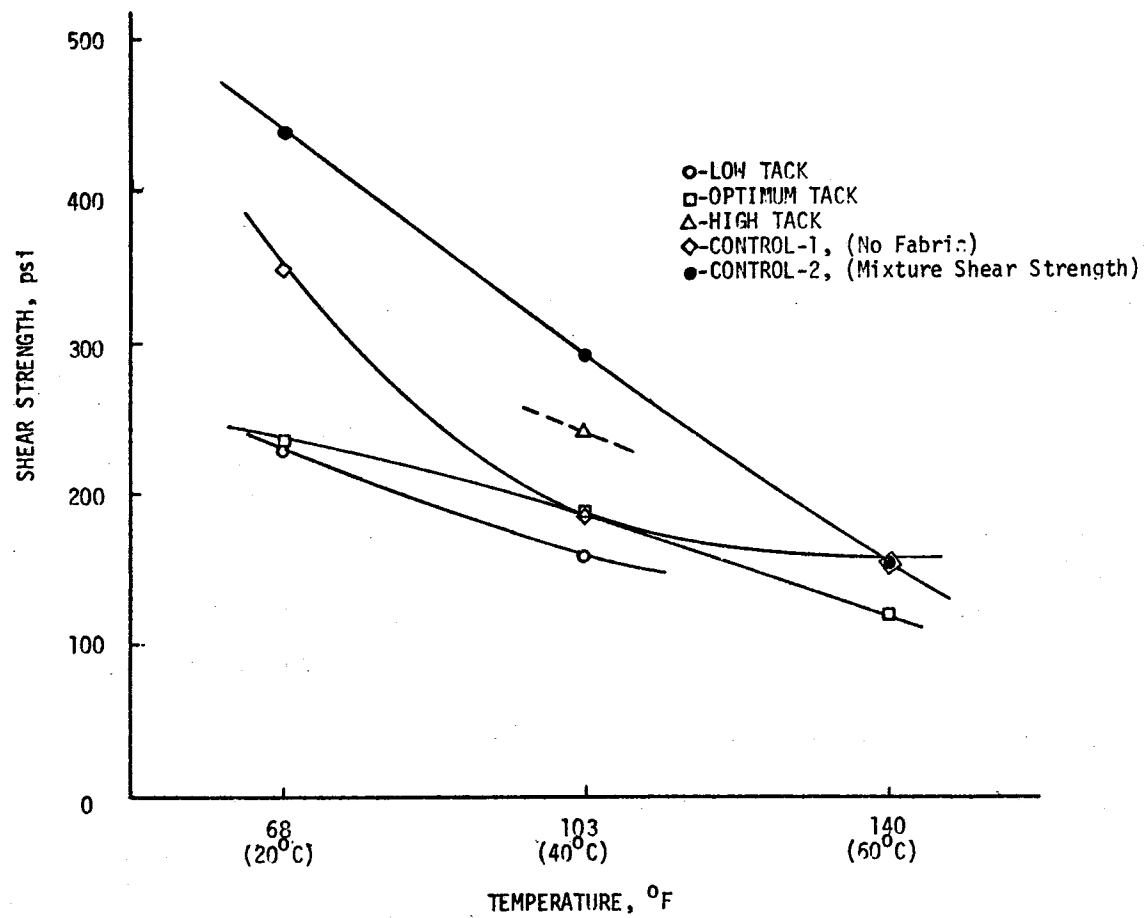


FIGURE 20. Overlay Shear Test Results with Mixtures using Fabric A.

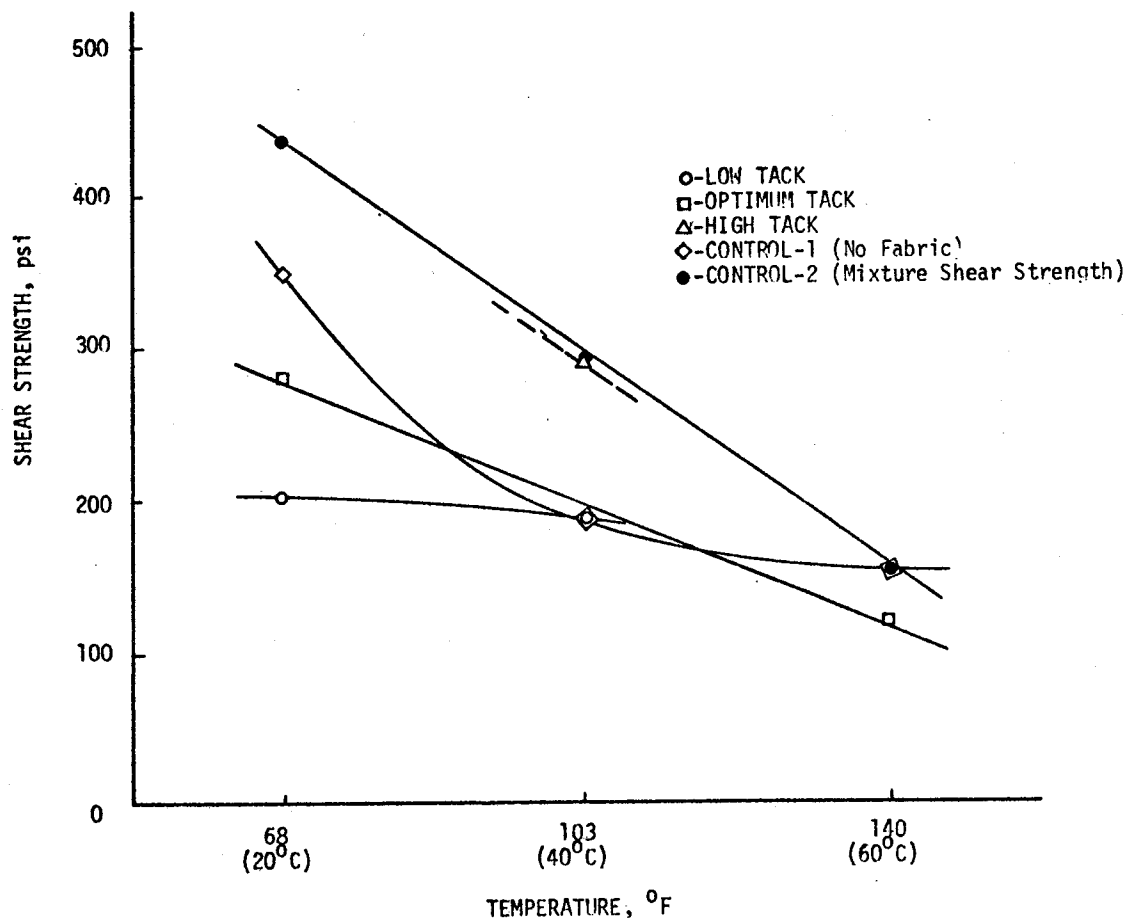


FIGURE 21. Overlay Shear Test Results with Mixtures using Fabric D.

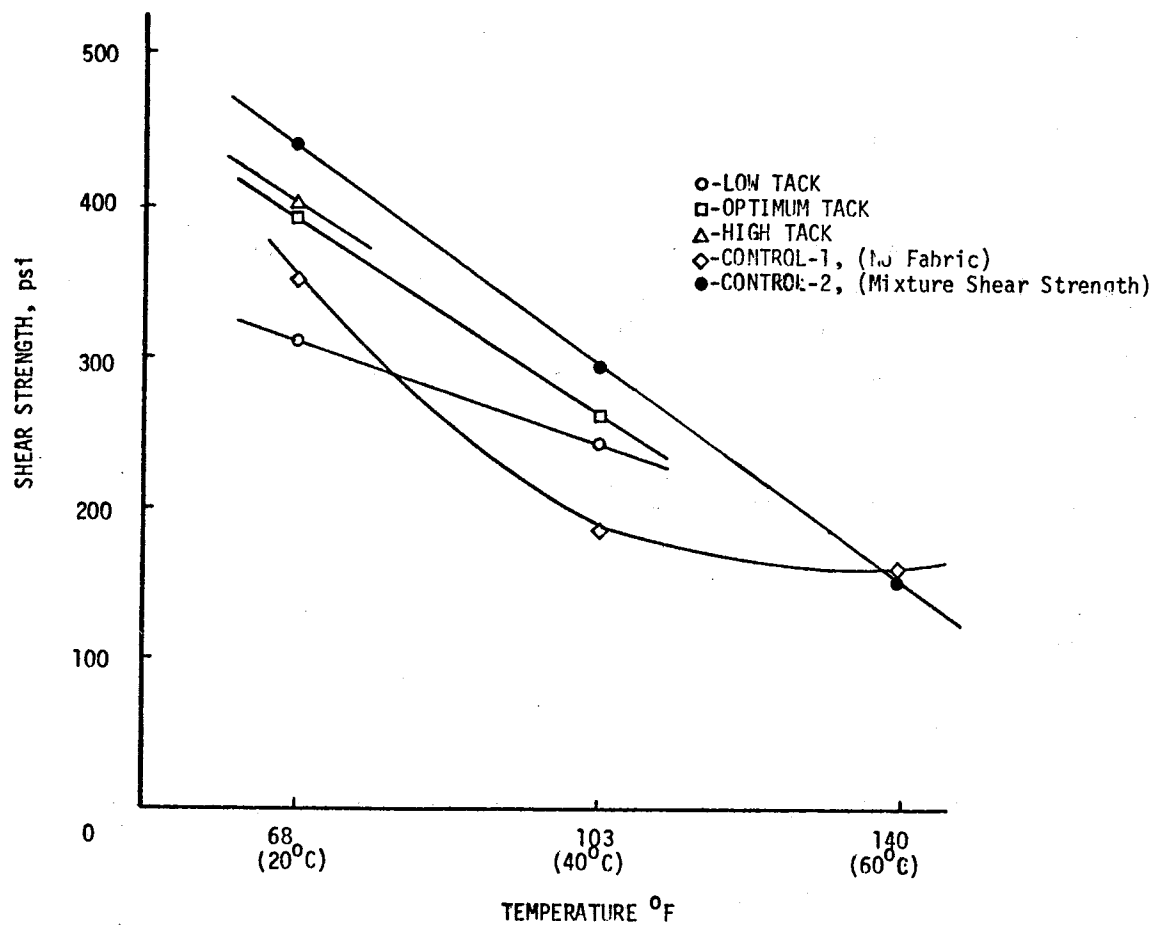


FIGURE 22. Overlay Shear Test Results with Mixtures using Fabric E.

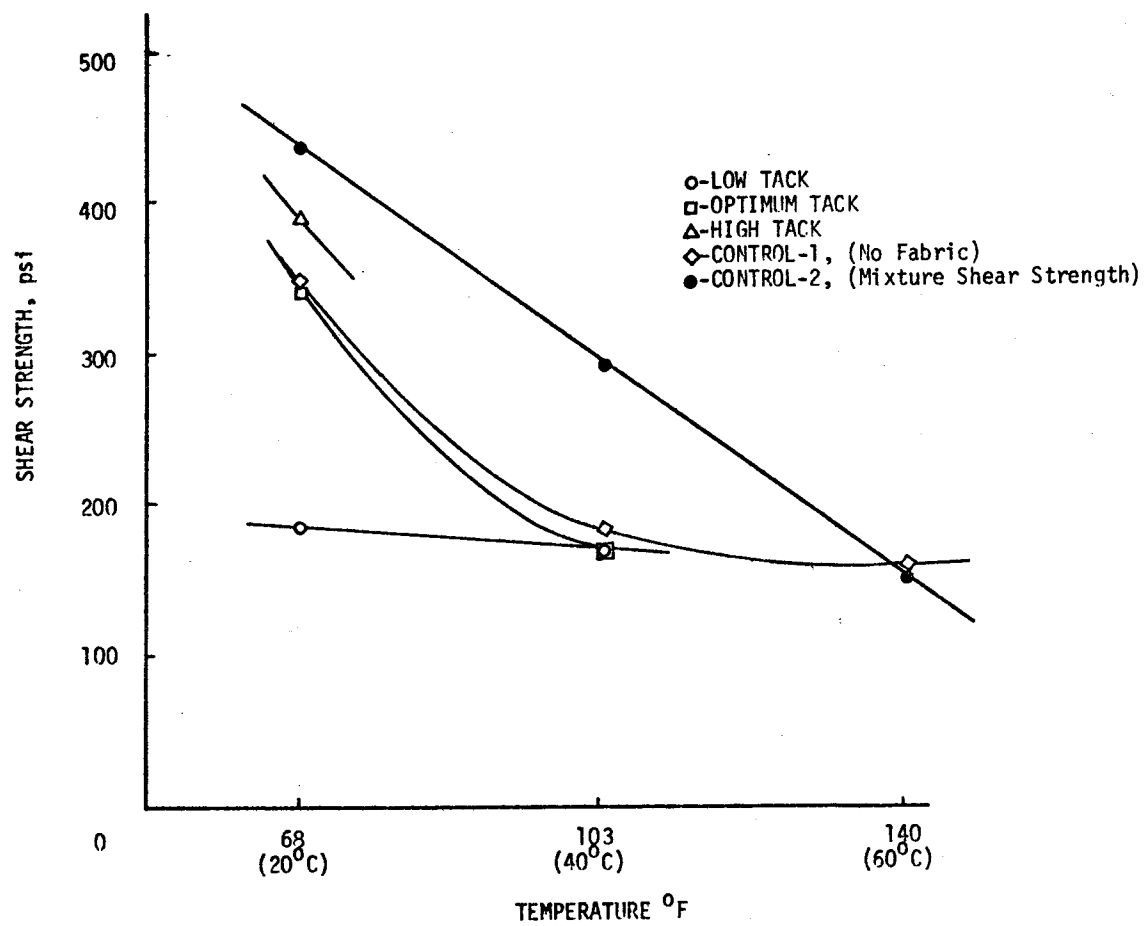


FIGURE 23. Overlay Shear Test Results with Mixtures using Fabric F.

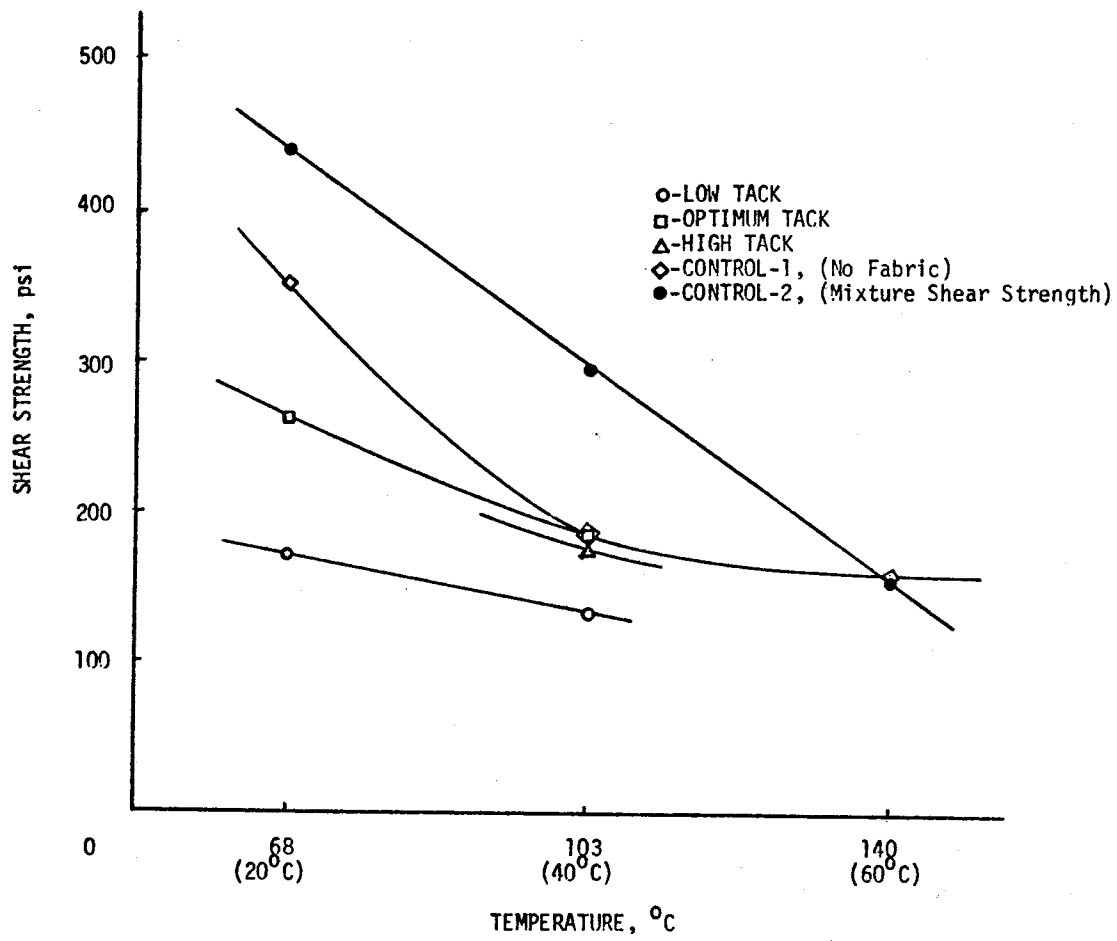


FIGURE 24. Overlay Shear Test Results with Mixtures using Fabric G.

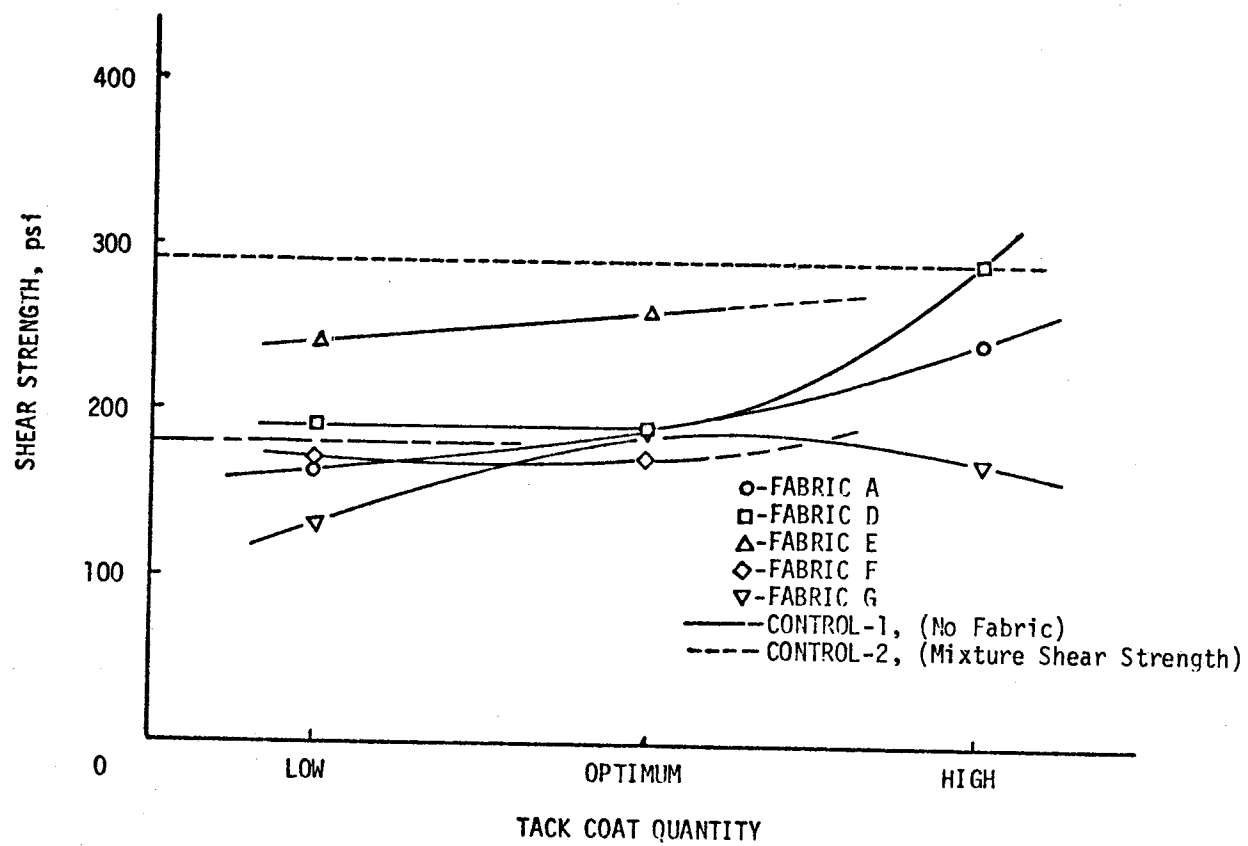


FIGURE 25. Shear Strength as a Function of Tack Coat Quantity at 103°F. (40°C)

the higher temperatures the shear strength of samples with fabric at the interface approaches the shear strength of those samples without fabric at the interface. Fabric E when placed at the interface actually increased the shear strength as compared to a no fabric interface.

Figure 25 indicates that the optimum tack coat based on maximizing shear strength is different from that indicated from Equation 1. Fabrics A and D illustrate increased shear strength with an increase in tack coat quantity. The dashed lines describing Fabrics E and F in Figure 25 are extrapolated based on data at 68°F (20°C).

The tack coat quantity called "high" was twice the optimum quantity and was without doubt more asphalt cement than should be used in an actual overlay operation. It was anticipated that the excess tack would act as a lubricant, especially above 100°F, and thus decrease the shear strength. Therefore, it was surprising when shear strength increased with increased tack coat for most of the fabrics.

The increase in shear strength with increased tack coat is probably due to additional asphalt which migrated into the mixture adjacent to the shear plane thus creating a more tenacious bond in the critical area. However, this may not always occur with certain fabrics especially at higher temperatures.

Shear strength with Fabric D is slightly higher than the other fabrics except Fabric E which is noticeably higher than Fabric D. It is noteworthy that Fabric D is somewhat thicker and "fuzzier" than the other fabrics, which were actually quite slick, and that Fabric E is even thicker and "fuzzier" than Fabric D. Therefore, it appears that shear strength is directly related to the bulk of a fabric which in turn are

related to the saturation level and surface friction of the fabric. This seems reasonable in that the "fuzz" could act as numerous little roots to provide reinforcement (interparticle friction) at the fabric interface and thus provide increased shear strength.

After the shear tests using Fabric A with low tack coat, it was observed that the fabric adhered to the lower portion of the specimen (where tack was applied). However, at optimum and high tack, the fabric randomly adhered to either the upper or lower portion of the specimen. (Figure C1, Appendix C). Apparently, the low permeability of the fabric prevented sufficient tack from migrating to the upper side of the fabric.

From a pavement performance standpoint, it is important to have sufficient shear strength at the interface between the old pavement and the new overlay to prevent slippage failures. The magnitude of the required shear strength is dependent upon the type of traffic, speed of traffic, temperature, severity of braking and wheel turning movements, and location of the interface within the pavement structure. At the present time an acceptable level of interface shear strength cannot be firmly established. A correlation between interfacial shear strength, mixture shear strength, mixture tensile strength, mixture compressive strength and pavement performance needs to be established.

As a general guide, it is desirable to have an interfacial shear strength of the same order of magnitude as that associated with conventionally constructed overlays (Control-1). Since shear strengths are low at elevated temperatures and hence critical, a reasonable desired value at 140°F (60°C) is about 150 psi (1.03 kPa). By adjusting tack coat quantity and/or grade, all fabrics can meet this interim criteria. It should be noted

that the above criteria are meaningful only when tests are performed using the same equipment and techniques upon which the criteria are based.

Conclusions. Based on the analysis of the shear tests within the scope of this study, the following conclusions are given:

1. Fabrics have less affect on the interfacial shear strength of an asphalt overlay at the higher temperatures where shear strength becomes critical.

2. Fabrics will decrease interfacial shear strength at lower temperatures where shear strength is more than adequate.

3. Fabrics will not compound slippage problems when properly installed to prevent reflection cracking in overlaid pavements.

4. Shear strength is directly related to surface texture and friction of fabrics and somewhat dependent on tack coat quantity.

5. The optimum tack coat quantity for maximum shear strength is generally higher than that described by Equation 1.

Flexural Fatigue

Peak stress, σ , initial bending strain (bending strain @ the 200th cycle), ϵ , initial stiffness modulus @ the 200th cycle), E , estimated total input energy, U_f , and estimated maximum energy density, U_d , were calculated for each fatigue test specimen in accordance with the formulae given in Appendix D. Table D2 gives the results of these calculations for individual specimens and Table 8 gives a statistical summary of those tests conducted at peak stress level of 100 psi.

Fifteen fatigue tests were conducted on the control beams to define the relationships between bending stress or initial bending strain and number of load applications to failure. These relationships including

TABLE 8. Simple Statistics of Flexural Fatigue Data.

Sample No.	Statistic	Specific Gravity, gm/cc	Air Voids, percent	Input Stress, psi	Bending Strain, in/in	Cycles to Failure*	Initial Stiffness Modulus, psi	Total Energy Input, lb-in	Max. Energy Density, ³ in-lb/in
Control**	Mean	2.38	4.2	105	.00074	6,400 (7,100***)	151,000	5,500	0.040
	Std. Dev.	0.005	0.15	12	.00026	----	36,000	5,700	0.018
	Coef. Var.	0.2	4	11	35	----	24	103	45
Fabric A (Low)	Mean	2.38	4.3	100	0.00130	3,100	80,000	4,800	0.0632
	Std. Dev.	0.007	0.25	0	0.0013	----	6,700	1,410	0.0054
	Coef. Var.	0.3	6	0	10	33	8	30	9
Fabric A (Optimum)	Mean	2.40	3.4	102	0.00064	9,200	177,000	7,200	0.0327
	Std. Dev.	0.0084	0.21	1.643	0.00020	----	69,400	3,030	0.0103
	Coef. Var.	0.4	6	2	32	82	39	42	31
Fabric A (High)	Mean	2.40	3.4	100	0.00130	4,900	78,000	7,800	0.0649
	Std. Dev.	0.0045	0.19	0	0.00127	----	7,500	1,720	0.00637
	Coef. Var.	0.2	6	0	10	31	10	23	10
Fabric D (Optimum)	Mean	2.36	5.3	102	0.00056	9,300	196,000	7,200	0.0288
	Std. Dev.	0.0336	1.33	1.414	0.00017	----	64,000	3,780	0.0087
	Coef. Var.	1	25	1	30	72	33	53	30
Fabric E** (Optimum)	Mean	2.39	3.8	102	0.00087	79,000	147,000	76,000	0.0475
	Std. Dev.	0.01	0.4	2.83	0.00062	----	102,000	33,000	0.0346
	Coef. Var.	0.4	9	3	72	62	70	43	73
Fabric F (Optimum)	Mean	2.37	4.6	101	0.00123	4,600	88,000	6,500	0.0547
	Std. Dev.	0.0058	0.4	1.2	0.00045	----	26,000	770	0.0115
	Coef. Var.	0.2	8	1	37	40	30	12	21
Fabric G (Low)	Mean	2.38	4.1	101	0.00077	7,400	133,000	7,600	0.0388
	Std. Dev.	0.0045	0.19	3.89	0.00009	----	16,300	4,031	0.0050
	Coef. Var.	0.2	5	4	12	61	12	53	13
Fabric G** (Optimum)	Mean	2.39	3.91	101	0.00081	8,600	134,000	9,600	0.0411
	Std. Dev.	0.0096	0.342	2.4	0.10016	----	25,000	5,800	0.0082
	Coef. Var.	0.4	9	2	20	73	19	60	20
Fabric G (High)	Mean	2.39	3.60	99	0.00064	16,200	133,000	7,600	9.028
	Std. Dev.	0.0055	0.10	1.342	0.00012	----	16,300	4,037	0.0119
	Coef. Var.	0.2	3	1	18	25	12	53	50

*Log mean

**Only those specimens tested at a stress near 100 psi are included in the mean

***Value computed from $\sigma-N_f$ regression equation

regression equations and correlation coefficients are given in Figures 26 and 27. The correlation coefficients greater than 0.80 should be considered quite good for fatigue tests of this type.

One of the fabrics (Fabric G with optimum asphalt tack) was selected to conduct a similar series of 15 fatigue tests. The plotted results with regression equations and correlation coefficients are given in Figures 28 and 29. Dashed lines on these figures represent the locus of the regression equations for the control specimens. Observation of Figures 28 and 29 indicates superior fatigue characteristics of the specimens containing Fabric G. That is, at a given bending stress or strain the control beam would fail in fewer load applications than the beam containing Fabric G (see examples in Figures 28 and 29).

Fabrics A, D, E and F were tested at a single stress level of approximately 100 psi. Optimum tack coats were used to fabricate the samples for testing. Plots of strain as a function of fatigue life are presented in Appendix D (Figures D1 through D5).

Figure 30 shows the mean number of load applications to failure for those specimens tested at 100 psi. Generally, the test results indicate certain fabrics with appropriate tack coats implanted within a flexural fatigue specimen in the region of tensile stress will improve fatigue life. The total input energy required to produce failure in these test beams shows a similar trend (Figure D7).

A comparison of Figures 30 and 31 shows specimen stiffness is affected by the fabrics and tack coats in a manner similar to fatigue life, that is, increased specimen stiffness produces a corresponding increase in number of applications to failure. This admittedly weak

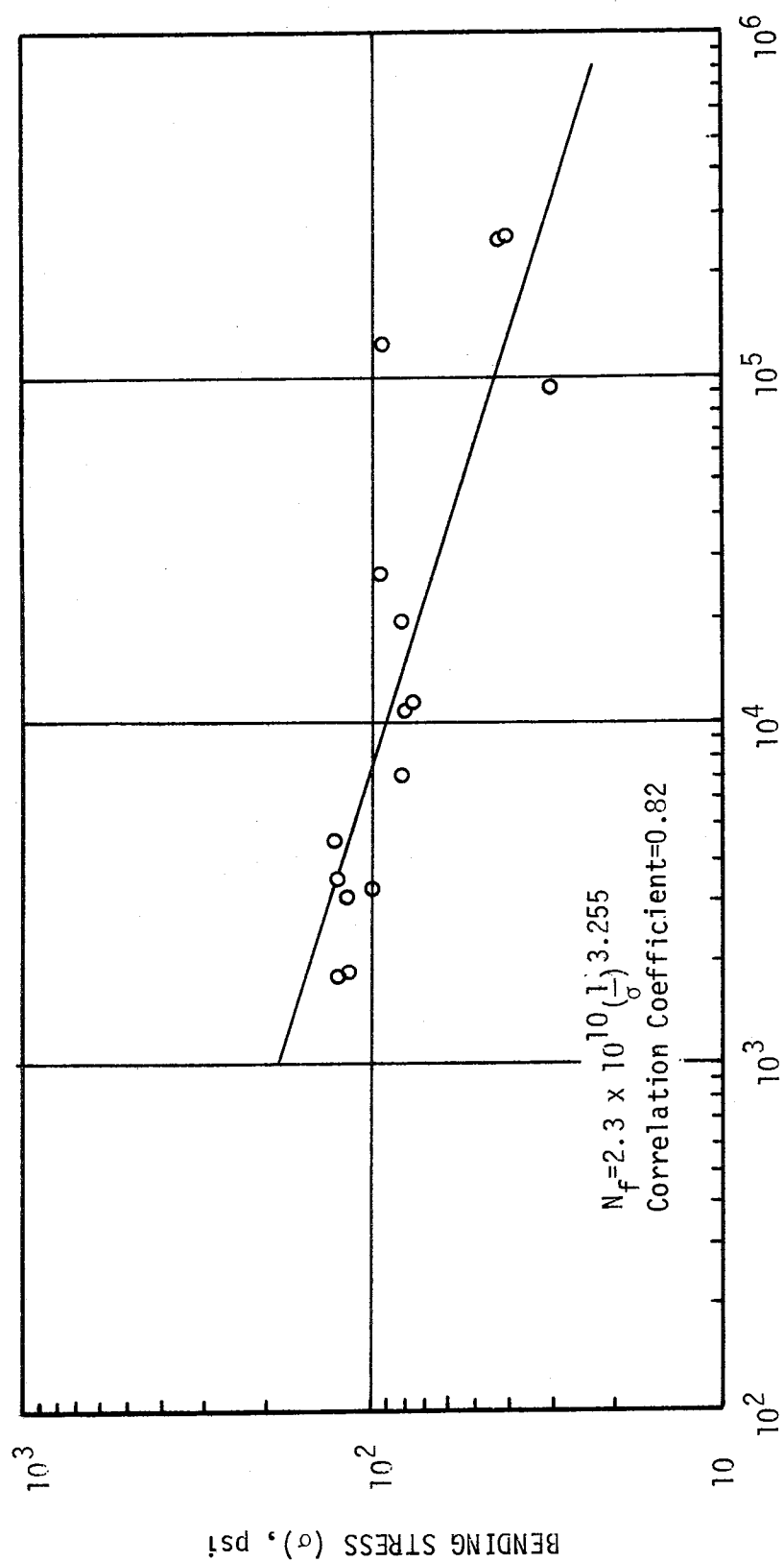


FIGURE 26. Stress versus Load Applications to Failure for Control Specimens.

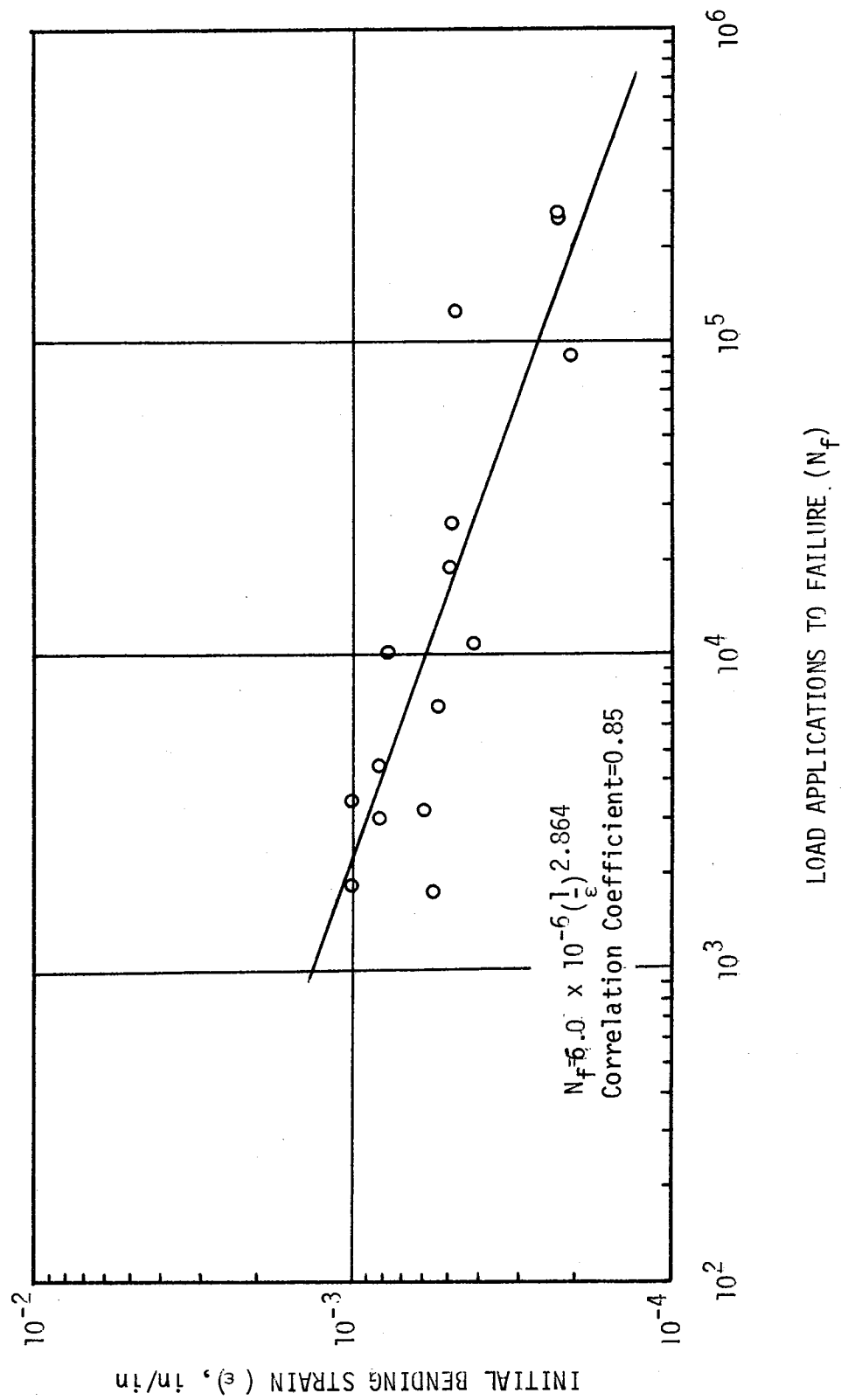


FIGURE 27. Strain versus Load Applications to Failure for Control Specimens.

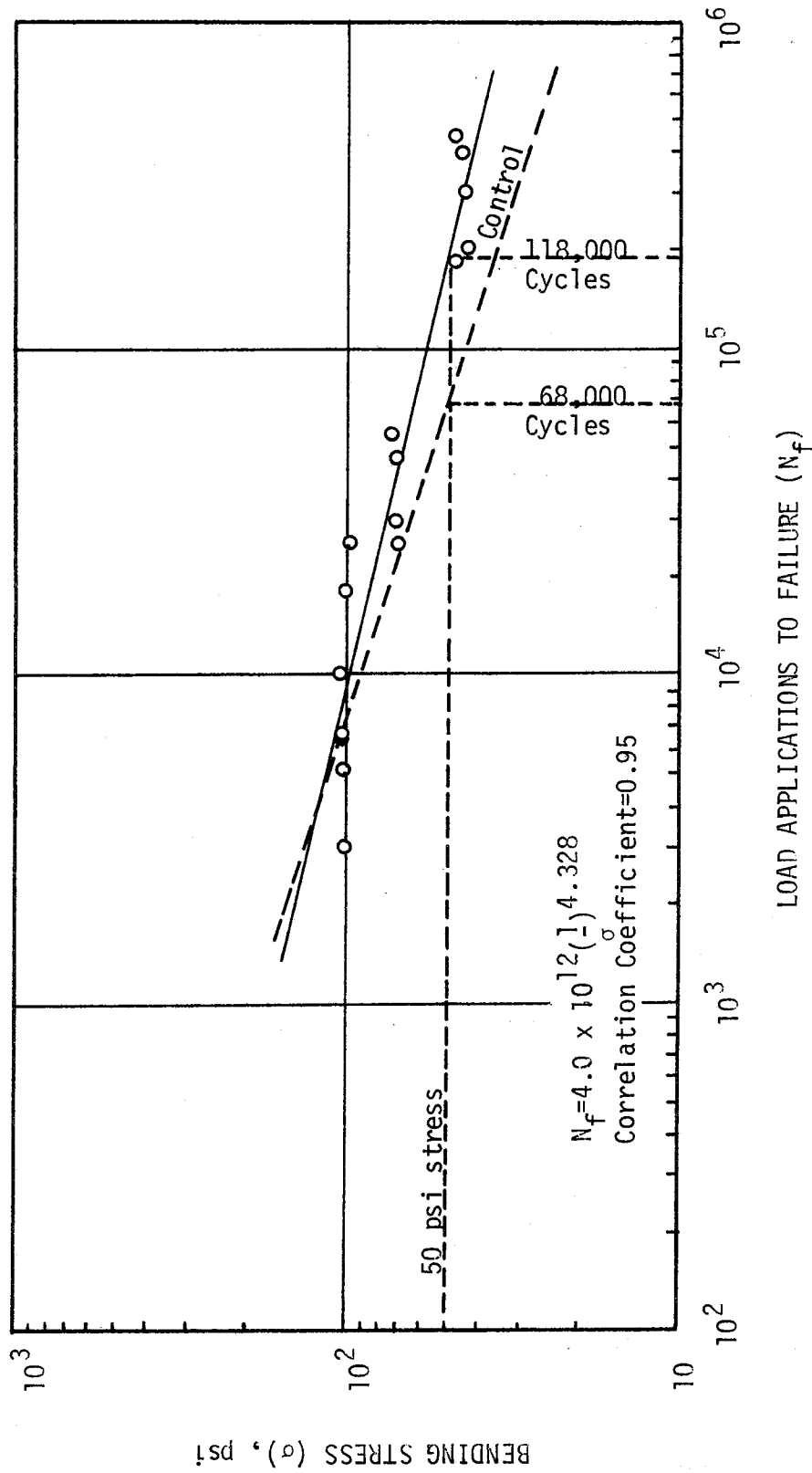


FIGURE 28. Stress versus Load Applications to Failure for Specimens Containing Fabric G at Optimum Asphalt Content.

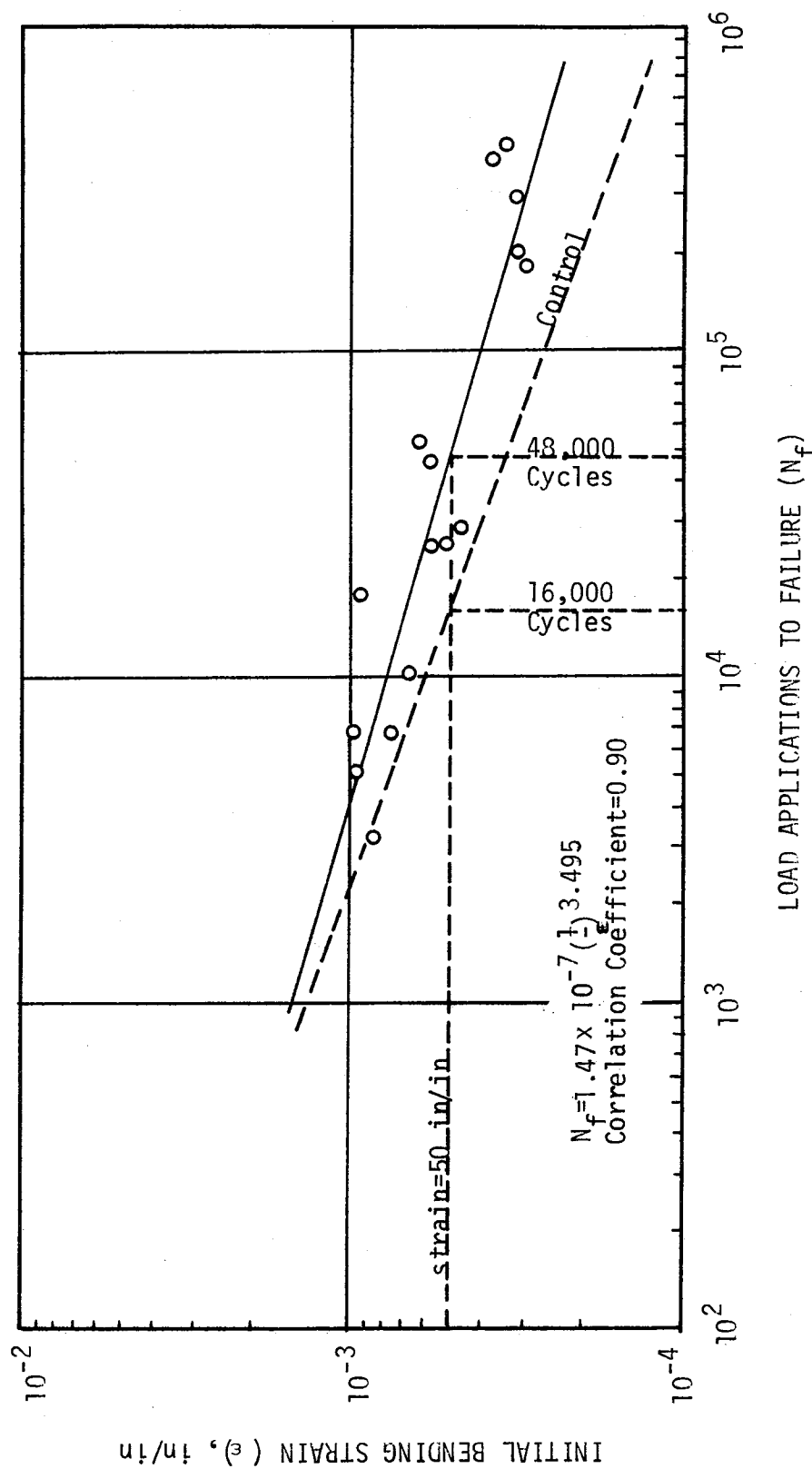


FIGURE 29. Strain versus Load Applications to Failure for Specimens Containing Fabric G at Optimum Asphalt Content.

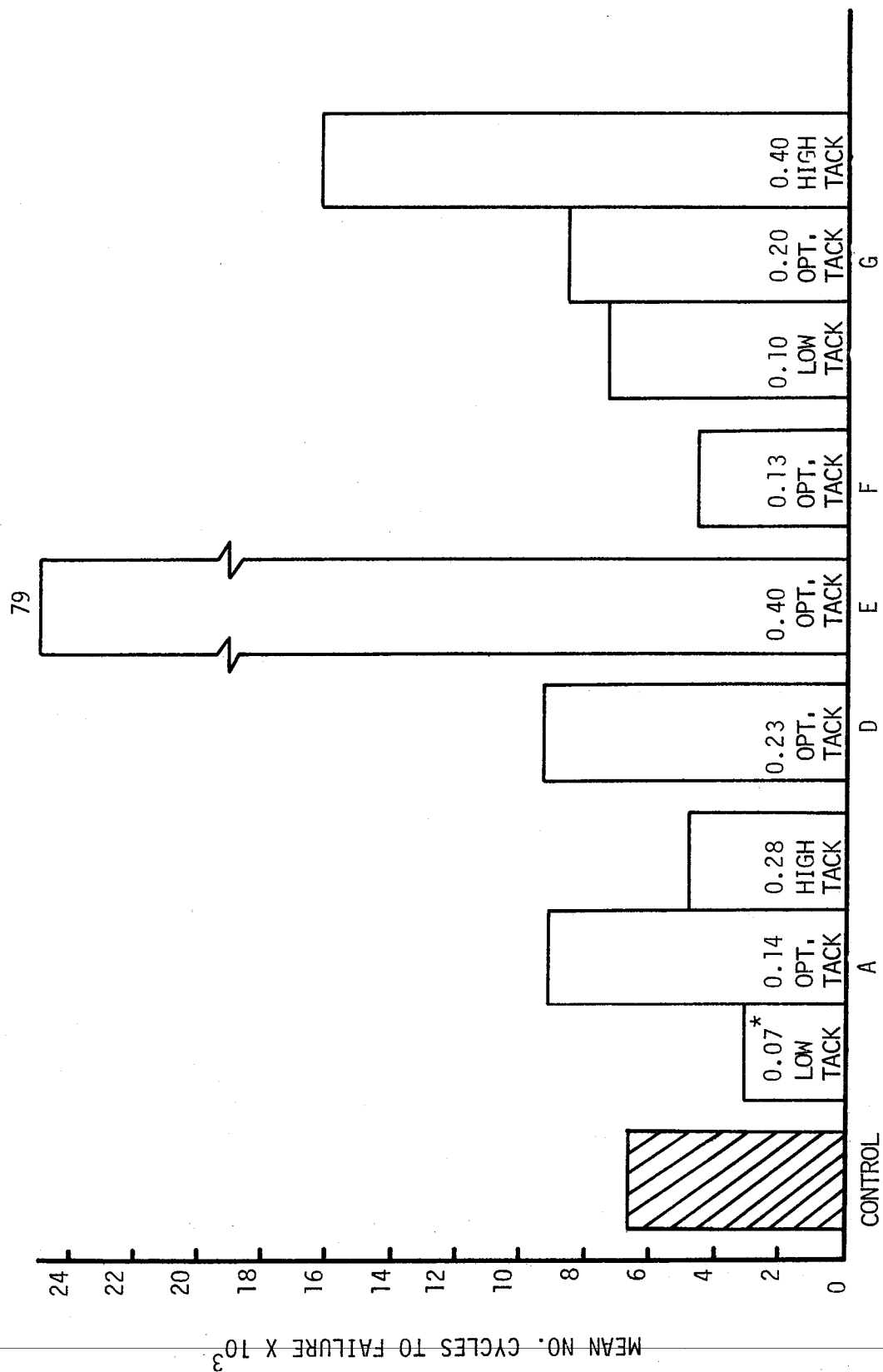


FIGURE 30. Mean No. of Load Cycles to Failure from Flexural Fatigue Test.
(Only those specimens tested at or near 100 psi)

*Tack quantities given have units of gallon per square yard.

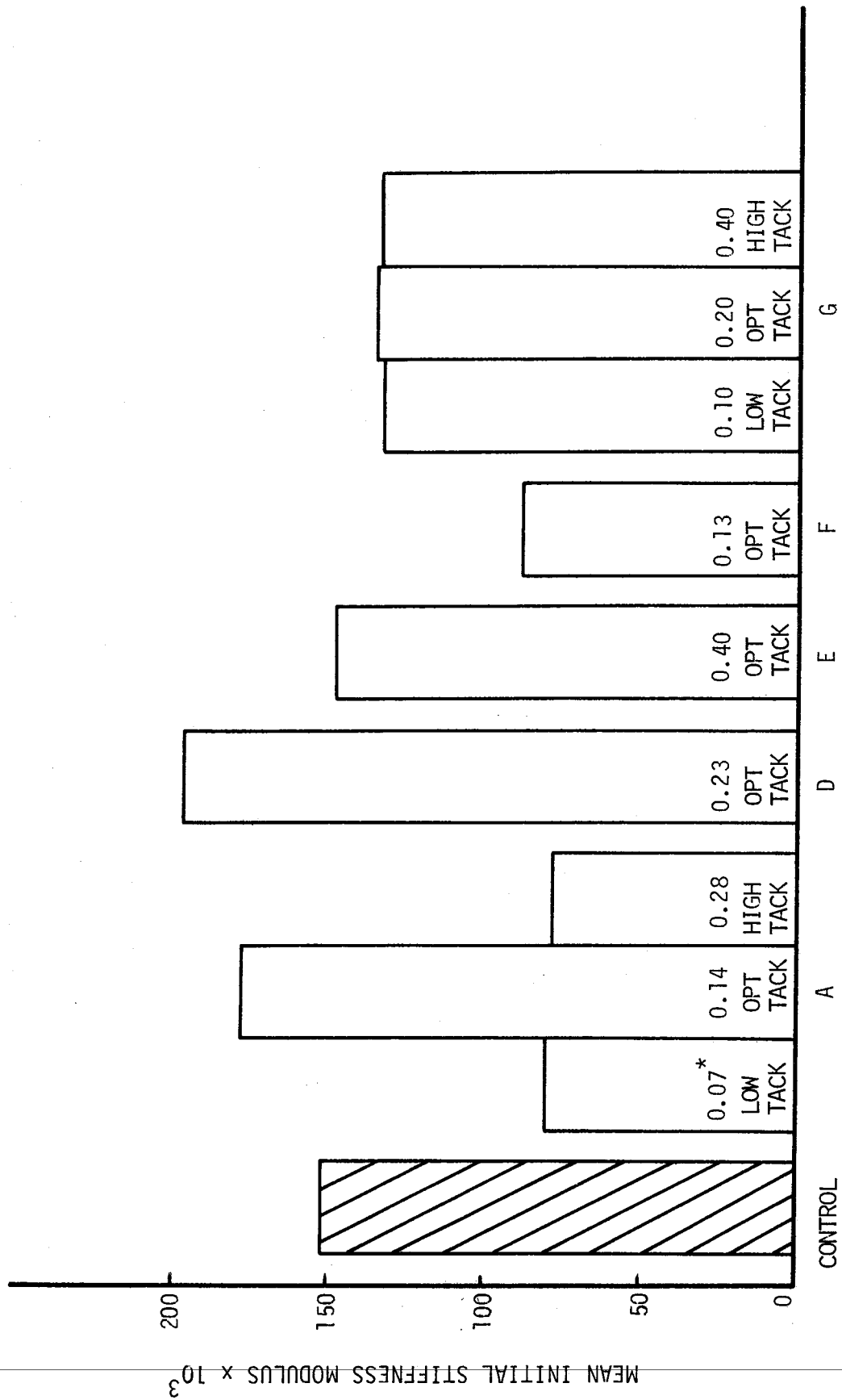


FIGURE 31. Initial Stiffness Modulus (200th Cycle) From Flexural Fatigue Test

*Tack quantities given have units of gallon per square yard.

trend is illustrated in Figure 32. These results are in agreement with earlier studies of fatigue life of asphalt paving mixtures (9, 10).

Fabrics A and F are thin, slick fabrics not capable of retaining an appreciable quantity of asphalt cement. From an asphalt tack coat cost standpoint this is a desirable fabric characteristic; however, from a fatigue life standpoint there are definite advantages with fabrics capable of holding more asphalt (Figure 32 and D7). Fabric A is shown to be quite sensitive to tack coat quantity. Insufficient asphalt at the upper surface of this low porosity fabric probably did not provide an adequate bond (side opposite tack coat application), whereas, excessive asphalt may have over-lubricated the slick fabric thus allowing slippage at the fabric layer and in turn excessive strain within the specimen, or that is, decreasing specimen stiffness. Improved fatigue performance of Fabric G samples was achieved with increased tack coat quantities.

There appeared to be some relationship between fatigue characteristics of a specimen and the fabric's ability to hold asphalt as well as the fabric's surface texture. That is, those "fuzzier" fabrics with a higher asphalt demand demonstrated superior fatigue performance during laboratory testing. Evidence to support this statement is given in Figure 33. For example, specimens made with Fabric E, a thick, fuzzy fabric with the ability to retain a considerable quantity of asphalt, exhibited significantly longer fatigue lives than any of the other specimens (Figures 30 and D7). Note, however, that stiffness of the specimens was not appreciably affected by Fabric E (Figure 31). It

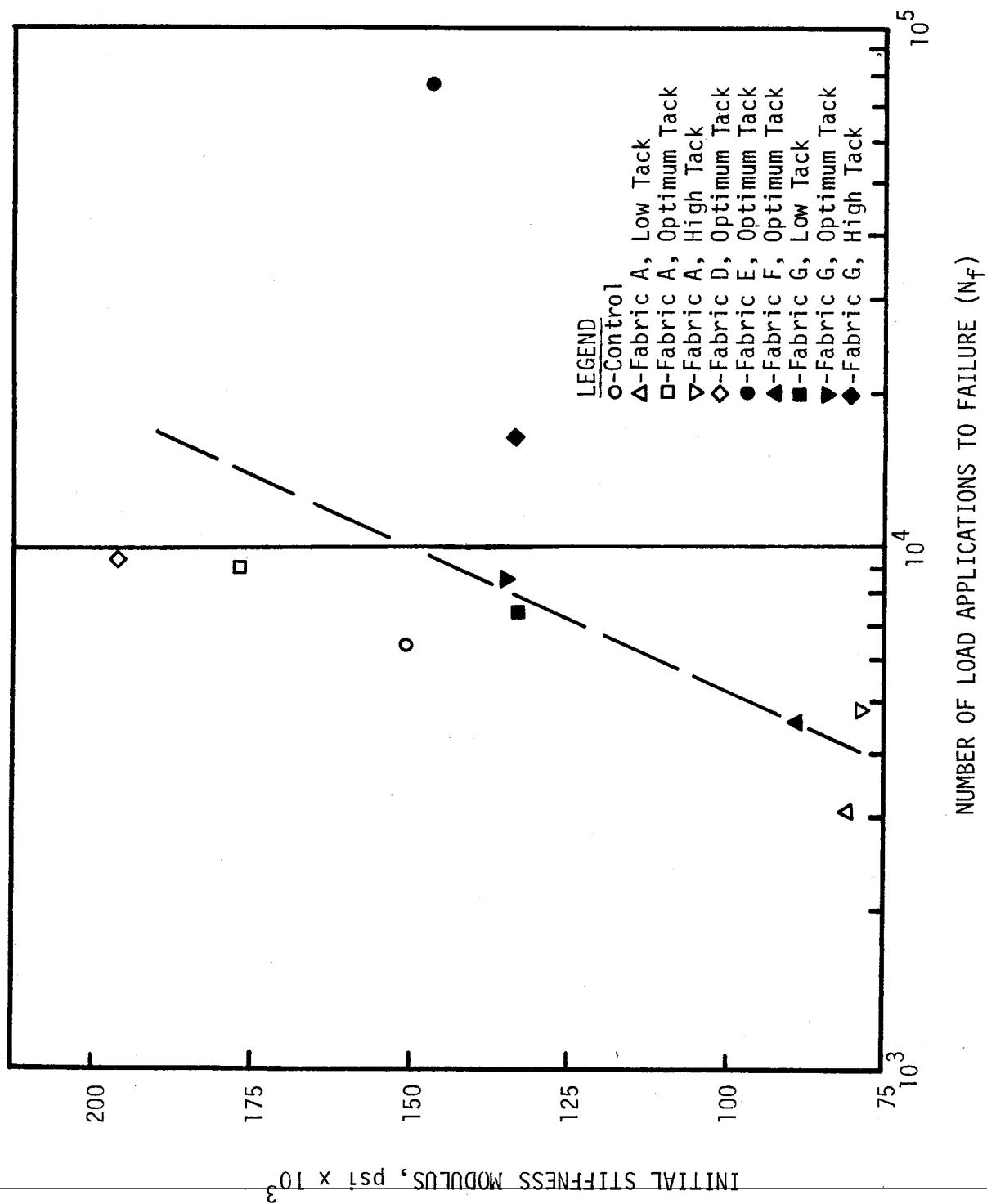


FIGURE 32. Relationship Between Specimen Stiffness Modulus and Number of Load Applications to Failure.

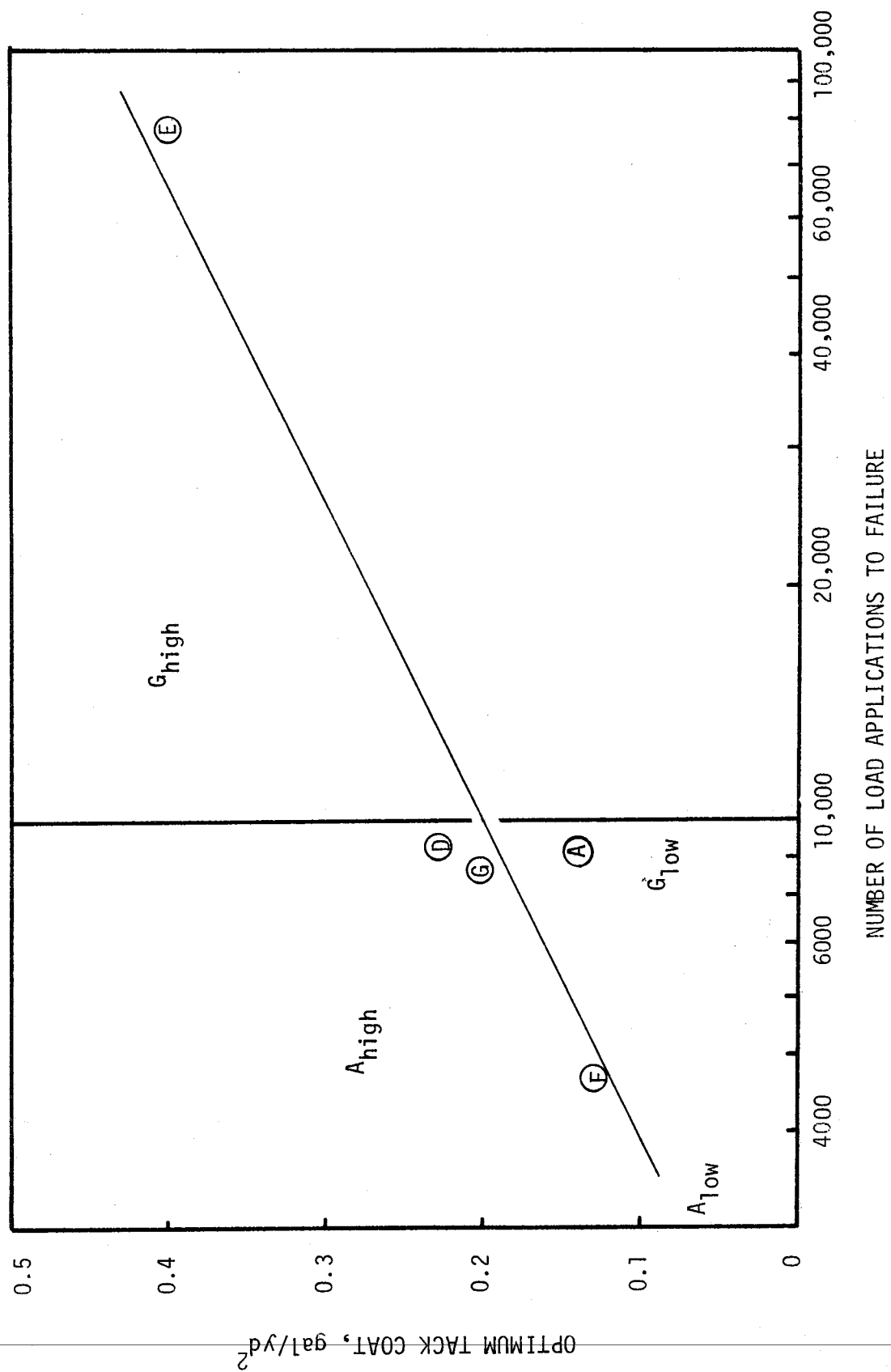


FIGURE 33. Relationship Between Optimum Tack Coat and Number of Cycles to Failure - Flexural Fatigue.

is surmised that the comparatively thick asphalt impregnated layer offset the stiffening effects one might otherwise expect from the fabric. However, more data would be necessary to sustain this argument.

It should be noted that increased fatigue performance, especially at high asphalt tack rates, may be attributed in part to the excess asphalt which migrated into the hot asphalt mixture as a result of the kneading action during compaction. The additional asphalt cement would decrease air voids in the critical region of the specimen and thus enhance fatigue performance (10). In order to dispel this notion, it would be desirable to fatigue-test specimens with interlayers containing asphalt tack coat but no fabric.

Conclusions. From the foregoing results on flexural fatigue tests, the following conclusions appear warranted:

1. Certain fabrics with appropriate tack coats will improve fatigue performance of asphalt paving mixtures.
2. Thin fabrics are more sensitive to asphalt tack application rate.
3. Thick fabrics hold more asphalt which enhances their ability as a stress relieving interlayer (11) as well as a waterproofing membrane.
4. Fabrics with fuzzy surfaces and the appropriate tack coat appear to give the best fatigue performance.
5. Fatigue performance is directly related to the amount of tack coat.
6. Fabrics remain intact after complete rupture of the asphalt concrete specimens.

Resistance to Thermal Reflection Cracking

Table 9 gives air void contents and number of load cycles to

TABLE 9. Results from "Overlay" Test Specimens

FABRIC	SAMPLE NO.	AIR VOIDS PERCENT	MEAN AIR VOIDS PERCENT	NO. CYCLES TO FAILURE	MEAN NO. CYCLES TO FAILURE
NO FABRIC (CONTROL)	CT-1	3.8	3.7	48	40
	CT-2	3.8		42	
	CT-3	3.5		30	
A (OPT TACK)	A-1	5.0	4.8	69	216
	A-2	4.6		363	
D (OPT TACK)	D-6	3.7	4.4	693	559
	D-7	4.5		495	
	D-8	4.0		585	
	D-9	5.3		500	
	D-10	4.5		523	
E (OPT TACK)	E-4	3.8	4.4	200	225
	E-5	4.5		130	
	E-6	5.0		346	
F (OPT TACK)	F-4	4.9	4.9	116	120
	F-5	4.9		134	
	F-6	5.0		110	
G (LOW TACK)	G-1	4.4	4.5	200	277
	G-2	4.4		325	
	G-3	4.8		305	
G (OPT TACK)	G-4	4.6	4.5	300	335
	G-5	4.5		355	
	G-6	4.5		350	
G (HIGH TACK)	G-7	5.0	4.2	1350	1164
	G-8	4.0		838	
	G-9	3.6		1350	
(OPT TACK) G* (OLDER SPECIMENS)	G-11	3.7	3.8	500	756
	G-12	3.8		900	
	G-13	3.8		742	
	G-14	3.9		1350	
	G-15	3.9		288	
H (OPT TACK)	H-1	3.9	4.1	664	465
	H-2	4.3		265	

failure for individual reflection cracking test specimens, as well as average values. Figures E1 through E10 show crack height as a function of number of load cycles. (Due to scheduling changes resulting from equipment modifications, the specimens labeled G* were aged about one year at 35°F (2°C) prior to testing).

All the fabrics greatly enhance reflection cracking performance of asphalt concrete in this mode of testing. A histogram of the mean number of cycles to failure (Figure 34) indicates that relative performance appears to be proportional to tack coat quantity. This demonstrates the stress-relieving ability of the thicker asphalt layer, however, it may be at least partly a result of migration of excess asphalt into the voids within the adjacent asphalt concrete during compaction which would improve tensile properties of the asphalt concrete. Although the data are scant, evidence to support this statement (Figure 35) shows increasing number of cycles to failure with decreasing air voids. Having anticipated these effects, the specimen air void content was controlled to range between 4 and 5 percent for the new specimens containing fabric, which was thought to be reasonable. In order to separate the effects of the asphalt tack and the fabrics it would be desirable to conduct similar tests with specimens containing an interface with various quantities of tack coat but no fabric.

Figures 36 and 37 show approximate peak loads as a function of number of load cycles. These curves are based on average values of peak load from each type of specimen tested. Those specimens containing fabric exhibit about six times more cycles to failure than the control specimens which contained no fabric. At the point of failure, as

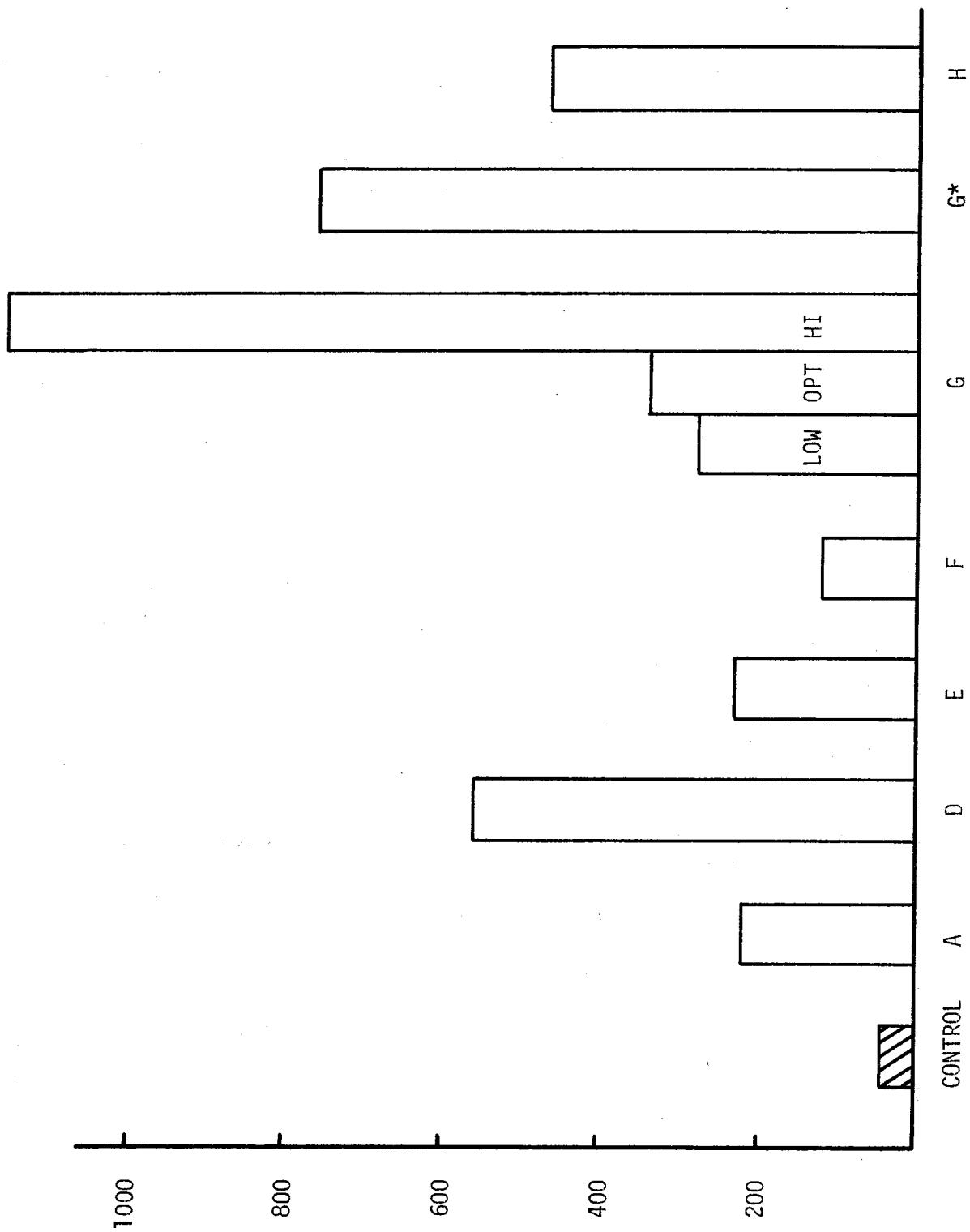


FIGURE 34. Mean Number of Cycles to Failure from Overlay Tests.
(Specimens **about** one year older than all others.)

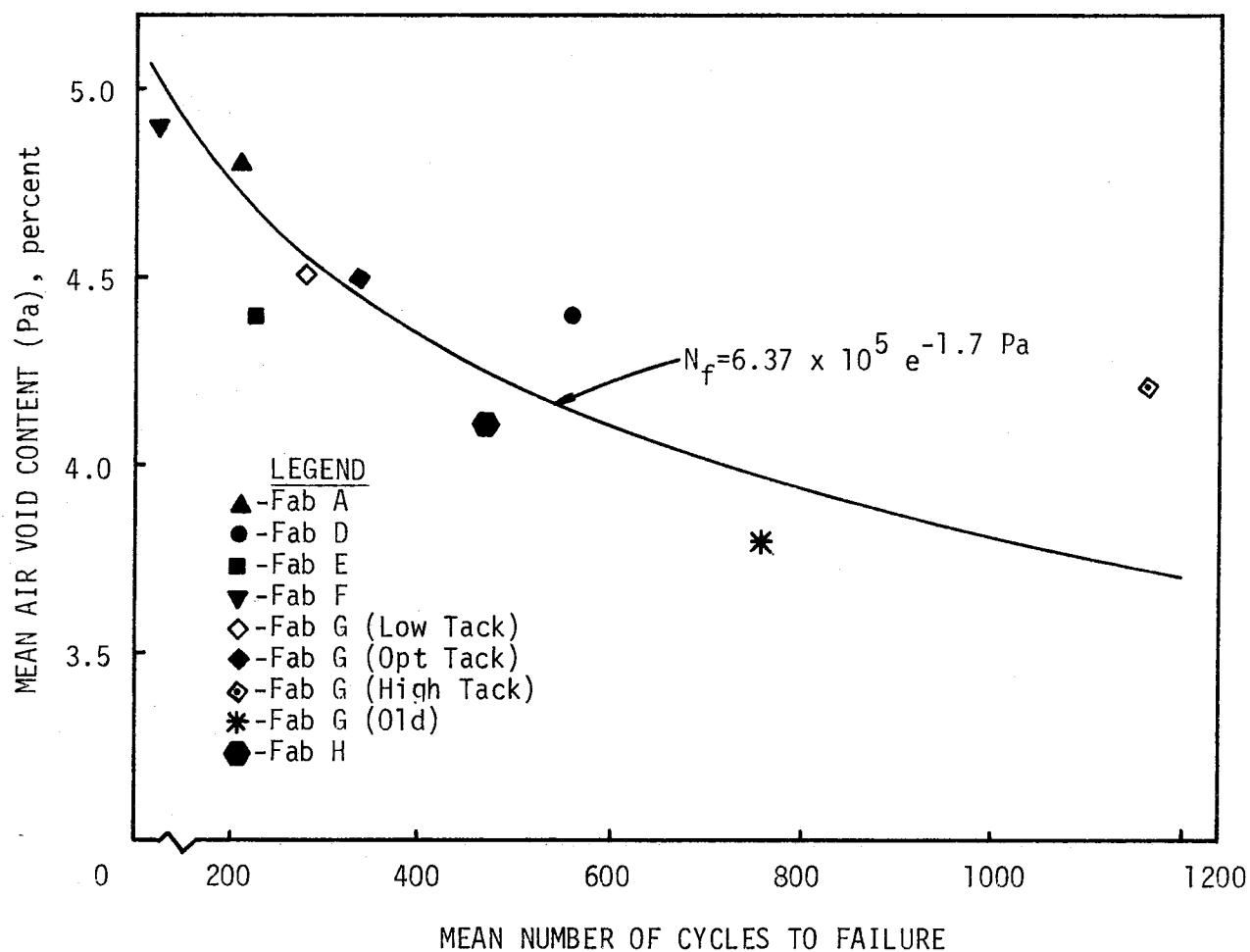


FIGURE 35. Effects of Air Void Content on Overlay Life.

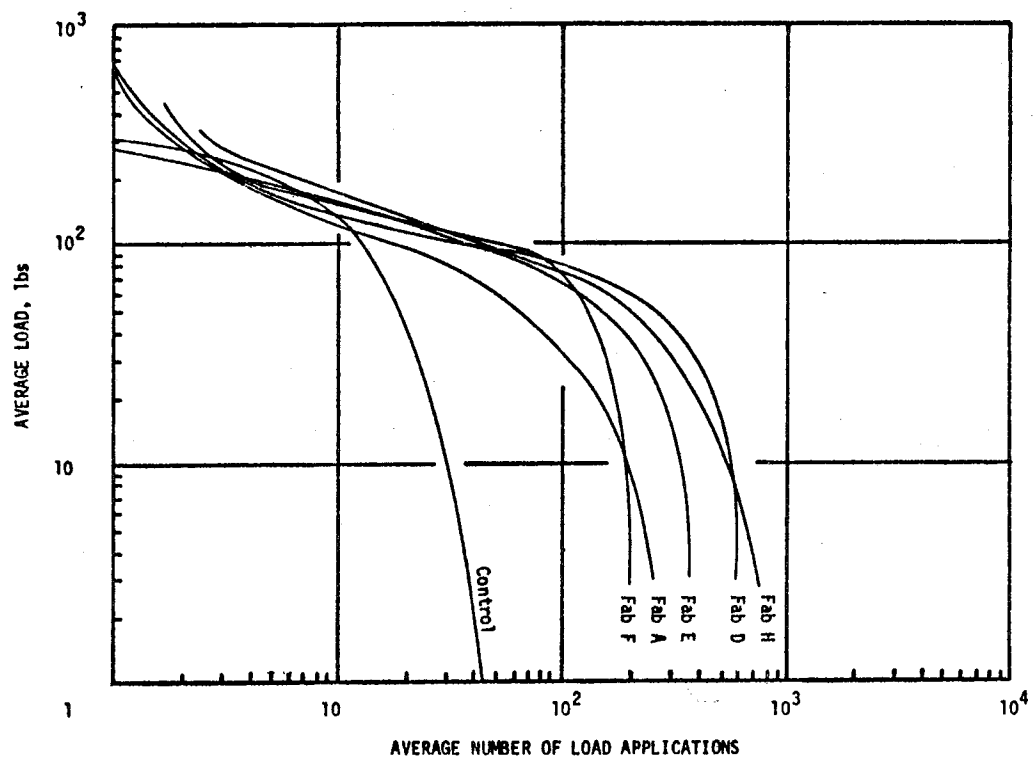


FIGURE 36. Peak Load Supported by Specimens Containing Different Fabrics.

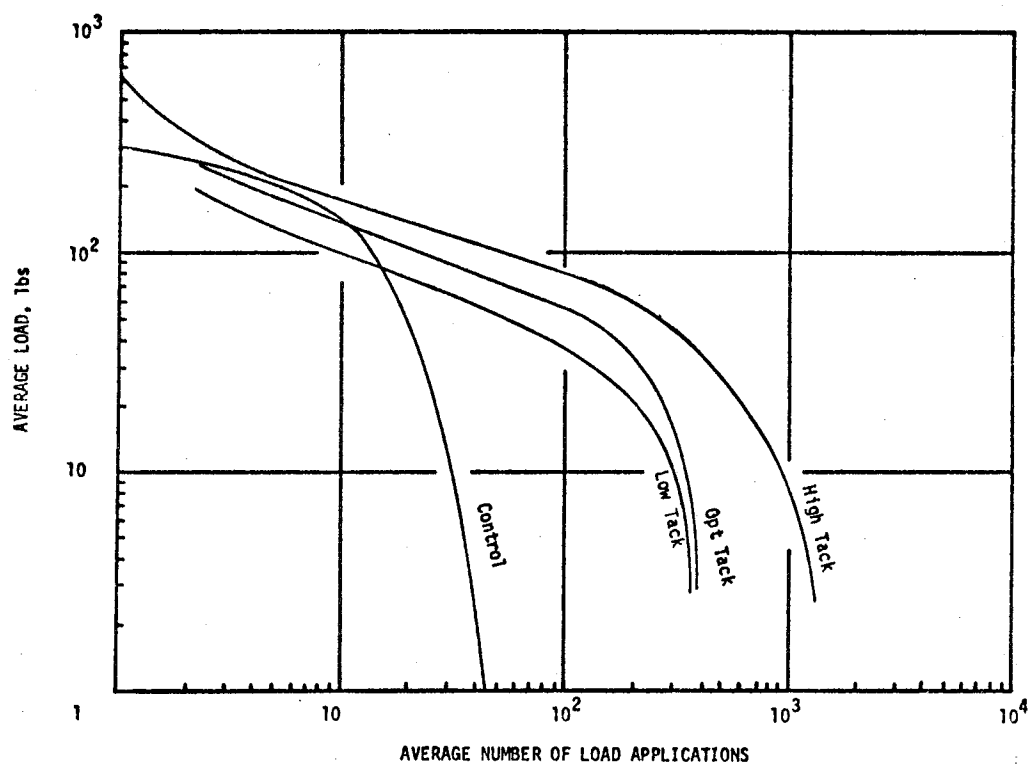


FIGURE 37. Peak Load Supported by Specimens Containing Fabric G.

described earlier, the fabrics remained intact and even supported a small load (typically, 5 to 10 lbs. or 22 to 44 N). Under these test conditions the fabrics probably would have remained intact indefinitely. Figure 37 illustrates the benefits of increasing the quantity of tack coat used with Fabric G. Changing tack coat quantity with Fabric G exhibits as much variation in specimen life as changing fabrics.

A comparison of fabric properties (Table 4) with the number of load applications to failure does not reveal any noteworthy correlations. Additional testing at low stress conditions will have to be performed on a variety of variants prior to establishment of a meaningful correlation. Techniques useful in establishing this correlation have been developed and appear in Appendix F.

Conclusions. This experimental technique, employing cyclic constant displacement tensile loading, which stimulates the action responsible for thermal reflective cracking, demonstrates several important features of fabrics when applied to retard reflective cracking in asphalt concrete overlays:

1. Fabrics retard reflective cracking in asphalt concrete.
2. Fabrics do not support a significant load once the asphalt concrete is completely ruptured.
3. Fabrics remain intact after asphalt concrete fails in tension; asphalt soaked fabric would, therefore, retard intrusion of moisture.
4. High tack coat rates improve the fabrics ability to retard reflective cracks; tack coat design should, however, be approached with caution.

Direct Tension Tests

Ultimate tensile stress and strain with initial tangent modulus and secant modulus are given in Table G1, Appendix G. A statistical summary of this data is presented in Table 10.

Air void content can have considerable effects on the tensile properties of asphaltic concrete. In an attempt to produce specimens with a narrow range in air voids, identical compaction procedures were followed in the preparation of all specimens. The control specimens and those containing fabric with the optimum tack coat were fabricated and tested about six months earlier than the remainder of the specimens. The second group of test specimens fabricated and tested contained significantly lower air voids than the first group (Table G2). Values of stress and strain at failure have been plotted as a function of air void content and a linear regression equation was determined for each (Figures G1 and G2). This linear relationship was used to "normalize" the stress and strain data or, that is, determine the value of stress or strain that would have been obtained if all specimens contained a similar quantity of air voids. Histograms showing the normalized values of stress and strain in Figures 38 and 39.

Figure 38 indicates that tensile strength of asphalt concrete can be improved by the installation of fabric and appropriate quantities of asphalt tack. As expected, the tensile strength is dependent upon the quantity of tack coat as well as the type of fabrics. Optimum tack coat quantities for maximizing tensile strength may not be identical to that required for peel strength, fatigue, crack resistance, etc.

TABLE 10. Statistical Summary of Direct Tension Test Results.

Fabric	Statistic	Tensile Strength, psi,			Failure Strain, (ϵ), in/in x 10 ⁻⁶ ($\mu\epsilon$)			Secant Modulus (E), psi x 10 ³			Initial Modulus (E _i), psi x 10 ³		
		Low	Opt	High	Low	Opt	High	Low	Opt	High	Low	Opt	High
A	Mean	72	97	127	5100	5000	8100	16.0	19.7	16.7	169	300	193
	Std Dev	14	17	15	2200	900	1700	6.9	2.9	5.7	30	123	116
	Coef Var	20%	18%	12%	44%	19%	21%	43%	15%	34%	18%	41%	60%
D	Mean		94			4900			20.1			234	
	Std Dev	-	19	-	-	1100	-	-	6.3	-	-	98	-
	Coef Var		20%			23%			31%			42%	
E	Mean	152	51	99	4600	4500	4900	34.8	12.2	20.9	528	-	349
	Std Dev	15	9	7	1300	1800	950	9.8	3.3	5.1	80	-	209
	Coef Var	10%	17%	7%	27%	40%	19%	28%	27%	24%	15%	-	60%
F	Mean	110	67	124	6200	3600	8300	19.3	19.4	15	343	614	178
	Std Dev	13	5	9	2300	700	1100	6.4	3.6	3.3	160	320	35
	Coef Var	11%	7%	7%	37%	20%	13%	33%	19%	22%	47%	50%	20%
G	Mean	87	112	157	5100	4700	5600	17.0	24.7	27.7	268	268	537
	Std Dev	28	12	12	1200	900	800	2.6	5.0	5.8	98	58	370
	Coef Var	33%	11%	8%	23%	20%	14%	16%	20%	21%	36%	21%	69%
Control	Mean		77			3700			24.0			141	
	Std Dev		14			1500			9.5			52	
	Coef Var		18%			41%			40%			37%	

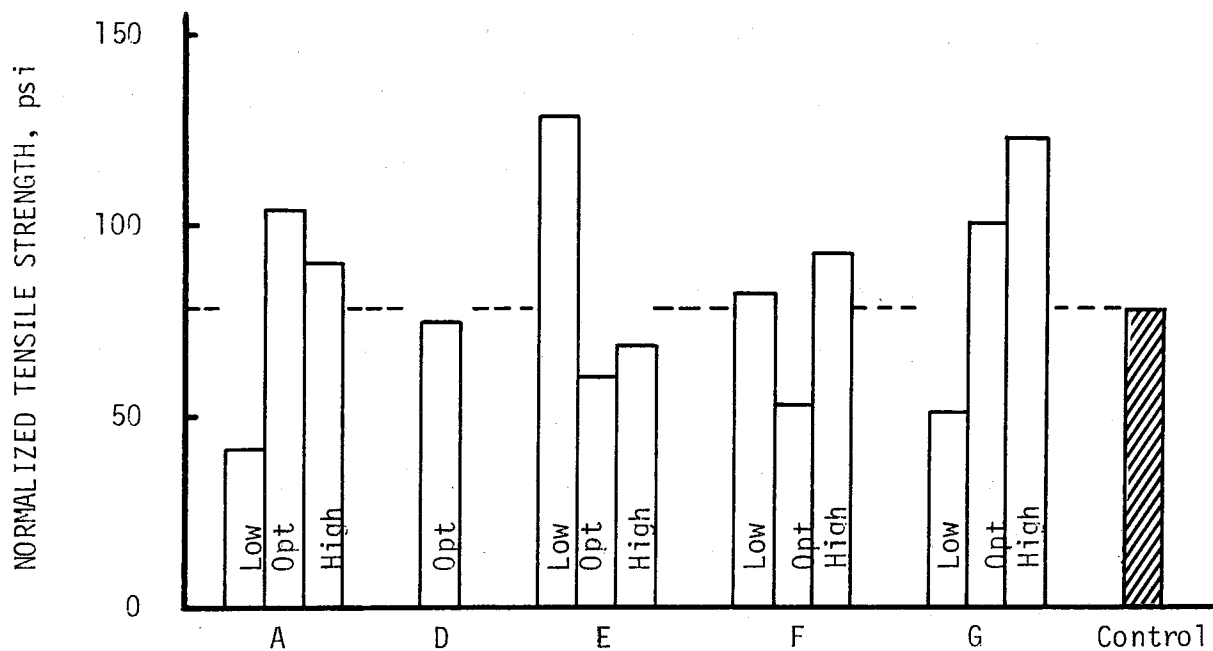


FIGURE 38. Normalized Average Tensile Strength of Test Specimens.

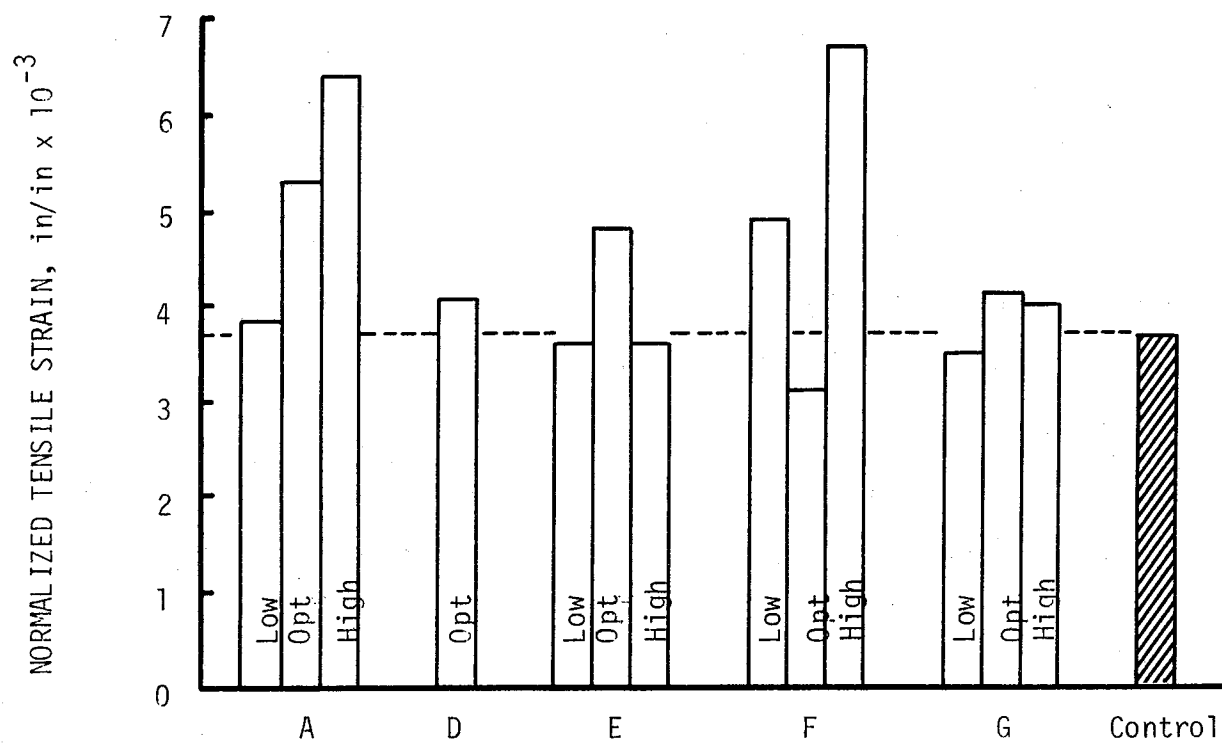


FIGURE 39. Normalized Average Ultimate Tensile Strain of Test Specimens.

Figure 39 indicates that tensile strain at failure can be improved by placing fabrics in asphalt mixtures. The tensile strain at failure is dependent upon the tack coat quantity as well as the type of fabric.

Figure 40 shows that the initial tangent modulus in tension can be improved by the use of fabrics which illustrates the reinforcing effects of the fabrics at very low strains. The type of fabric as well as the amount of tack influences the initial tangent modulus.

Correlations between fabric properties and mixture tensile strength are not readily evident from a review of the data. The thin, smooth surfaced fabrics (A and F) produced high tensile strains at failure. Specimens containing fabrics with high tack coat requirements (D and E) show no outstanding behavior.

Conclusions. Direct tensile test results of fabric-asphalt concrete systems under the conditions described above support the following conclusions.

1. Tensile strength at failure, tensile strain at failure and initial tangent modulus can be improved by the use of fabrics.
2. Fabrics remain intact after the asphalt concrete fails in tension.
3. Optimum tack coat quantities for maximizing tensile strength may not be identical to that required for peel strength, fatigue, crack resistance, etc.

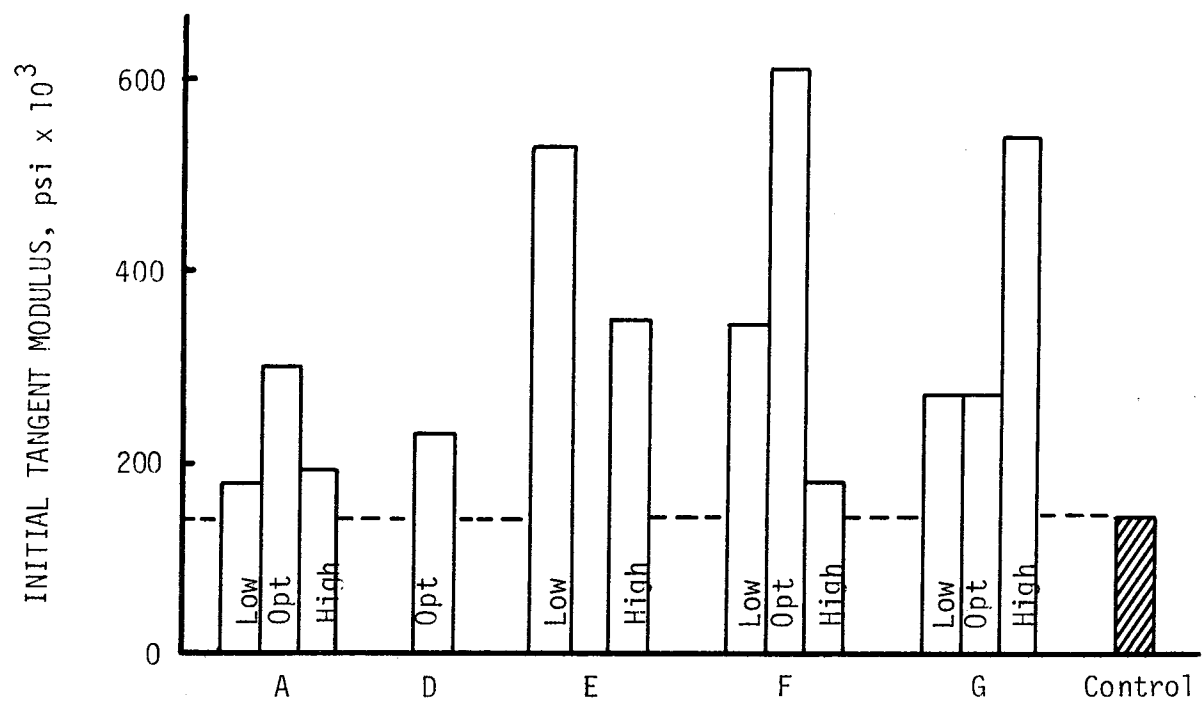


FIGURE 40. Average Initial Tangent Modulus of Tensile Test Specimens.

SYSTEMS TO REDUCE REFLECTION CRACKING

(FIELD EXPERIENCE)

Based on available literature (See Bibliography, Table 11) it is evident that a number of overlay systems including those given below have been utilized in an attempt to eliminate or reduce reflection cracking:

1. stone dust bond breakers
2. unstabilized aggregate layers
3. thick overlays of dense graded asphalt concrete
4. thick overlay of large maximum size open graded asphalt stabilized mixtures
5. reinforcing steel or wire mesh
6. low rubber content asphalt concrete seal coats and asphalt concrete mixtures
7. asphalt-rubber chip seals (high rubber content asphalt cements)
8. fiber reinforced asphalt concrete mixtures
9. heater-scarification
10. surface spray applications of asphalt cement softening materials
11. fabrics

Results of field trials conducted by state departments of transportation to investigate methods for reducing reflection cracking to bituminous overlays are to a large extent inconclusive. However, results do indicate that the most promising overlay systems appear to be the following:

1. thick overlays of asphalt concrete (dense or open graded)

TABLE 11. Summary of State Field Trials.

State	Description of Treatment	Comments	Old Pavement
Arizona Dept. of Transportation (8)	1 1/4 AC + Sahuaro asphalt rubber chip seal 3/4" heater-scarification + Petroset + 1 1/4 AC + 1/2" OGFC 1 1/4 AC + Sahuaro asphalt rubber chip seal + 1/2" OGFC 1 1/4 asbestos AC + 1/2" OGFC 1 3/4" AC 1 1/4 AC + 1/2" OGFC 1 1/4" OGFC (emulsions) + 1/2" OGFC Petromat + 1/4" AC + 1/2 OGFC Fiberglass + 1/4 AC + 1/2 OGFC 1/4 AC + Petroset + 1/2 OGFC fill cracks with Petroset + 1/4 AC + 1/2 OGFC fill cracks with Reclamite + 1/4 AC + 1/2 OGFC Reclamite + 1/4 AC + 1/2 OGFC 3/4 heater-scarification + Reclamite + 1/4, 1/2 or 3 AC + 1/2 OGFC Control Section 1/4, 1/2 or 3 AC + 1/2 OGFC	After four years of service the following five treatments were found to have significantly reduce reflective cracking; 1) heater-scarification with Petroset, 2) asphalt rubber membrane seal coat under OGFC, 3) Fiberglass membrane, 4) heater-scarification with reclamite, 5) overlays made with 200-300 penetration asphalt.	FLEXIBLE 3.5" AC 3.0" Asphalt Treated Base 6 to 15" subbase 4" AC 6" Base 15-21" Subbase
California Dept. of Transportation (9)	Thick Sections of AC OGFC + AC Rubberized Slurry seal Slurry Seal Petrolastic Stone Dust Petromat Cerex Asphalt rubber chip seal Heater-scarification Petroset Reclamite	After two to four years of service on nine projects it appears as if an additional 2.4 in. AC overlay performs better than most other overlay systems. Petromat has proven to be effect on pavements exhibiting alligator cracking. Emulsion slurry seal, rubberized slurry seal and Petroset were not effective on one project.	FLEXIBLE & RIGID
Colorado Division of Highways (7)	Reclamite + 2 1/2 in. AC Petromat + 2 1/2 in. AC Slurry Seal + 2 1/2 in. AC Squeegee Seal of Asphalt and Limestone Dust + 2 1/2 in. AC 5/8" Heater Scarification + Rejuvenating Agent + 2 in. AC 5/8 in. OGFC + 2 1/2 in. AC Crack Sealing + 2 1/2 in. AC 2 in. AC containing 15% rubberized asphalt 2 1/2 in AC + Petroset Control - 2 1/2 in. AC	After five years of service the sections had the following percentage of reflection cracking; Reclamite (96), Petromat (0), slurry seal (29), squeegee seal (87), heater-scarification (100), Plant mix seal (40), crack sealing (80), AC with rubberized asphalt (35), Petroset (21), control (80). The most promising treatment appears to be the use of a fabric.	FLEXIBLE 3" AC 4" Base 6-17" Subbase
Florida Dept. of Transportation (6)	1 in. AC + Structofors + 2 in. AC 3 in. AC + Reclamite 1 in. AC + Petromat + 2 in. AC 1 in. AC + 1 in. AC + Petroset + 1 in. AC + Petroset chip seal + 3 in. AC 1 in. AC + 1" OGFC + 1" AC 4 in. AC control - 3 in. AC	After seven years of service the Petromat section had 70 percent reflection cracking, extra thickness 85 percent reflective cracking, open graded 100% reflective cracking. All other sections had more cracks than in old pavement. For example; the control section had 33% more cracking, structofors 76% more cracking and the minimal seal 66% more cracking.	FLEXIBLE 3" AC 10" Base 12" Lime Stabilized Subgrade
Georgia Dept. of Transportation (10)	3/4 in. AC + Mirafi + 2, 4, 6 in. AC OGFC 3/4 in. AC + Petromat + 2, 4, 6 in. AC + OGFC Waterproofing membrane + 2, 4, 6 in. AC + OGFC 3.5 in. Coarse Open Graded Base + 3.5" AC Control - 2, 4, 6 in. AC + OGFC 3, 4, 5, 6.0 in. PCC	After one year of service the data indicate that fabrics retard reflective cracking. The coarse open graded base section is also performing well.	RIGID 9" PCC 3" Asphalt Stabilized 5" Subbase
Iowa Dept. of Transportation	Structofors + 3 in. AC Petromat + 3 in. AC control - 3 in. AC Cerex + 3 in. AC	After five years of service reflection cracking at the widening joint was 35% for the control section (3 inch overlay), 6 percent for Cerex, 1% for structofors and 0% for Petromat. After five years of service reflection cracking at transverse cracks was 51 percent for the central section, 25% for Cerex and structofors and 16 percent for Petromat.	RIGID + FLEXIBLE WIDENING
New York State Dept. of Transportation (12, 13)	Broken Pavement + Overlay Stone-Dust Bond-Breaker + overlay Wire Mesh Reinforcement with overlay	Over 90 pavement sections were studied indicating the stone-dust is not an effective method while wire mesh and broken pavement section studies have been inconclusive.	RIGID
North Carolina Dept. of Transportation (11)	Mirafi + 2" AC Petromat + 2" AC Structofors + 2" AC Fiberglass + 2" AC OGFC + 2" AC Sand Seal + 2" AC Control - 2" AC	After one year of service insufficient data have been accumulated to permit definite conclusions. However, the Mirafi fabric has performed better than the control section.	RIGID 7-9" PCC Subgrade

State	Description of Treatment	Comments	Old Pavement
North Dakota State Highway Department (24)	Asphalt treated sand with 3 1/2 fly ash + 3 1/2 in. AC Asphalt treated sand + 2 1/2 in. AC Structofors + 2 1/2 in. AC Petromat + 3 1/2 in. AC 1/2 in. OGFC + 3 1/2 in. AC Emulsion slurry seal + 3 1/2 in. AC Rubberized slurry seal + 3 1/2 in. AC		
Oklahoma Dept. of Highways (4, 40)	Petromat (fabric) + 1 in. AC + 3/4 OGFC Mirafi (fabric + 1 in. AC + 3/4 OGFC Control - 1 in. AC + 3/4 OGFC	After three months of service on IH 40 minor cracking has occurred in Petromat section and no cracking in the Mirafi section. Cracking was evident in the control section. Three other test sections have been placed. Fabric sections have performed equal to or better than control sections.	FLEXIBLE 4.5" AC .8" Base 6-10" Subbase
South Dakota Dept. of Highway (1)	Petromat (fabric) + 0.5 to 2.0 in. of Asphalt mixture Protecto-Wrap (fabric + coal tar) + 0.5 to 2.0 in. Asphalt mixture Control - 2 in. of asphalt mixture	After three years of service cracks have reflected in both sections but an adequate seal has been obtained.	FLEXIBLE
Texas State Department of Highways and Public Transportation (16, 17, 18, 19, 20, 21, 22, 23)	SC + AC AC + Petromat + SC + AC SC + OGFC Petromat + SC + OGFC AC + Petromat + AC Petromat + AC Fiberglass + Wire Mesh	After several years of experience on several sections good performance has been obtained with fabrics and wire mesh.	FLEXIBLE RIGID
Vermont Department of Highways (2, 3)	Recycle - Pulverize in-place + emulsion + 2 in. AC Recycle - Pulverize in-place + 2 in. AC Rubberized Crack Filler + 2 in. AC Rubberized Crack Filler + 3/8" Slurry + 2 in. AC Rubberized Crack Filler Control - 2 in. AC	After two years of service recycled sections show no cracking, rubberized crack filler + overlay reflected transverse cracking and rubber slurry seal, extensive cracking.	FLEXIBLE
Los Angeles County Road Department (14)	Wire Mesh with overlay Sheet Metal + overlay Saturated Building Paper + overlay Aluminum Foil Waxpaper Stone Dust	After 4 years of service the stone dust treatment was acceptable.	RIGID
Ontario Ministry of Transport and Communications (15)	Granular Interlayers 1, 3, 6 in. + overlay OGFC + overlay Remove & Replace Surface Pulverize Existing Surface + overlay Saw Transverse Joints in overlay	After 4 years of service the stone dust treatment was acceptable.	RIGID

AC - Asphalt Concrete

SC - Chip Seal Coat

OGFC - Open Graded Friction Course

2. asphalt-rubber chip seals with an overlay
3. heater-scarification in combination with softening agents and an asphalt concrete overlay
4. fabrics in combination with overlays

Performance of fabrics has been addressed on a national scale by the Federal Highway Administration in their National Experimental and Evaluation Program Project No. 10 (NEEP No. 10) (37). This program was initiated in 1970 and contained a number of state projects which evaluated the use of a Phillips Petroleum Company fabric. The conclusion of the Federal Highway Administration can be briefly summarized as follows:

1. There is no strong evidence that "Petromat" provides a universal mechanism for extending the crack-free life of an overlay. Reports from the states of Colorado, California, Florida and Texas support the use of fabrics while reports from Arizona, Louisiana, Wyoming and North Dakota are not in general support of fabrics. These data, in general, support the concepts that fabrics perform well in mild climates.

2. Insufficient quantitative data have been obtained in the majority of the test sections. This lack of data makes it nearly impossible to classify those pavements and environmental conditions under which fabrics have performed satisfactorily. Some reports, however, have indicated that fabrics are most suited for prevention of reflection cracks when placed over pavements that exhibit alligator cracking. Fabrics in general do not demonstrate good performance over thermally cracked asphalt concrete pavements and portland cement

concrete pavements.

The conclusion as to the performance of fabric overlay systems reached by the Federal Highway Administration is in general agreement with the literature presented in Table 11. Other general conclusions that can be inferred from this literature review and based on the authors experience are as follows:

Conclusion

1. For flexible pavements with alligator cracking a fabric with a one inch asphalt concrete overlay will perform about equivalent to a 2-inch asphalt concrete overlay. This statement does not imply that a fabric with a 2-inch overlay will perform about the same as a 4-inch overlay without fabric. Performance of fabrics placed with thicker overlay sections of asphalt concrete have not been well established.

2. For flexible pavements with transverse (thermal type) cracks, improved early performance may be obtained with fabric overlay systems. This advantageous performance may not extend past 3 years or through severe winters.

3. Fabrics have been used for routine surface patching operations. Chip seals placed over fabrics and utilized to repair isolated alligator type cracking has been successful in Texas.

Several new experimental projects placed in the last 2 to 3 years will supply data on the performance of several types of fabrics including those shown in Table 12. Experimental sections placed in Georgia over concrete pavement should provide valuable performance data. Test sections planned in Texas for the summer of 1979 will be

TABLE 12. Fabric Manufacturers.

Material	Manufacturer
Structofors	American Enka Corporation Enka, North Carolina
Petromat	Phillips Fibers Corporation Petromat Marketing Office Post Office Box 66 Greenville, South Carolina 29602
Cerex Bidim	Monsanto Company 800 North Lindberg Road St. Louis, Missouri 63166
Mirafi	Mirafi Inc Post Office Box 240967 Charlotte, North Carolina 28224
Fiberglass	Burlington Glass Fabric Company
Typar	DuPont Company Explosive Products Division Wilmington, Delaware 19800
Bithuthene Strips	

designed in such a manner that the structural or load carrying ability of the pavement will be considered as an input to performance. Additional field performance information should be collected in a systematic and continuous fashion.

ECONOMIC CONSIDERATIONS

The engineer has a number of rehabilitation alternatives which are suitable for eliminating or reducing the occurrence of reflection cracking. Overlays and reconstruction including the concepts of materials recycling are commonly used. The most successful overlay systems for reducing the occurrence of reflection cracking are thick overlays and asphalt-rubber chip seals, heater-scarification and fabrics in combination with asphalt concrete overlay. Cost comparisons of these alternatives on both a first cost and life cycle basis are of interest to the engineer and should be considered when selecting the optimum rehabilitation alternative for a particular segment of pavement.

First costs for a number of rehabilitation alternatives are shown in Table 13. These costs data are intended to be representative only. Relative costs can be expected to vary depending on the location in the country, cost of materials, cost of labor, cost and availability of equipment and productivity. For a particular project the engineer is encouraged to obtain and utilize local cost information.

As noted on Table 13 the first costs of the fabric interlayers, asphalt-rubber interlayers and heater-scarification operations are nearly identical. In addition, the first cost of one inch of asphalt concrete is about equivalent to the various interlayer approaches to reducing reflection cracking. Thus, from a first cost standpoint none of the recommended systems have a decided advantage. Performance of the various systems therefore must be considered.

TABLE 13. Typical Costs for Rehabilitation Alternatives Suitable for Reducing or Eliminating Reflection Cracking.

Material or Operation	Typical Cost Range \$ per sq. yd.	Representative Cost \$ per sq. yd.
Asphalt Concrete	0.80 - 1.40 [*]	1.25 [*]
Recycled Asphalt Concrete	0.70 - 1.40 [*]	1.00 [*]
Chip Seal Coat	0.25 - 0.75	0.55
Fabric Interlayer	0.80 - 1.50	1.25
Heater-Scarification and Softening Agent	0.40 - 1.30	0.90
Asphalt-Rubber Interlayer	0.80 - 1.50	1.25

^{*}Cost per square yard for 1-inch thickness

Life cycle analysis techniques are used to compare rehabilitation strategies which have different performance periods. Costs over the life of a facility for various rehabilitation alternatives are reduced to an equal annual cost or to a present worth. The rate of return of capital is commonly considered in these standard engineering economic analysis techniques.

As an example of the aforementioned technique, ten different rehabilitation strategies have been proposed for a 9-mile (2 lane) pavement in West Texas (Tables 14 and 15). This pavement has 7 to 9 transverse cracks per 100 feet of roadway and in excess of 200 feet of longitudinal cracks per lane, 100 feet in length. The pavement is structurally sound but is becoming rough riding and requires a large expenditure for routine maintenance. First costs for the 10 techniques considered are shown on Table 16 together with their expected maintenance and rehabilitation costs for a 20-year period. Present worth of the various alternatives is shown on both a square yard basis and for the entire 9-mile pavement section based on a 0 and 8 percent rate of return (Table 16). Performance of the various rehabilitation alternatives is based on the available literature and the authors' experience. Maintenance costs were estimated based on information contained on Table 17.

Utilizing this type of analysis framework, it is possible to perform "what if games". For example:

1. "What if" the life of the fabric reinforcement plus two-inch overlay (alternate 3) were 15 years rather than 10 years.
2. "What if" the first cost of the fabric reinforcement plus two-inch overlay were \$3.00 rather than \$3.75.

TABLE 14. Rehabilitation Alternatives Defined.

- Plan 1: Two-inch asphalt concrete overlay with maintenance on a 7 year cycle (asphalt concrete \$25.00 per ton).
- Plan 2: Chip seal plus 2-inch asphalt concrete overlay with maintenance (chip seal \$0.55 per square yard, asphalt concrete \$25.00 per ton).
- Plan 3: Fabric reinforcement plus 2-inch asphalt concrete overlay with maintenance (fabric reinforcement \$1.25 per square yard, asphalt concrete \$25.00 per ton).
- Plan 4: Recycle existing 4 inches of material and blend a selected aggregate into recycled mixture. A 2-inch overlay is scheduled after 5 years (recycling at \$20.00 per ton and overlay at \$25.00 per ton).
- Plan 5: Recycling existing 4 inches of asphalt materials and 2 inches of asphalt concrete overlay with maintenance (recycling \$16.00 per ton, asphalt concrete \$25.00 per ton).
- Plan 6: Recycling existing 4 inches of asphalt materials and 2 inches of asphalt concrete overlay with maintenance which includes a two-inch overlay (recycling \$16.00 per ton, asphalt concrete \$25.00 per ton).
- Plan 7: Recycling existing 4 inches of asphalt materials and 2 inches of asphalt concrete overlay with maintenance (recycling \$20.00 per ton, asphalt concrete \$25.00 per ton).
- Plan 8: Delay recycling 4 years and then recycle and add 2 inches of asphalt concrete overlay with maintenance (recycling \$16.00 per ton, asphalt concrete \$25.00 per ton).
- Plan 9: Heater-scarify to a depth of 1 to 1.5 inch and 2 inches of asphalt concrete overlay with maintenance (heater-scarification \$0.90 per square yard, asphalt concrete \$25.00 per ton).
- Plan 10: Asphalt-rubber interlayer and 2 inches of asphalt concrete overlay with maintenance (asphalt-rubber interlayer \$1.25 per square yard, asphalt concrete \$25.00 per ton).

TABLE 15. Rehabilitation Alternatives Cost Schedules.*

Year	Plan 1 2" A.C. Overlay	Plan 2 Seal Coat +2" A.C. Overlay	Plan 3 Fabric Rein- force- ment +2" A.C. Overlay	Plan 4 Recycle	Plan 5 Recycle +2" A.C. Overlay	Plan 6 Recycle +2" A.C. Overlay	Plan 7 Recycle +2" A.C. Overlay	Plan 8 Recycle +2" A.C. Overlay	Plan 9 Heater-Scarify + 2" A.C. Overlay	Plan 10 Asphalt-Rubber Interlayer + 2" A.C. Overlay
1980	2.50	3.05	3.75	4.00	5.70	5.70	6.50	.15	3.40	3.75
1981								.15		
1982								.15		
1983	.08							.15		
1984	.13	.08	.08					6.50	.08	.08
1985	.15	.13		2.50						
1986	.15	.15	.13						.13	.13
1987	2.50	.15								
1988		.15	.15		.08	.08	.08		.15	.15
1989	.08	2.50								
1990	.13		2.50	.08	.13	.13	.13	.08	2.50	2.50
1991	.15	.08			.15	.15	.15			
1992	.15	.13	.08	.13	.15	.15	.15	.13	.08	.08
1993	2.50	.15	.13	.15	.15	2.50	.15	.15	.13	.13
1994		.15	.15	.15	.15		.15	.15	.15	.15
1995		3.05	.15	.15	.15		.15	.15	.15	.15
1996	.08		.15	.15	.15		.15	.15	.15	.15
1997	.13		.15	.15	.15	.08	.15	.15	.15	.15
1998	.15		.15	.15	.15		.15	.15	.15	.15
1999	.15		.15	.15	.15	.13	.15	.15	.15	.15
2000	.15	.08	.15		.15	.13	.15		.15	.15

* Numbers represent costs per square yard.

TABLE 16. Cost of Rehabilitation Alternatives *

Basis of Costs	Interest Rate	Plan 1	Plan 2	Plan 3	Plan 4	Plan 5	Plan 6	Plan 7	Plan 8	Plan 9	Plan 10
Square Yard	0	9.03	9.85	7.72	7.16	6.66	8.77	7.46	7.76	7.37	7.72
	8	5.50	5.80	5.44	5.91	6.03	6.76	6.83	5.52	5.09	5.44
Entire 9 Miles	0	1,144,000	1,248,000	978,000	907,000	844,000	1,111,000	945,000	983,000	934,000	978,000
	8	697,000	735,000	689,000	749,000	746,000	857,000	865,000	700,000	645,000	689,000

* Costs do not include improvements to shoulders and patching that would be required in Plans 1, 2, 3, 9 and 10. Patching will cost about \$100,000.

TABLE 17. Representative Costs for Maintenance and Rehabilitation Activities.

Maintenance Activity	Cost Dollars * Per		Percent of Total Pavement Area Treated
	Sq Yd	Lane Miles	
Fog Seal - Partial Width	0.045	320	50 percent
Fog Seal - Full Width	0.06	420	100 percent
Chip Seal - Partial Width	0.06	420	15 percent
Chip Seal - Full Width	0.21	1,500	100 percent
Surface Patch - Hand Method	0.10	700	2.5 percent 1 inch thick
Surface Patch - Machine Method	0.08	560	10 percent 1 inch thick
Digout & Repair - Hand Method	0.25	1,760	2 percent 4 inches thick
Digout & Repair - Machine Method	0.20	1,400	5 percent 6 inches thick
Crack Pouring	0.12	850	250 lin. ft. Per Station
Asphalt Concrete Overlay	1.90	13,400	100 percent 2 inches thick

*Costs are for square yards of total pavement surface maintained. For example, surface patching by the hand method may have been applied over only 5 percent of total pavement surface area, yet costs reported are for the total pavement area maintained or one mile of pavement.

Metric Conversions:

$$1 \text{ yd}^2 = 0.83 \text{ m}^2$$

$$1 \text{ mi} = 1609 \text{ m}$$

$$1 \text{ in.} = 0.024 \text{ m}$$

$$1 \text{ ft} = 0.305 \text{ m}$$

These types of "what if" analyses can be performed to determine a competitive cost for new products, provided the competition and its cost is identified and the life of the competition and new product can be obtained or predicted. The major competition for fabrics has been identified and their first cost range established. The relative performance of the competing products needs to be firmly established for various pavement conditions.

Figure 41 which assumes a 0% rate of return and no maintenance cost can be utilized to simply combine the effects of first cost on performance life. For example, if the first cost of a suitable overlay system is \$1.00 per square yard and it normally performs for a period of 5 years, a competitive system that cost \$1.20 must last 6 years, a competitive system that cost \$1.60 must last 8 years and a system that cost \$2.00 must last 10 years. This simplified approach is appropriate for a general comparison only. The approach method described above and shown on Table 16 is suggested for detailed analysis purposes.

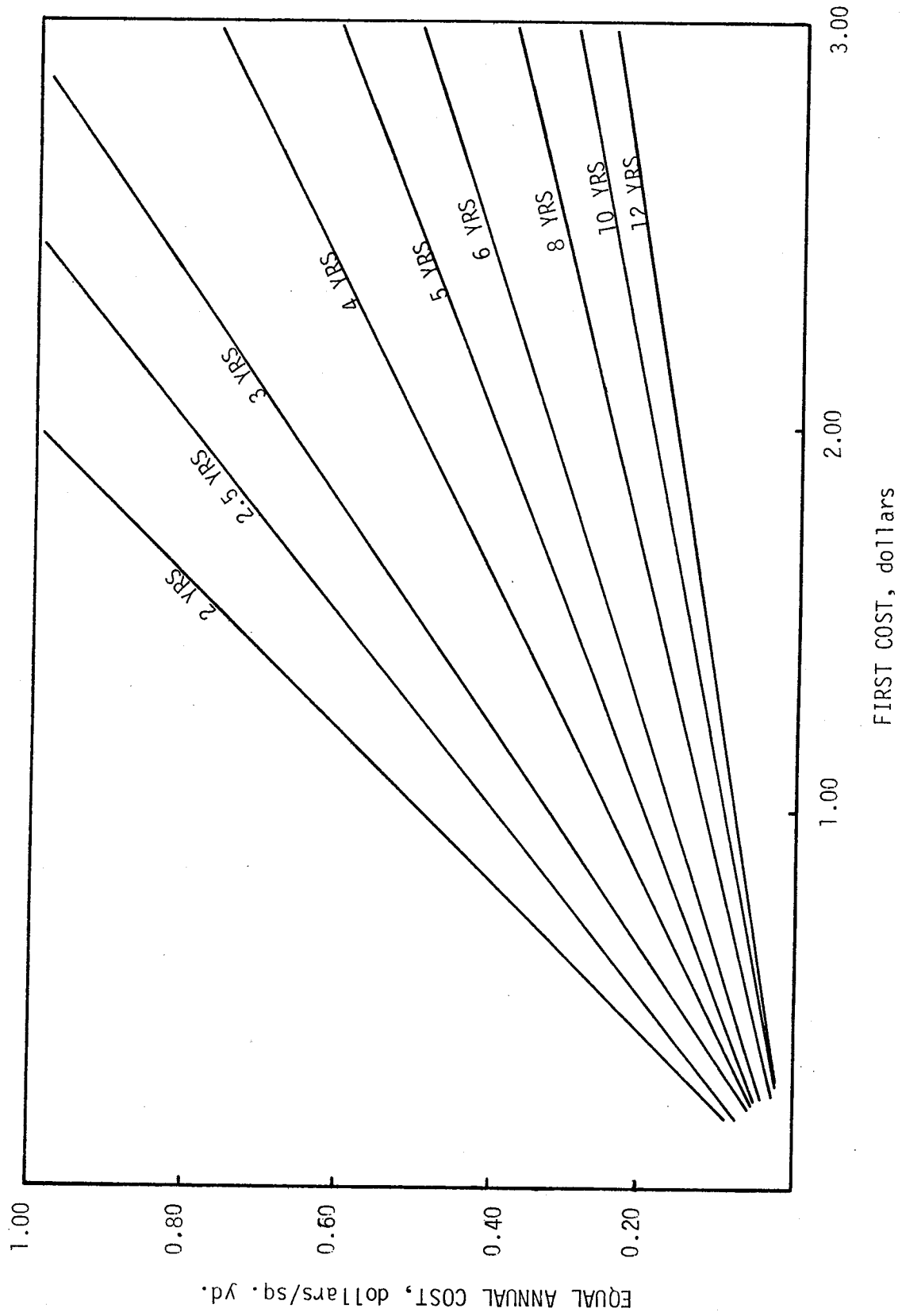


FIGURE 41. Simplified Relationship Between Equal Annual Cost and First Cost.

GENERAL CONCLUSIONS

Based on the previously discussed laboratory test results, analysis of existing field data, economic considerations and fracture mechanics theory, the following conclusions appear warranted:

1. To date, field performance is not well defined, however, fabrics show promise in retarding reflection cracking from pavement exhibiting fatigue distress.

2. At the current state-of-the-art, economic benefits to be gained from the use of fabrics in overlay applications is marginal.

3. Shrinkage of some fabrics associated with the high temperatures of newly placed asphalt concrete can cause premature cracking of the overlay. This cracking can be controlled by utilizing proper construction techniques and by modifying the fabrics shrinkage characteristics.

4. The potential for pavement slippage at the fabric-pavement interface is no greater for fabric overlay systems than for conventional overlays.

5. Fabrics will improve pavement fatigue performance.

6. Fabrics will improve resistance to reflective cracking in asphalt concrete overlays.

7. Tensile properties of asphalt concrete is improved by the use of fabrics.

REFERENCES

1. Epps, J. A. and Button, J. W., "MIRAFI[®] Fabric Tack Coat Requirements for Asphalt Overlays", Interim Report RF 3424-1, Texas Transportation Institute, July 1977.
2. Button, J. W. and Epps, J. A., "Asphalt Overlays with MIRAFI[®] Fabric - The Slippage Question on Airport Pavements", Interim Report RF 3424-2, Texas Transportation Institute, September 1977.
3. Button, J. W., Epps, J. A. and Gallaway, B. M., "Test Results on Laboratory Standard Asphalt, Aggregates and Mixtures", Research Brief No. 1, Materials Division, Texas Transportation Institute, January 1977.
4. Hveem, F. N., "Establishing the Oil Content for Dense-Graded Bituminous Mixtures", California Highways and Public Works, July-August 1942.
5. Dickson, P. F., and Corlew, J. S., "Thermal Computations Related to the Study of Pavement Compaction Cessation Requirements", Proceedings of the Association of Asphalt Paving Technologists, Volume 39, (1970).
6. Gallaway, B. M., and Rose, J. G., "Macro-Texture, Friction, Cross Slope and Wheel Track Depression Measurements on 41 Typical Texas Highway Pavements", Report No. 138-2, Texas Transportation Institute, June 1970.
7. Irwin, L. H., "Evaluation of Stabilized Soils in Flexural Fatigue for Rational Pavement Design", Doctoral Dissertation, Texas A&M University, May 1973.
8. Deacon, J. A., "Fatigue of Asphalt Concrete", Graduate Report, The Institute of Transportation and Traffic Engineering, University of California, Berkeley, 1965.
9. Pell, P. S., "Fatigue of Asphalt Pavement Mixtures", Proceedings, Second International Conference on the Structural Design of Asphalt Pavements, University of Michigan, 1967.
10. Epps, J. A., "Influence of Mixture Variables on the Flexural Fatigue and Tensile Properties of Asphalt Concrete", Doctoral Dissertation, University of California, Berkeley, September, 1968.
11. Steward, J., Williamson, R., and Mahoney, J., "Guidelines for Use of Fabrics in Construction and Maintenance of Low-Volume Roads, Report No. FHWA-TS-78-205, USDA, Forest Service, Portland, Oregon, June 1977, p. 9-4.

12. Way, George, "Prevention of Reflection Cracking in Arizona Minnetonka-East", Report No. 11, Arizona Department of Transportation, May, 1976.
13. Bushey, Roy W., "Experimental Overlays to Minimize Reflection Cracking", Interim Report FHWA-CA-TL-3167-76-28, September, 1976, sponsored by California Department of Transportation.
14. Donnelly, Davis E., McCabe, Philip J. and Swanson, Herbert N., "Reflection Cracking in Bituminous Overlays", Report No. CDOH-P&R-R-76-6, Final Report, Colorado Division of Highways, December, 1976.
15. Fish, G. W. and McNamara, R. L., "Reduction of Reflective Cracking in Bituminous Overlays", Payne's Prairie Experimental Project, Research Report 176-A, Office of Materials and Research, Florida Department of Transportation, June 1977.
16. Gulden, Wouter, "Rehabilitation of Plain Portland Cement Concrete Pavements with Asphaltic Concrete Overlays", Georgia Department of Transportation, February 13-15, 1978, presented at the Annual Meeting of the Association of Asphalt Paving Technologists.
17. Smith, Richard D., "Prevention of Reflection Cracking in Asphalt Overlays with Structofors", Petromat and Cerex, Iowa Highway Research Board, Project HR-158, Final Report, Iowa Department of Transportation, May, 1977.
18. McCullagh, F. R., "Reflection Cracking of Bituminous Overlays on Rigid Pavements", Special Report 16, New York State Department of Transportation, February, 1973.
19. "Wire Mesh Reinforcement of Bituminous Concrete Overlays", Research Report 66-1, New York State Department of Public Works, October, 1966.
20. Head, W. J., Interim Report "Evaluation of the Effectiveness of Fabric Reinforcement in Extending the In-Service Life of Bituminous Concrete Overlays", Project ERD-110-715, June, 1974 - not for publication.
21. North Dakota State Highway Department.
22. Leary, Michael T., "Construction with Reinforcement Fabric in Oklahoma", Federal Highway Administration, Oklahoma Division, Region Six, February, 1977.
23. Middleton, E. D. and Smith, M. D., "An Experimental Product Evaluation Fabric Reinforced Asphalt Concrete", Oklahoma Department of Transportation, Report 73-06-1, December, 1977.

24. McDonald, E. B., "Reduction of Reflective Cracking by Use of Impervious Membrane", U.S. #12 Project F 044-2(8), Carson County HR0206 (3645), South Dakota Department of Highways.
25. Day, D. D., "Evaluation of Surface-Sealing Systems Utilizing Seal Coats and Poly-Fab Underseal", Experimental Project Report Number: 606-4, Texas State Department of Highways and Public Transportation, February, 1978.
26. A Survey of Reflective Crack Retardation by Fabric Materials in Texas", Experimental Project Report No. 606-2, Texas State Department of Highways and Public Transportation, August, 1977.
27. Huffman, M. D., "Comparison of Reflective Crack Retardation by Fabric Material (Petromat), Open-Graded Friction, Courses, and Conventional Hot Mix", Experimental Project Report No. 606-3, Texas State Department of Highways and Public Transportation, February, 1978.
28. Coleman, P. H., "Texas Uses Fabric to Protect Pavement from Cracks", Civil Engineer, ASCE, December, 1977.
29. Buttler, L. J., "Performance of Metal Reinforced Bituminous Overlays in Texas", Special Study 9.0, Departmental Research, Texas Highway Department, August, 1978.
30. "Performance of Metal Reinforced Bituminous Overlays in Texas", Supplement to Report Number SS 9.0, Departmental Research, Texas Highway Department, June, 1971.
31. "Fibrous Reinforced Concrete Overlay", Experimental Project, Report 606-1, Texas State Department of Highways and Public Transportation.
32. "Fiberglass Placement", Experimental Project, Report 608-1, Texas State Department of Highways and Public Transportation.
33. Gray, J. T., Stickney, E. H. and Nickolson. R. F., "Alternative Reflection Crack Treatment Pulverization and Rubberized Slurry SRI", Initial Report 75-1, March, 1975, Vermont Department of Highways.
34. "Relieving Reflection Cracking in Bituminous Overlays Utilizing a Strain Relieving Inter-Layer of Rubberized Slurry", Report 74-3, Vermont Department of Highways.
35. Vicelja, J. L., "Methods to Eliminate Reflection Cracking in Asphalt Concrete Resurfacing Over Portland Cement Concrete Pavements", Proceedings, AAPT, Vol. 32, 1963.
36. Kher, R., "Road Test to Determine Implications of Preventing Thermal Reflection Cracking in Asphalt Overlays", TRB Record 632, 1977.

37. "NEEP No. 10 - Reducing Reflection Cracking in Bituminous Overlays Status of Synthetic Fabrics", Federal Highway Administration Memorandum, March 9, 1978.
38. Schapery, R. A., "A Theory of Crack Growth in Viscoelastic Media", Office of Naval Research, Department of the Navy, MM 2764-73-1, Mechanics and Materials Research Center, Texas A&M University, March 1973.
39. Germann, F. P., Lytton, R. L., "Methodology for Predicting the Reflection Cracking Life of Asphalt Concrete Overlays", Research Report 207-5, Texas Transportation Institute, March 1979.

BIBLIOGRAPHY

1. Dallaire, G., "Filter Fabrics: Bright Future in Road and Highway Construction", Civil Engineering, ASCE, May, 1976, also March, 1975, March, 1977.
2. Mirafi 140 Fabric for Longer Lasting Pavement Overlays, Leaflet, Celanese Fibers Marketing Company, 1978.
3. Special Specifications - Texas Department of Highways and Public Transportation Items 3099, Fabric Underseal.
4. "NEEP No. 10 - Reducing Reflection Cracking in Bituminous Overlays Status of Synthetic Fabrics", Federal Highway Administration Memorandum, dated March 9, 1978.
5. Brownie, R. B., "Evaluation of Rubber-Asphalt Binder for Seal Coating Asphaltic Concrete", Technical Memorandum, Civil Engineering Laboratory, Naval Construction Battalion Center, Port Hueneme, California, August, 1977.
6. Lansdon, H. G., "Construction Techniques of Placement of Asphalt-Rubber Membranes", paper presented at the 13th Paving Conference, University of New Mexico, January 8-9, 1976.
7. LaGrone, B. G., and Huff, B. J., "Utilization of Waste Rubber to Improve Highway Performance and Durability", paper presented at the 52nd Annual Meeting of the Highway Research Board, January, 1973.
8. Status Report, "National Experimental and Evaluation Program", FHWA Notice N 5080.73, April 8, 1978.
9. Interim Report, "National Experiment and Evaluation Program Project No. 10 - Reducing Reflection Cracking in Bituminous Overlays", FHWA Notice N 5140.9, January 19, 1976.
10. Rubber-Asphalt Binder for Seal Coat Construction, HHO-31, FHWA, February, 1973.
11. Oliver, J. W. H., "A Critical Review of the Use of Rubber and Polymers in Bitumen Bound Paving Materials", Australian Road Research Board, Vistoria, March, 1977.
12. "Field Performance Report Surface Treatments on Van Buren Street City of Phoenix, Arizona, Arizona Refining Company, Technical Report ARS-502, August, 1975 through December, 1977.
13. "Field Audit of Arm - R. Shield Surface Treatments on Van Buren Road City of Phoenix, Arizona Refining Company, Technical Report ARS-501, Dexember, 1977.

14. Morris, Gene R., "Asphalt-Rubber Membranes Development Use Potential", Arizona Department of Transportation.
15. Jimenez, R. A., "Testing Methods for Asphalt-Rubber", Final Report - Phase K, Arizona Department of Transportation, ADOT-RS-15 (164), January, 1978.
16. Frobel, R. K., "Laboratory and Field Development of Asphalt-Rubber for Use as a Waterproof Membrane", Final Report, Arizona Department of Transportation, ADOT-RD-14(167), July, 1977.
17. Green, E. L., "The Chemical and Physical Properties of Asphalt-Rubber Mixtures", Arizona Department of Transportation, Final Report, ADOT-RS-14(162), July, 1977.
18. McLaughlin, A. L., "Reflection Cracking of Bituminous Overlays for Airport Pavements, A State of the Art", Report No. FAA-RD-79-57, U.S. Department of Transportation, Federal Aviation Administration, May 1979.

Appendix A

Cooling Time for Asphalt Mats

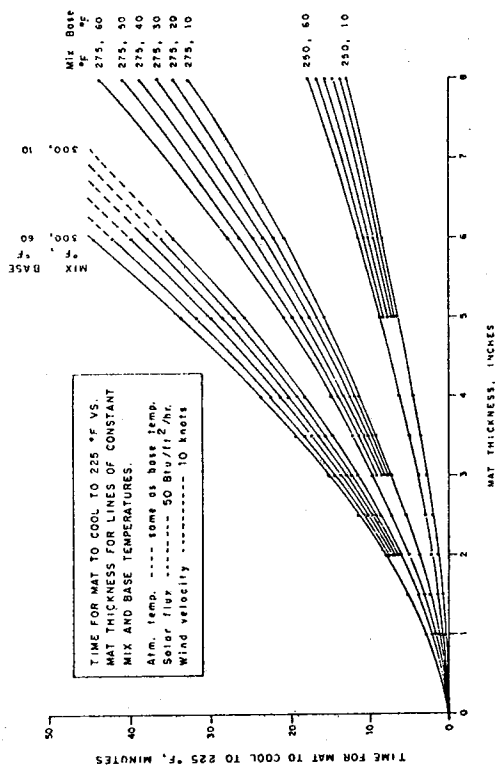


FIG A1. Time for Mat to Cool to 225 F vs. Mat Thickness for Lines of Constant Mix and Base Temperatures. (5)

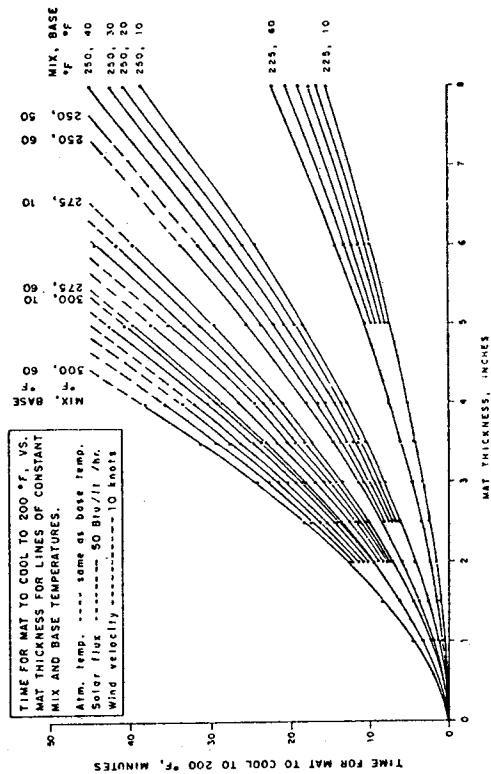


FIG A2. Time for Mat to Cool to 200 F vs. Mat Thickness for Lines of Constant Mix and Base Temperatures. (5)

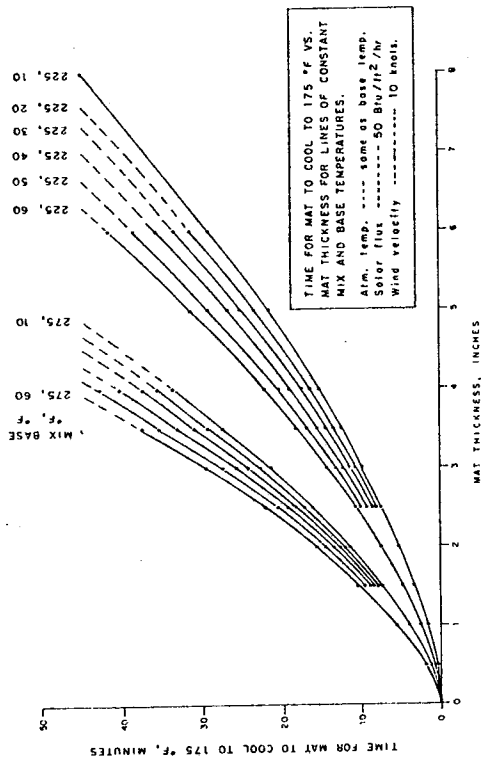


FIG A3. Time for Mat to Cool to 175 F vs. Mat Thickness for Lines of Constant Mix and Base Temperatures. (5)

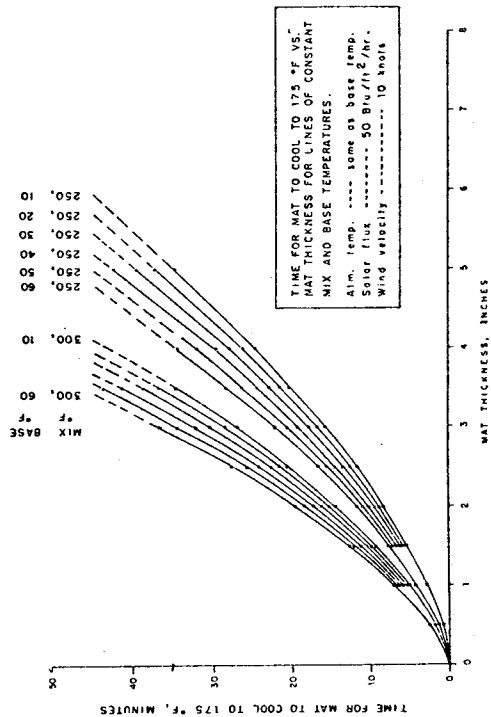


FIG A4. Time for Mat to Cool to 175 F vs. Mat Thickness for Lines of Constant Mix and Base Temperatures. (5)

Appendix B

Peel Strength Test Data

TABLE B-1. Individual and Mean Peel Strength Test Results at 122°F (50°C).

Surface Peel Rate Tack Quan.	Peel Strength, lbs/inch width											
	Portland Cement Concrete						Asphalt Concrete					
	5 in/min			20 in/min			5 in/min			20 in/min		
	Low	Opt	High	Low	Opt	High	Low	Opt	High	Low	Opt	High
A	0.31	0.26	0.24	0.83	0.94	0.81	0.11	0.20	0.74	0.37	0.77	0.86
	0.35	0.23	0.23	1.09	0.83	0.90	0.20	0.23	0.19	0.32	0.80	0.72
		0.21	0.24	1.14	0.81	0.82	0.13	0.23	0.23	0.16	0.77	0.86
	0.33	0.24	0.24	1.02	0.86	0.84	0.15	0.22	0.39	0.43	0.78	0.81
B	0.04	0.04	0.17	0.54	0.50	0.54	0.10	0.05	0.08	0.42	0.39	0.45
	0.06	0.10	0.10	0.36	0.50	0.54	0.10	0.08	0.10	0.39	0.36	0.45
	0.08	0.13	0.13	0.30	0.48	0.57	0.18	0.09	0.11	0.49	0.33	0.48
	0.06	0.09	0.13	0.40	0.49	0.55	0.13	0.07	0.10	0.43	0.36	0.46
C	0.05	0.08	0.07	0.26	0.29	0.30	0.02	0.05	0.06	0.09	0.24	0.25
	0.05	0.08	0.09	0.29	0.26	0.30	0.05	0.08	0.06	0.14	0.25	0.25
	0.05	0.08	0.08	0.22	0.29	0.34	0.03	0.05	0.06	0.15	0.24	0.25
	0.05	0.08	0.08	0.26	0.28	0.31	0.03	0.06	0.06	0.13	0.24	0.25
D	0.35	0.27	0.35	1.00	0.92	0.93	0.10	0.21	0.20	0.41	0.69	0.84
	0.32	0.29	0.36	0.96	0.86	0.98	0.12	0.23	0.23	0.47	0.69	0.75
	0.28	0.30	0.29	0.82	0.94	0.93		0.19	0.23	0.27	0.68	0.75
	0.32	0.29	0.33	0.93	0.91	0.94	0.11	0.21	0.22	0.38	0.69	0.78
G*	0.02	0.12	0.08	0.16	0.51	0.36	0.01	0.05	0.05	0.02	0.22	0.12

*Data interpolated at appropriate tack coat quantities from curves in Figures A-15 and A-16 of Report 3424-1 (3)

TABLE B-2. Coefficients of Variation of Peel Strength Measurements.

Coefficient of Variation, percent												
Surface Peel Rate Tack Quan. Fabric	Portland Cement Concrete						Asphalt Concrete					
	5 in/min			20 in/min			5 in/min			20 in/min		
	Low	Opt	High	Low	Opt	High	Low	Opt	High	Low	Opt	High
A	9	11	4	16	8	6	30	7	78	37	2	10
B	33	51	27	31	2	3	36	30	15	12	8	4
C	0	0	13	16	6	7	51	29	0	25	2	0
D	11	5	11	10	5	15	13	10	8	27	1	7

Appendix C

Shear Strength Test Data

TABLE C-1. Results of Shear Strength Tests .

Specimen Identification	Test Temp. °F (°C)	Shear Strength, psi					
		Low Tack		Opt. Tack		High Tack	
			Avg.		Avg.		Avg.
A	68 (20)	287 173	230	247 300 253 153	240	---	
	103 (40)	153 157 177	160	207 220 153 173	190	247 240 243 233	240
	140 (60)	---	---	123 130 106 115	120	---	---
D	68 (20)	147 260	200	293 300 280 253	280	---	---
	103 (40)	160 230 167 200	190	173 220 167 240 213 140	190	253 297 293 320	290
	140 (60)	---	---	119 121	120	---	---
E	68 (20)	293 332	310	379 402 425 390 362 407	390	425 329 439	400
	103 (40)	231 244 258	240	70 265	270	---	

TABLE C-1. Continued

Specimen Identification	Test Temp. °F (°C)	Shear Strength, psi					
		Low Tack		Opt. Tack		High Tack	
			Avg.		Avg.		Avg.
F	68 (20)	216 190 149	185	355 365 317 332	340	363 420 374	390
	103 (40)	161 182 168	170	202 126	170	---	---
G	68 (20)	172 121 170	150	199 297 288	260	---	---
	103 (40)	143 147 111	130	172 178 190 194	180	185 166 166	170
Control - 1 No Fabric 0.05 Tack	68 (20)	NA	NA	356 340	350	NA	NA
	103 (40)	NA	NA	160 178 196 200	180	NA	NA
	140 (60)	NA	NA	121 144 118	130	NA	NA
Control - 2 Asphalt Conc. No Interface	68 (20)	NA	NA	427 453	440	NA	NA
	103 (40)	NA	NA	273 293 310	290	NA	NA
	140 (60)	NA	NA	155 148 158	150	NA	NA

TABLE C2. Physical Properties of Shear Test Specimens.

FABRIC CODE	TACK COAT gal/yd ²	SPECIFIC GRAVITY	AIR VOIDS percent
A	LOW-0.07	2.33	6.3
	OPT-0.14	2.33	6.5
	HIGH-0.28	2.34	6.1
D	LOW-0.11	2.34	5.8
	OPT-0.23	2.32	6.9
	HIGH-0.46	2.36	5.1
E	LOW-0.20	2.34	7.4
	OPT-0.40	2.35	6.9
	HIGH-0.75	2.38	5.9
F	LOW-0.07	2.34	7.6
	OPT-0.13	2.34	7.5
	HIGH-0.26	2.34	7.5
G	LOW-0.10	2.27	8.5
	OPT-0.20	2.29	8.1
	HIGH-0.40	2.27	8.8
CONTROL-1 NO FABRIC	0.05	2.27	8.5
CONTROL-2 NO INTERFACE	0	2.37	8.0

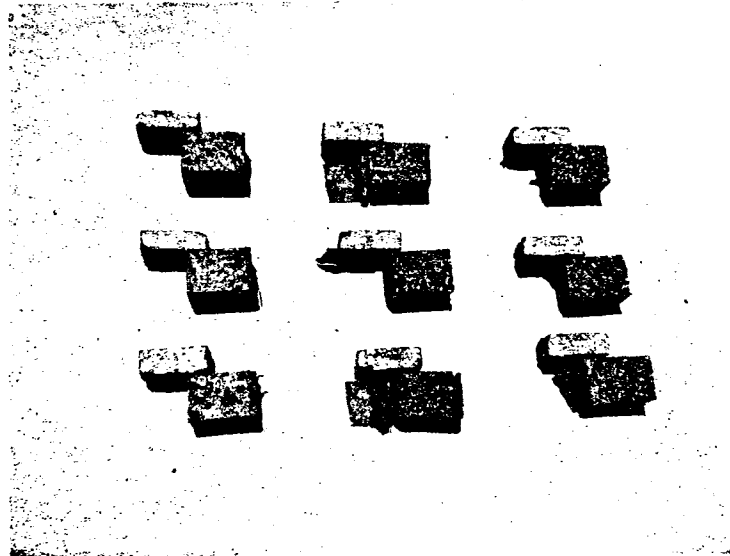


FIGURE C1. Airport Shear Test Specimens after Testing with Fabric A (Tack Coat Rate Increases from Left to Right-Low, Optimum, and High).

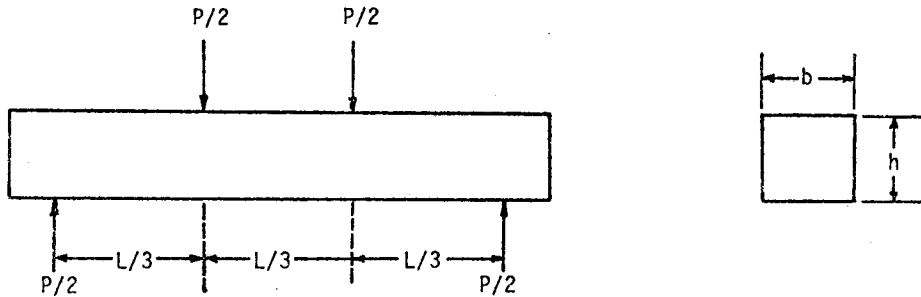
Appendix D

Flexural Fatigue Test Data

TABLE D1. Test Results from Fatigue Specimens Fabricated by Two Techniques.

Fabrication Technique	Sample No. or Item	Input Stress psi	Bending Strain, in/in $\times 10^{-4}$	Cycles to Failure	Stiffness Modulus psi $\times 10^3$	Specific Gravity	Air Void, percent
Weathered Surface + Tack Coat + Dry Fabric	L-2	78	5.12	26,617	150	2.39	3.9
	L-2	83	6.86	16,504	120	2.38	4.1
	L-4	83	4.85	85,408	169	2.39	3.9
	L-5	80	4.75	40,001	170	2.39	3.9
	Mean	81	5.40	42,000	152	2.39	4.0
	Std. Dev.	2.4	0.99	30,000	23	0.005	0.1
	Coef. Var.	3%	18%	72%	15%	0.2%	3%
Presoaked Fabric	x-1	72	4.64	29,129	155	2.38	4.3
	x-2	71	5.21	25,430	136	2.38	4.3
	x-4	71	5.87	45,598	120	2.37	4.7
	x-5	79	6.23	53,573	126	2.38	4.1
	Mean	73	5.49	38,433	134	2.38	4.4
	Std. Dev.	3.9	0.71	13,000	15	0.005	0.3
	Coef. Var.	5%	13%	35%	11%	0.2%	6%

Summary of Formulae
for
Third-Point Loaded Beam (7)



Equation No.

$$\text{Peak stress in extreme fiber} = \sigma_{\max} = \frac{PL}{bh^2}, \text{ psi} \quad (\text{D1})$$

$$\text{Initial stiffness modulus} = E = \frac{0.213 PL^3}{W_0 bh^3} + \frac{0.400 PL(1+\mu)}{W_0 bh}, \text{ psi} \quad (\text{D2})$$

$$\text{Initial bending strain in extreme fiber} = \epsilon = \frac{\sigma}{E}, \text{ in./in.} \quad (\text{D3})$$

(Hooke's Law)

$$\text{Total input energy} = U_f = \frac{10.2 P W_0 N_f}{23}, \text{ in.-lb} \quad (\text{D4})$$

$$\text{Maximum energy density} = U_d = \frac{(\sigma_{\max})^2}{2E}, \frac{\text{in.-lb}}{\text{in.}^3} \quad (\text{D5})$$

where

- P = applied load, lbs
- L = tested length of beam, in.
- b = width of beam, in.
- h = depth of beam, in.
- W₀ = center deflection of beam at 200th cycle, in.
- μ = Poisson's ratio (assumed 0.35)
- N_f = number of cycles to failure

An Explanation of Energy Terms

The total input energy, U_f , is the macroscopic amount of energy (or work) imparted to the specimen during the test (up to failure) by external forces. By contrast, the maximum energy density, U_d , is the microscopic strain energy per unit volume which occurs at a point in the most highly stressed region of the specimen at the peak of any given cycle (7). Total input energy is used herein as a comparative measure of fatigue performance.

TABLE D2. Beam Fatigue Data.

Type Sample	Sample No.	Specific Gravity,	Air Voids, percent	Input Stress, psi	Bending Strain, in/in x 10 ⁻⁴	Cycles To Failure	Modulus, psi x 10 ³	Total Energy Input, lb-in x 10 ³	Max. Energy Density, in-lb in ³ x 10 ⁻²
Control Beams	I-14	2.38	4.4	31	2.2	90,925	140	7	0.3
	I-15	2.38	4.2	40	2.3	251,554	172	28	0.5
	I-12	2.39	4.0	44	2.3	246,332	190	30	0.5
	I-4	2.38	4.2	75	4.2	11,099	178	4	1.6
	I-2	2.38	4.1	80	4.9	19,060	163	9	2.0
	I-6	2.38	4.4	80	5.4	6,846	149	3	2.1
	I-7	2.38	4.4	80	7.6	10,173	105	7	3.0
	I-1	2.39	4.0	92	4.8	122,631	190	64	2.2
	#1	----	----	93	4.8	26,226	193	14	2.2
	I-9	2.38	4.3	97	6.0	3,200	163	2	2.9
	I-3	2.39	4.0	115	10.7	1,856	107	3	6.2
Fabric A (Low Tack)	I-10	2.38	4.2	115	8.2	3,033	140	3	4.7
	I-5	2.38	4.2	125	10.7	3,466	117	5	6.7
	I-8	2.38	4.2	125	5.7	1,733	220	1	3.6
	I-11	2.39	4.0	125	8.2	4,441	153	5	5.1
	6	2.38	4.5	100	11.4	3,553	88	5	5.7
	7	2.39	3.9	100	12.3	4,780	81	7	6.2
	8	2.37	4.5	100	14.1	1,840	71	3	7.0
	9	2.38	4.4	100	12.0	2,925	83	4	6.0
	10	2.38	4.3	100	13.4	3,055	75	5	6.7

TABLE D2. Continued

Type Sample	Sample No.	Specific Gravity, gm/cc	Air Voids, percent	Input Stress, psi	Bending Strain, in/in x 10 ⁻⁴	Cycles To Failure	Modulus, psi x 10 ³	Total Energy Input, lb-in x 10 ³	Max. Energy Density, in-lb in ³ x 10 ⁻²
Fabric G (Low Tack)	11	2.39	3.9	98	8.2	7,407	119	7	4.0
	12	2.38	4.4	100	8.6	2,934	117	3	4.3
	13	2.38	4.3	100	7.0	16,720	142	14	3.5
	14	2.38	4.1	108	8.1	5,616	133	6	4.4
	10	2.38	4.2	100	6.4	11,014	156	8	3.2
Fabric G (Optimum Tack)	3	2.40	3.6	43	3.1	203,588	140	32	0.7
	1	2.39	3.9	44	3.2	299,544	137	50	0.7
	9	2.40	3.6	45	3.8	393,474	119	79	0.9
	4	2.40	3.6	47	2.9	181,851	159	30	0.7
	2R	-----	-----	48	3.5	430,000	136	86	0.8
	X4	2.37	4.7	65	5.8	45,598	122	19	1.7
	X2	2.38	4.3	71	5.2	25,430	136	11	1.9
	X1	2.38	4.3	72	4.6	29,129	155	12	1.7
	X5	2.38	4.1	74	6.2	53,573	126	29	2.2
	2	2.39	3.7	98	5.7	25,008	172	16	2.8
	15	-----	-----	98	9.3	17,504	105	19	4.6
	5	2.39	3.9	101	8.2	3,334	123	3	4.1
	6	2.40	3.7	103	6.5	10,340	158	8	3.4
	7	2.40	3.6	103	9.8	6,750	105	8	5.1
	8	2.39	3.7	103	7.6	6,793	135	6	3.9
	10	2.39	4.1	103	9.5	5,179	108	6	4.9

TABLE D2. Continued

Type Sample	Sample No.	Specific Gravity, gm/cc	Air Voids, percent	Input Stress, psi	Bending Strain, in/in x 10 ⁻⁴	Cycles To Failure	Modulus, psi x 10 ³	Total Energy Input, 1b-in x 10 ³	Max. Energy Density, in-lb $\frac{3}{in}$ x 10 ⁻²
Fabric A (Optimum Tack)	1	2.40	3.5	103	3.6	27,600	287	12	1.8
	2	2.40	3.4	100	6.7	7,377	150	6	3.3
	3	2.41	3.2	104	5.2	13,200	201	8	2.7
	4	2.39	3.7	103	8.1	5,380	127	5	4.2
	5	2.41	3.2	101	8.4	4,573	119	5	4.3
Fabric A (High Tack)	1	2.41	3.2	100	14.1	3,404	71	6	7.0
	2	2.40	3.3	100	11.8	7,023	85	10	5.9
	3	2.40	3.3	100	11.8	6,290	85	9	5.9
	4	2.40	3.7	100	14.5	3,638	69	6	7.2
	5	2.40	3.4	100	12.7	5,080	78	8	6.4
Fabric D (opt)	1	2.31	7.2	103	4.0	25,500	256	12	2.1
	2	2.34	5.8	104	6.7	2,186	155	2	3.5
	3	2.37	4.7	101	3.7	16,200	274	7	1.9
	4	2.36	5.2	101	7.6	7,320	133	7	3.8
	5	2.40	3.6	101	6.2	10,543	163	8	3.1
Fabric E (opt)	1	2.39	3.7	120	8.4	24,890	148	30	4.9
	2	2.40	3.6	100	4.3	102,201	220	53	2.3
	3	2.38	4.1	104	13.1	60,721	75	99	7.2
Fabric F (opt)	1	2.38	4.2	100	9.8	5,700	102	7	4.9
	2	2.37	4.7	102	17.5	2,701	58	6	8.6
	3	2.37	4.9	100	9.5	6,418	105	7	4.8

TABLE D2. Continued

Type Sample	Sample No.	Specific Gravity, gm/cc	Air Voids, percent	Input Stress, psi	Bending Strain, in/in x 10 ⁻⁴	Cycles To Failure	Modulus, psi x 10 ³	Total Energy Input, lb-in x 10 ³	Max. Energy Density, $\frac{\text{in-lb}}{\text{in}^3} \times 10^{-2}$
Fabric G (High Tack)	15	2.40	3.5	97	4.7	23,816	208	13	2.3
	16	2.40	3.6	100	7.4	16,116	135	14	0.4
	17	2.39	3.7	100	6.0	13,058	168	9	3.0
	18	2.40	3.5	100	6.4	15,461	155	12	3.2
	19	2.39	3.7	100	6.2	14,351	162	10	3.1

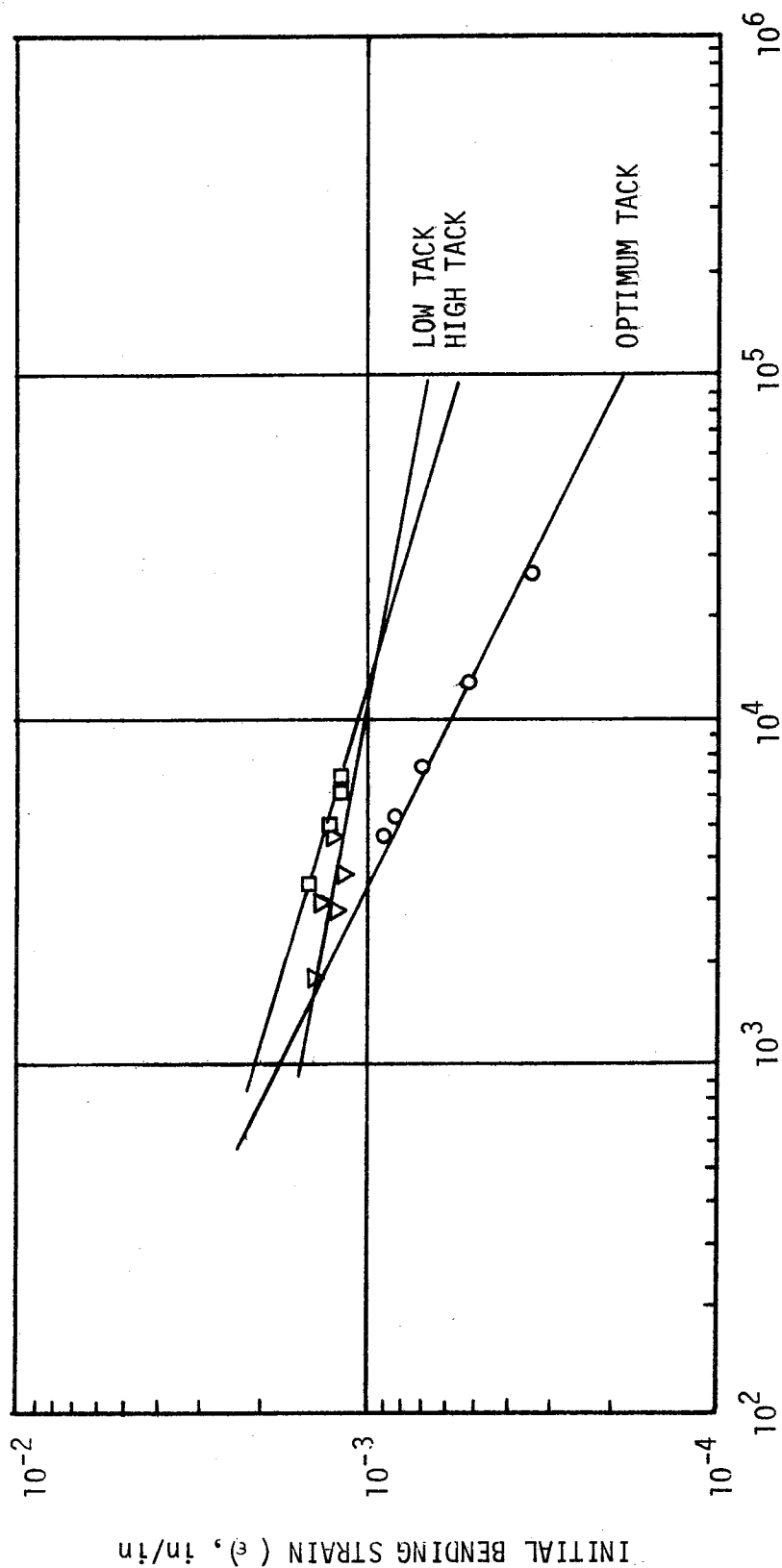


FIGURE D1. Strain versus Load Applications to Failure for Specimens Containing Fabric A.

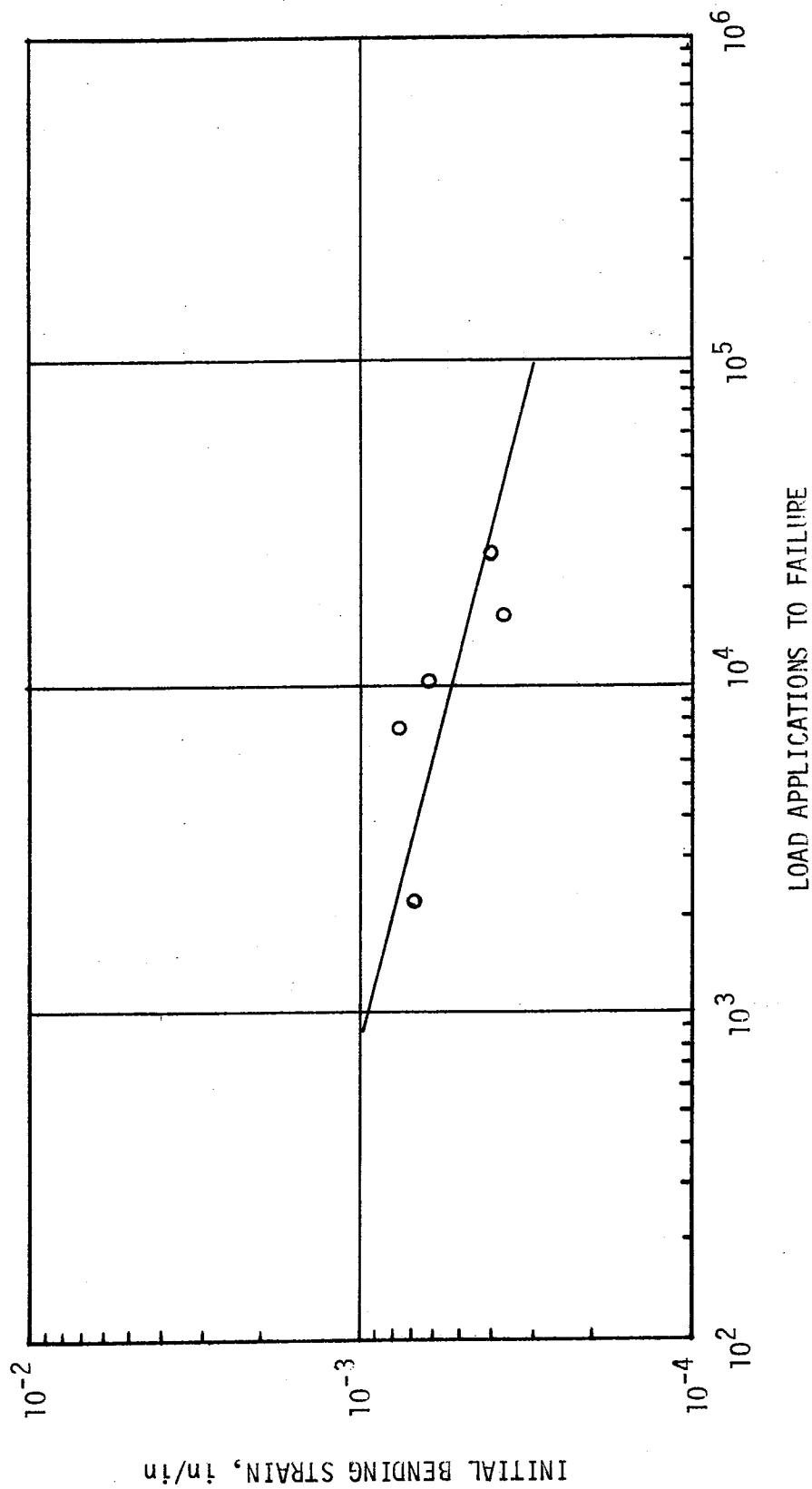


FIGURE D2. Strain versus Load Applications to Failure for Specimens Containing Fabric D.

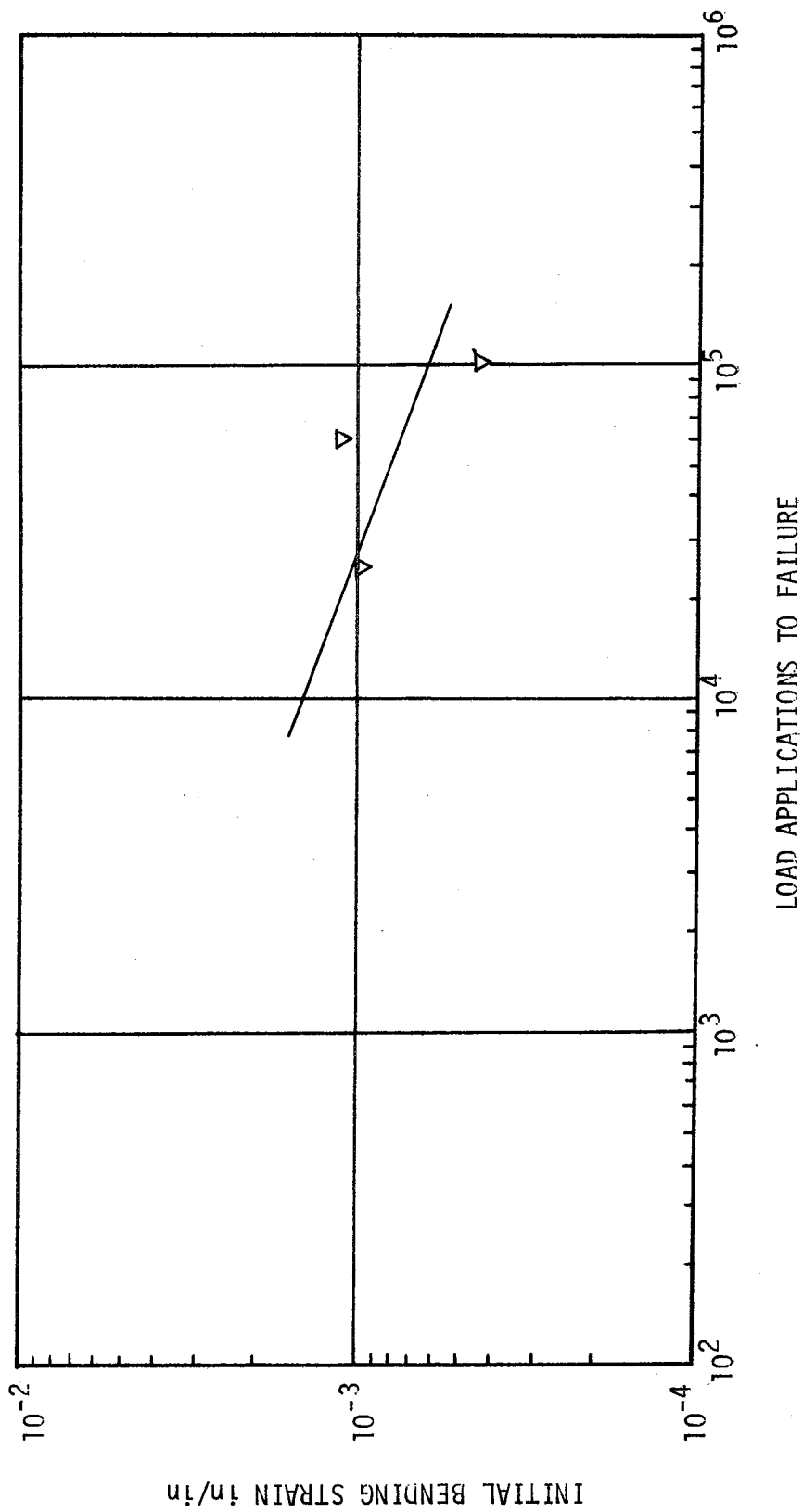


FIGURE D3. Strain versus Load Applications to Failure for Specimens Containing Fabric E.

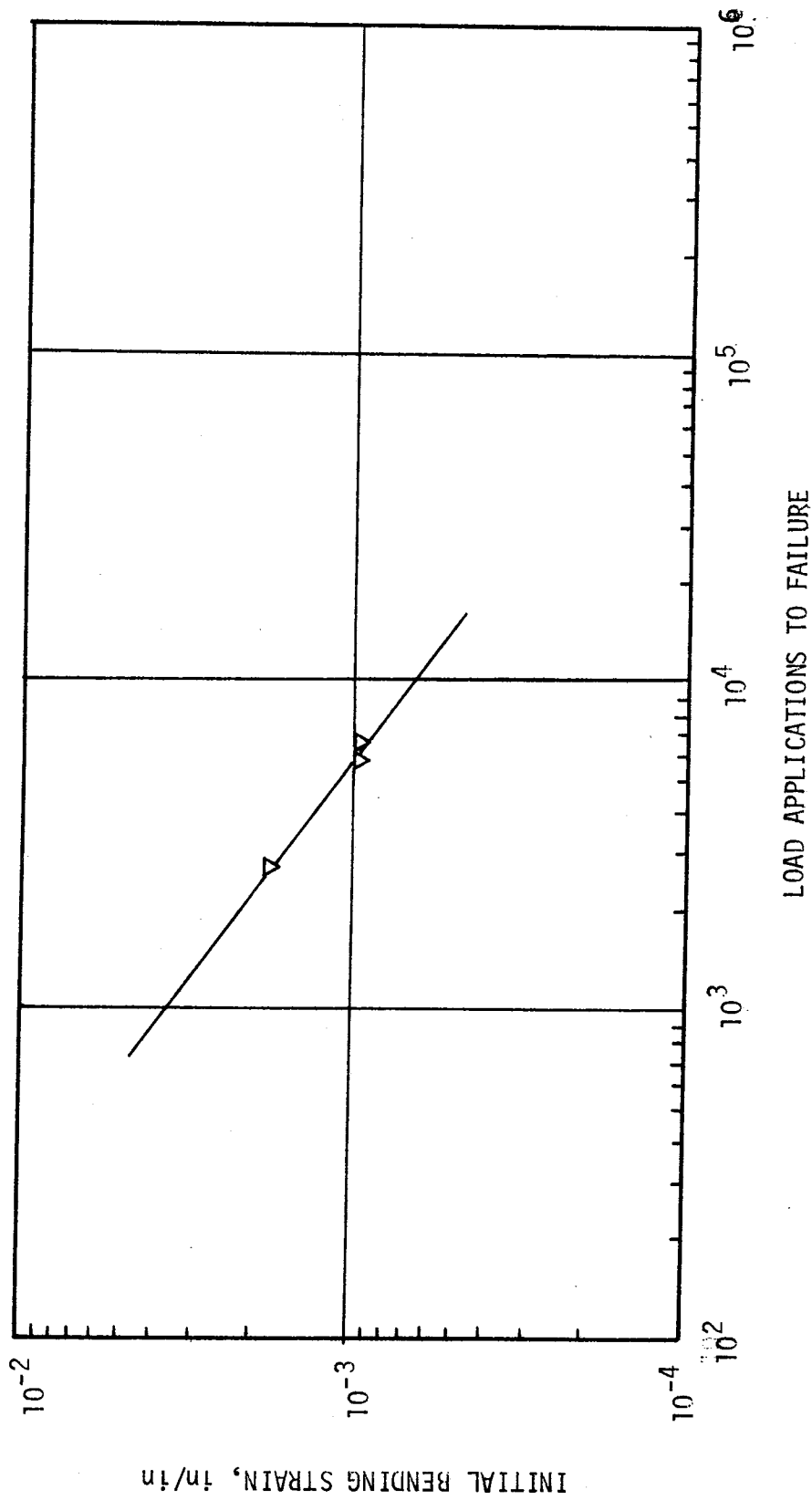


FIGURE D4. Strain versus Load Applications to Failure for Specimens Containing Fabric F.

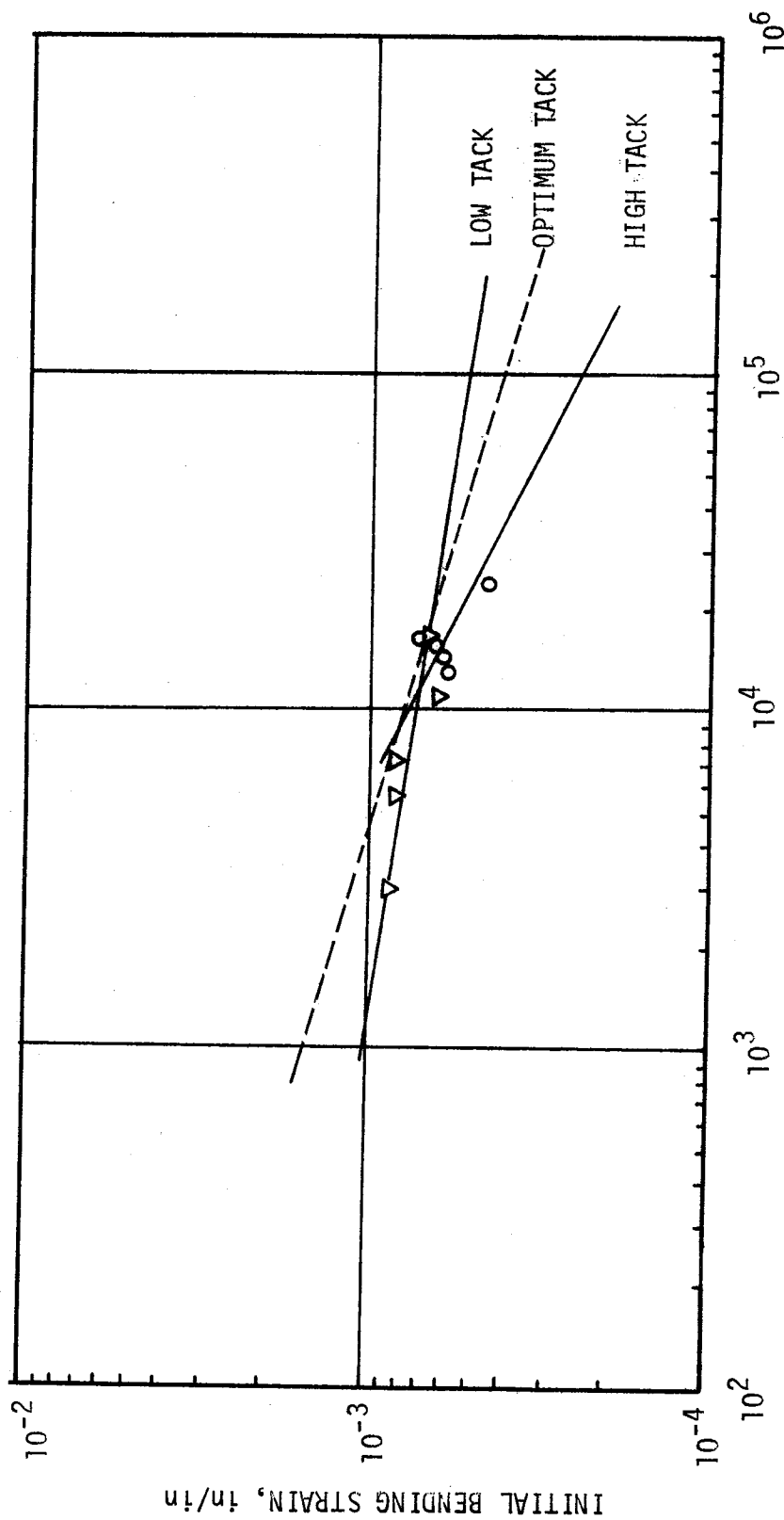


FIGURE D5. Strain versus Load Applications to Failure for Specimens Containing Fabric G.

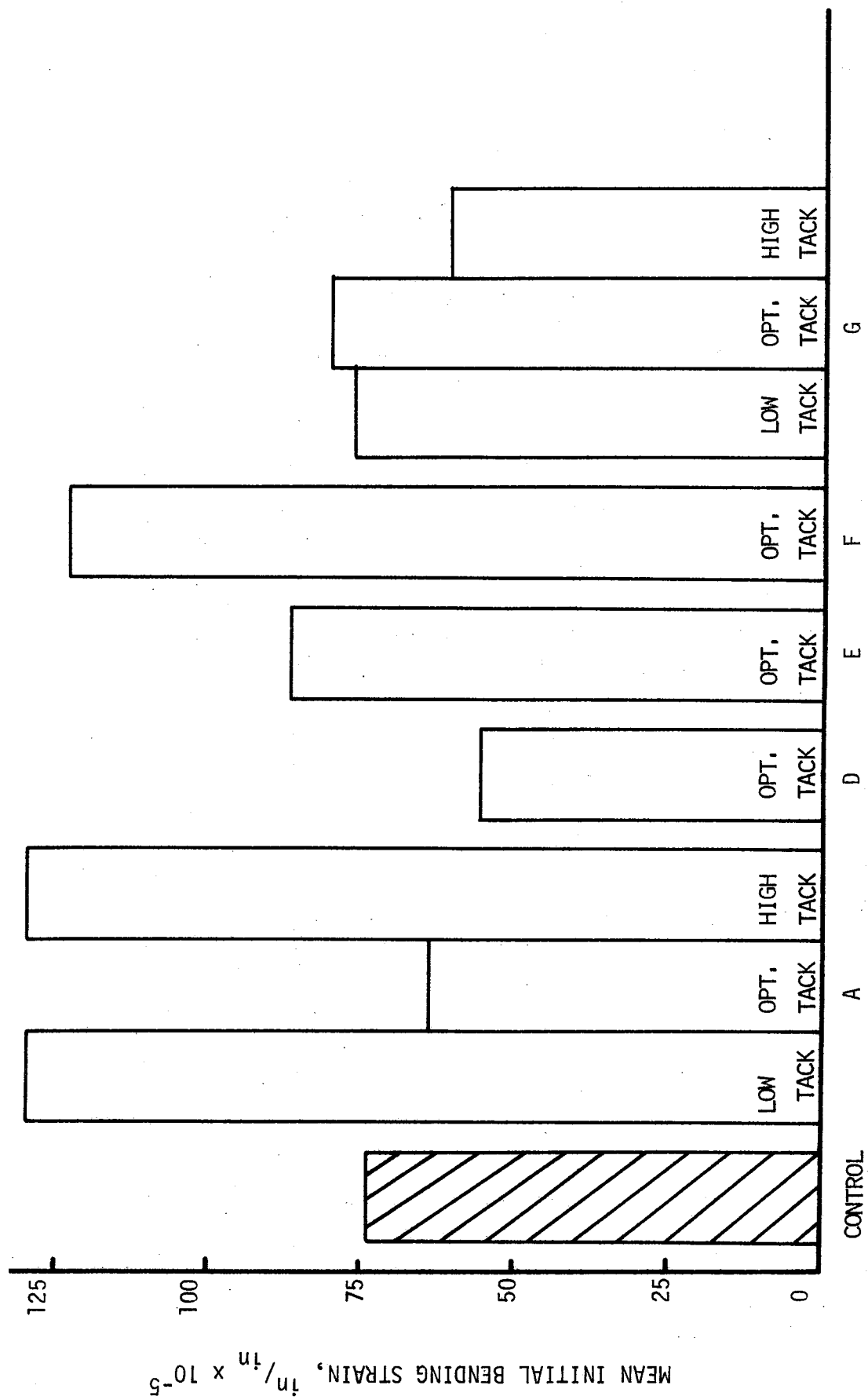


FIGURE D6. Initial Bending Strain (200th Cycle) from Flexural Fatigue Test

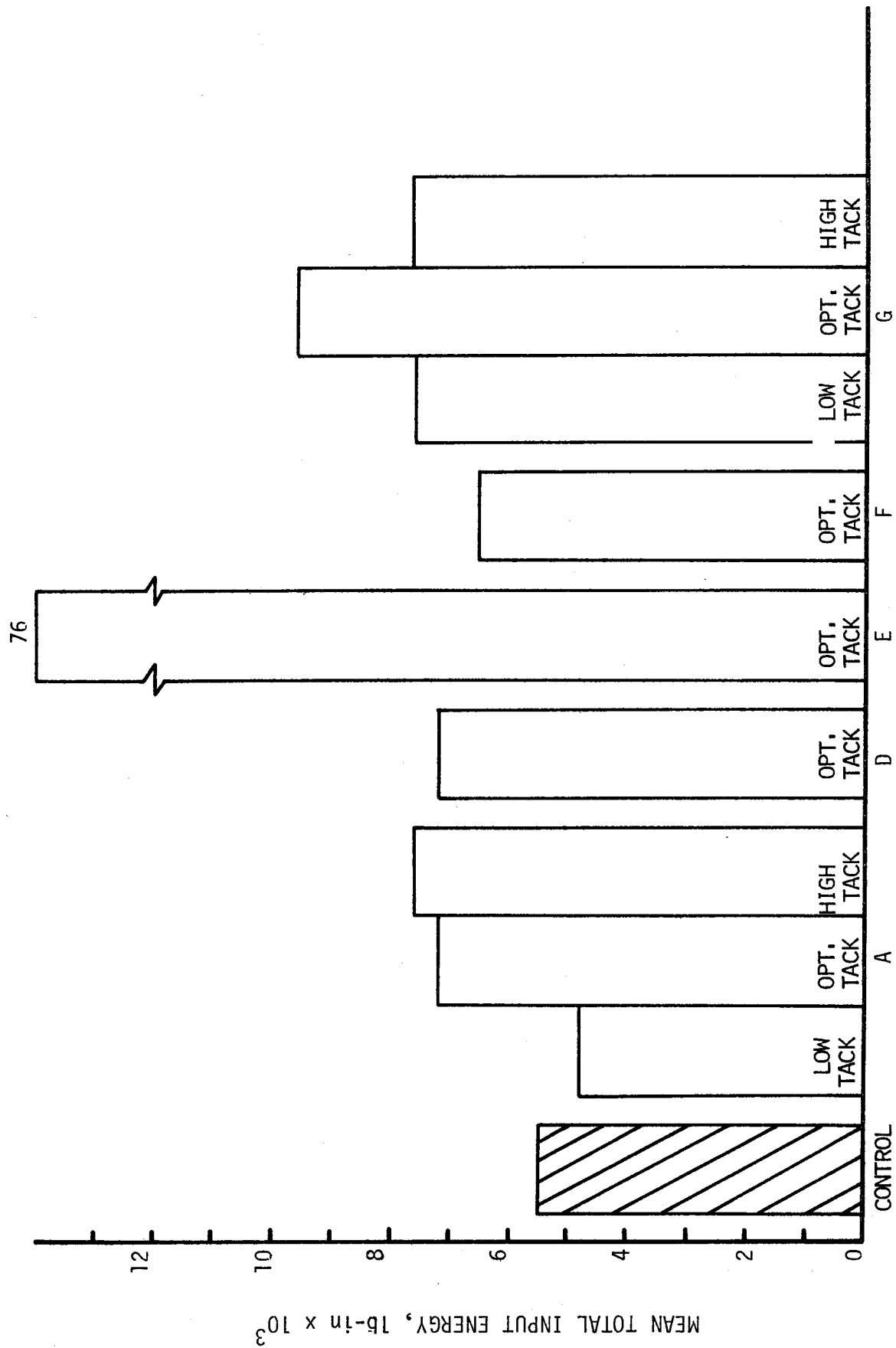


FIGURE D7. Comparison of Total Input Energy for Flexural Fatigue Test

Appendix E

Thermal Reflection Cracking Test Data

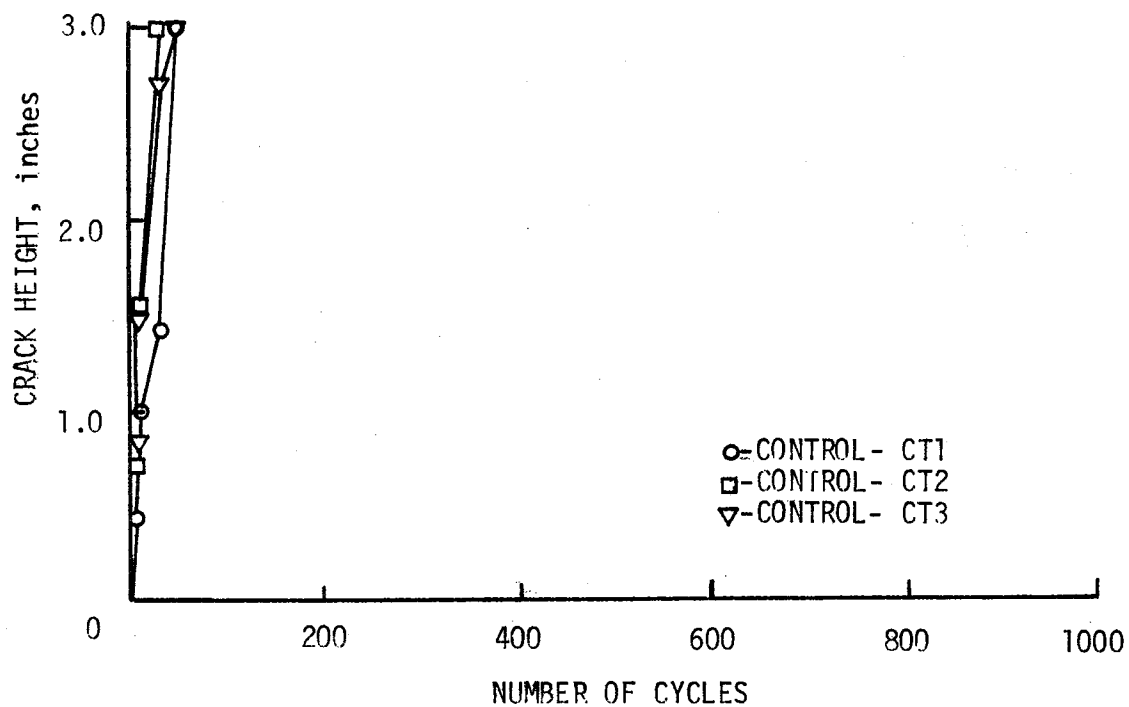


FIGURE E1. Crack Height versus Number of Cycles for Control Specimens.

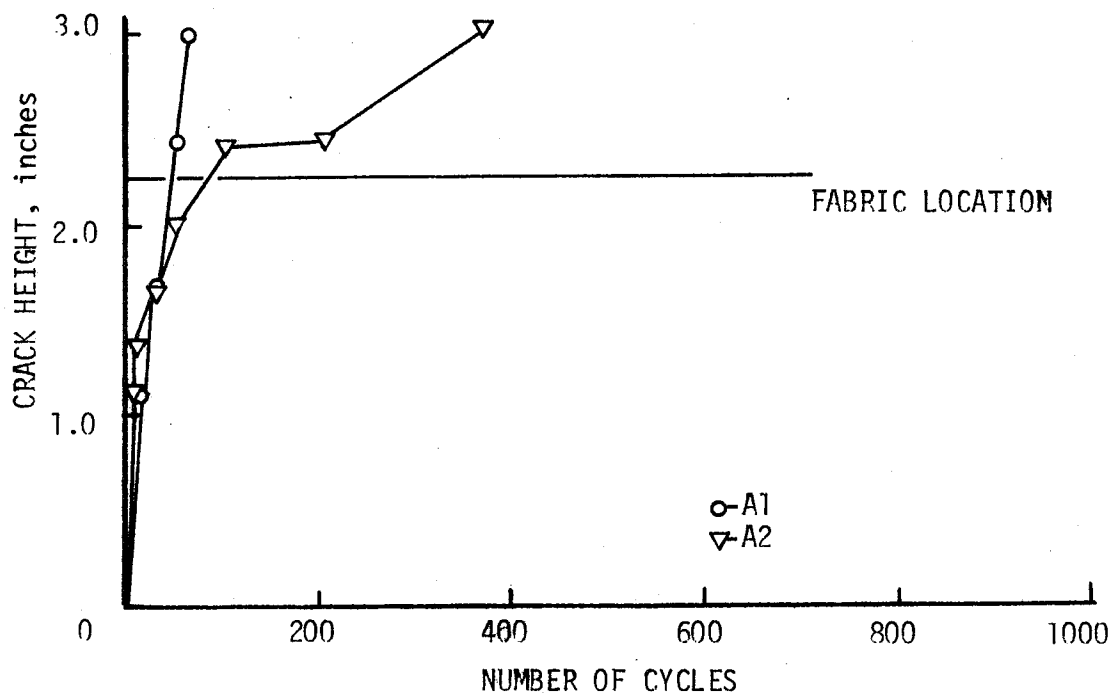


FIGURE E2. Crack Height versus Number of Cycles for Specimens with Fabric A.

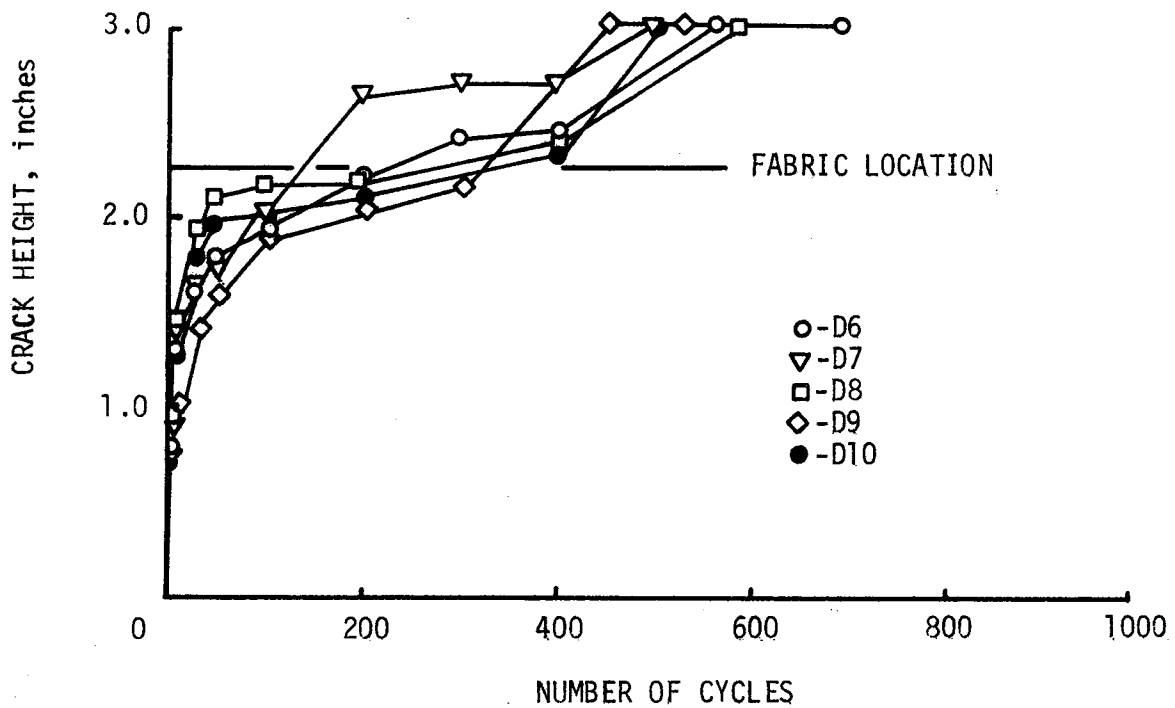


FIGURE E3. Crack Height versus Number of Cycles for Specimens with Fabric D.

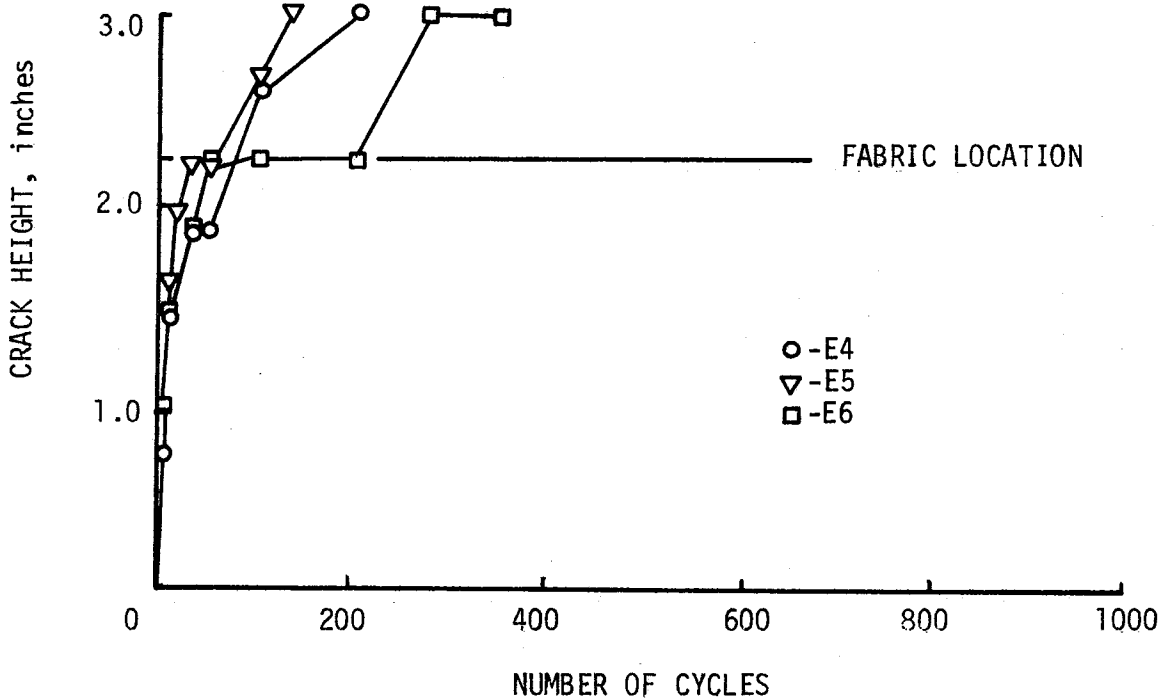


FIGURE E4. Crack Height versus Number of Cycles for Specimens with Fabric E.

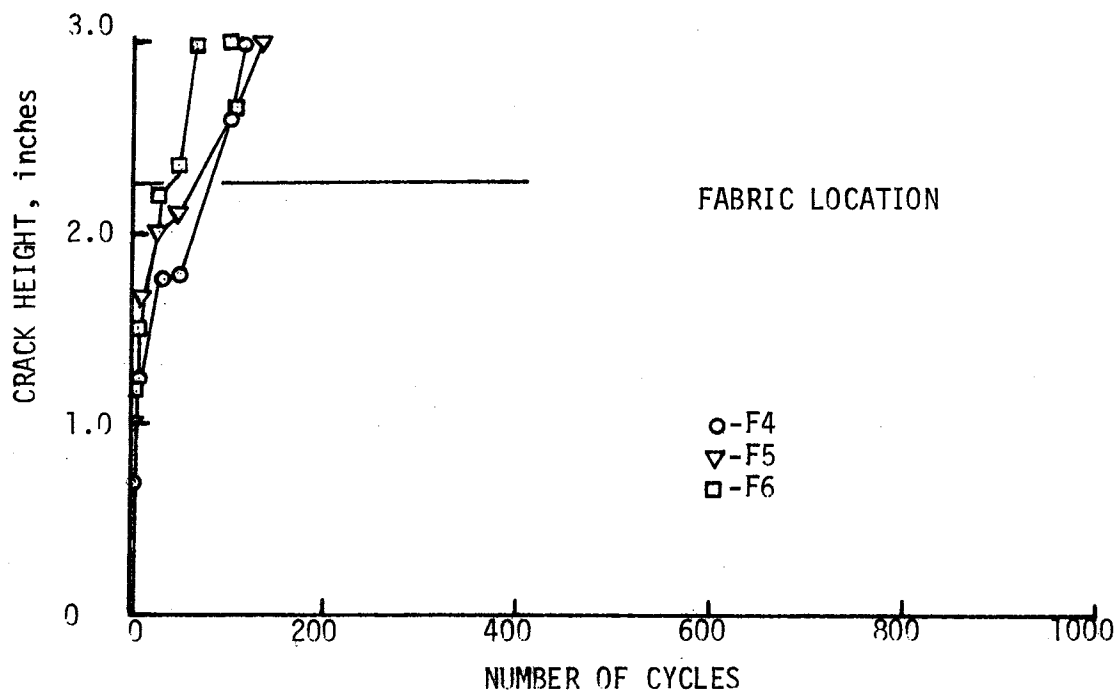


FIGURE E5. Crack Height versus Number of Cycles for Specimens with Fabric F.

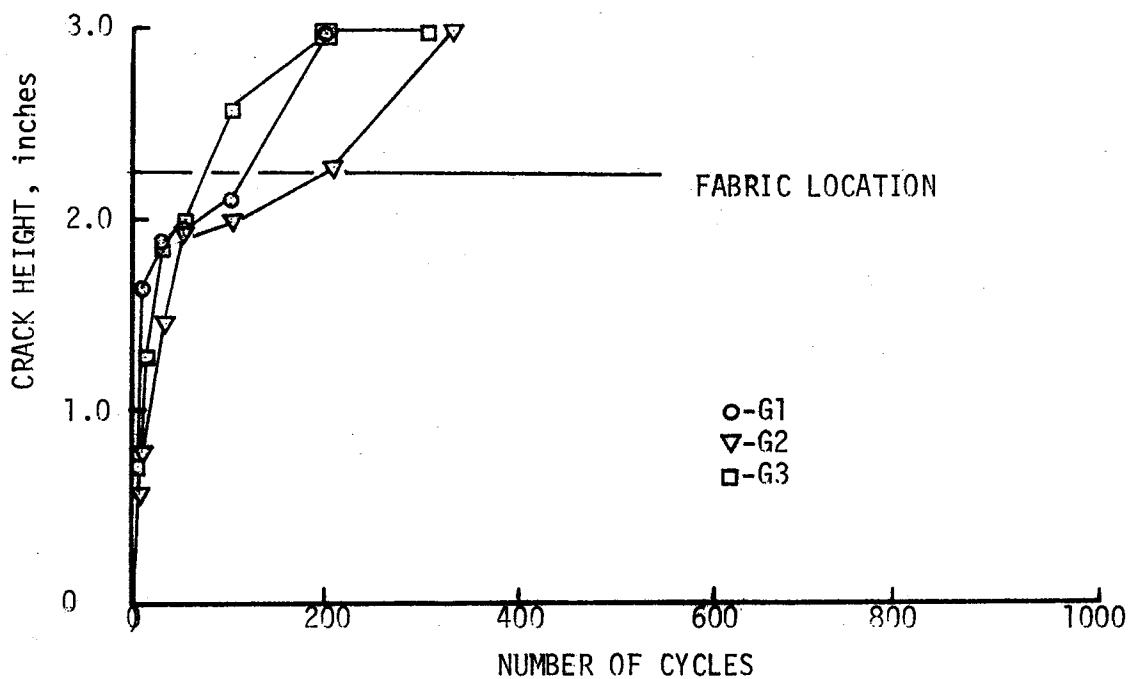


FIGURE E6. Crack Height versus Number of Cycles for Specimens with Fabric G and Low Tack Coat.

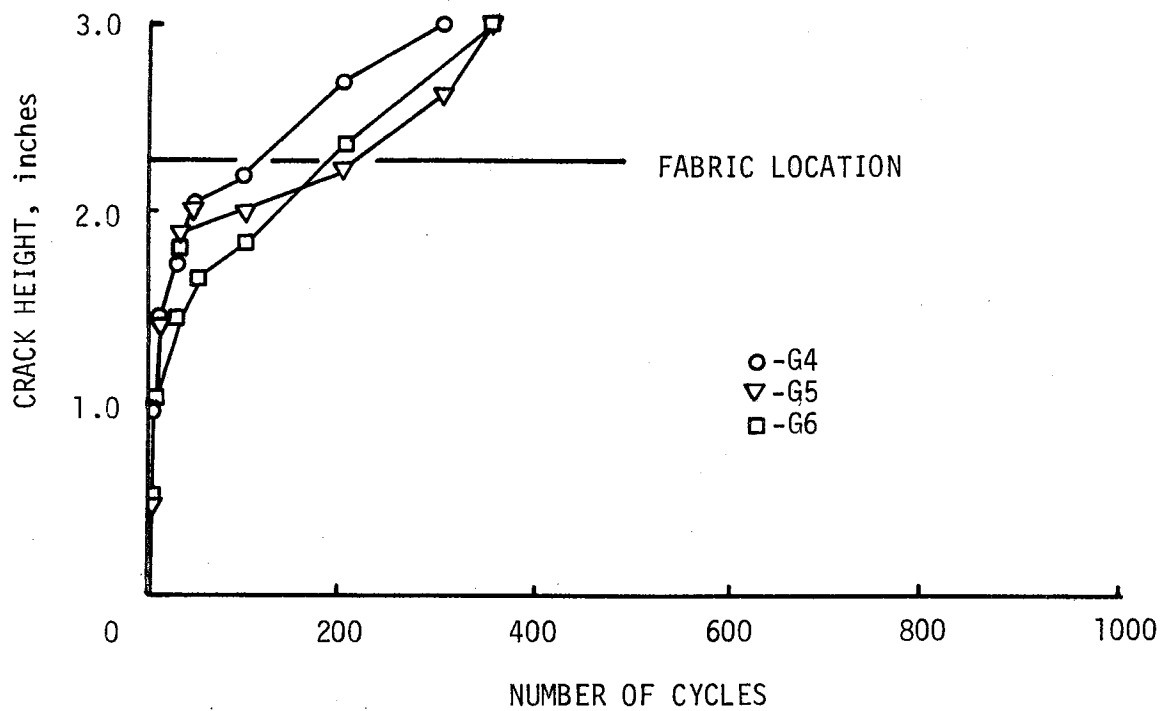


FIGURE E7. Crack Height versus Number of Cycles for Specimens with Fabric G and Optimum Tack.

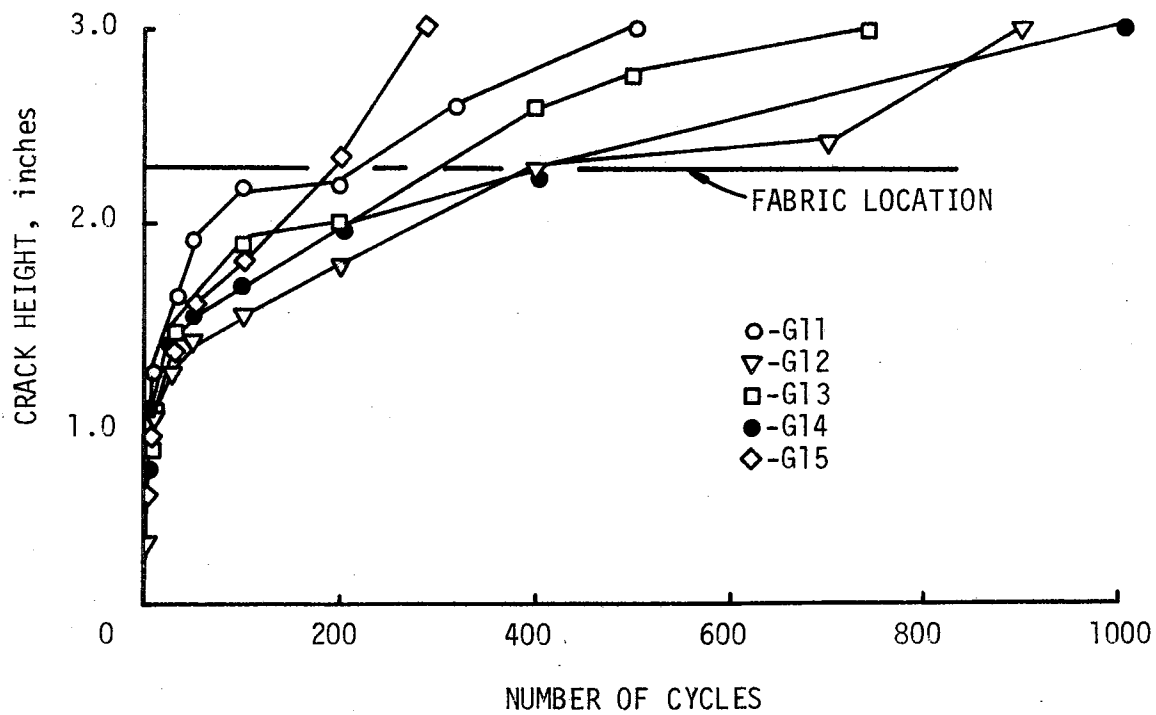


FIGURE E8. Crack Height versus Number of Cycles for Specimens with Fabric G and Optimum Tack (Old Specimens).

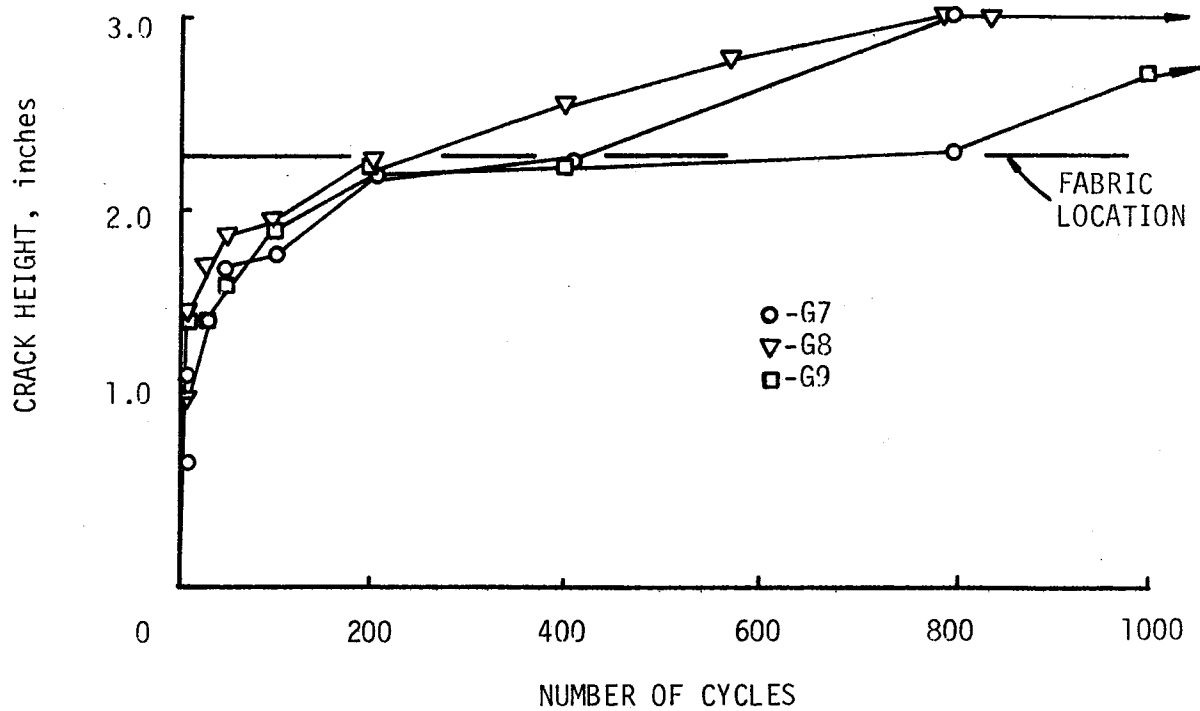


FIGURE E9. Crack Height versus Number of Cycles for Specimens with Fabric G and High Tack Coat

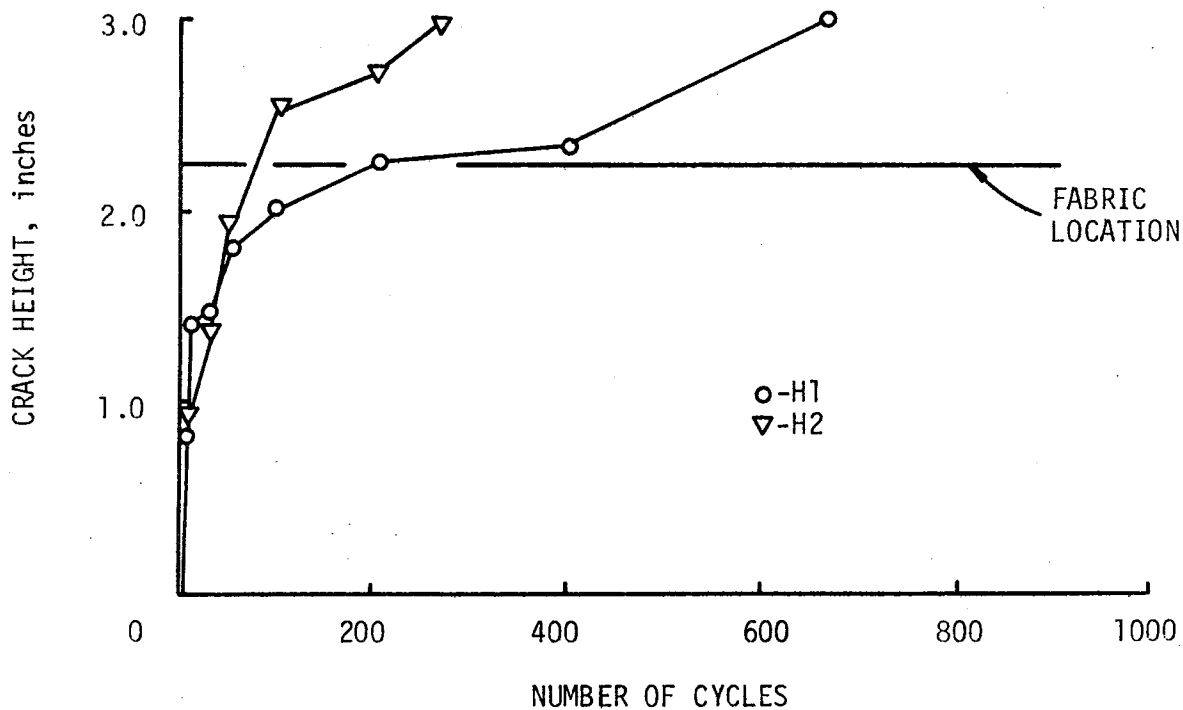


FIGURE E10. Crack Height versus Number of Cycles for Specimens with Fabric H

Appendix F

Application of Fracture Mechanics to Pavement Reflection Cracking

APPLICATION OF FRACTURE MECHANICS TO PAVEMENT THERMAL REFLECTION CRACKING

Introduction

Fracture mechanics principles together with the use of finite element analyses computer programs can be used to analyze the pavement reflection cracking problem. Details of this approach can be found in reference (38). The application of this approach is illustrated in this appendix.

Finite Element Analysis

Finite element calculations have been used to calculate values of the fracture mechanics factor, $2K/Eu$, as a function of the relative crack length, c/d . The following are the definitions of each of these symbols:

K = the stress intensity factor, $\text{lb} - \text{in}^{-3/2}$

E = the elastic modulus of the material, lb/in^2

u = the crack opening, inches

c = the crack length, inches

d = the height of the overlay specimen, inches

If the last four variables are known, then the stress intensity factor can be calculated using these results of the finite element calculations. The elastic modulus that is used to calculate the stress intensity factor in asphalt concrete should be measured at the same strain rate as used in the reflection cracking test on the same material. If this is not done, then the stress intensity factors calculated with these elastic moduli cannot be expected to obey the theory exactly. However, any elastic modulus which is measured in a consistent way may

be used to determine empirical relations that may closely resemble the theoretical expressions derived in the theory. Because the elastic moduli used in these calculations were taken from the direct tension tests which were performed at a different strain rate and a different percent of reinforcing fabric in the cross-sectional area than those used in the overlay tester, the empirical approach is adopted here. Two moduli were used: (1) the initial tangent modulus, E_i , from the initial slope of the stress-strain plot and (2) the final secant modulus, E_f , that was obtained by dividing the failure tensile stress by the failure strain. These values were obtained from the direct tension test data. The average values of these two moduli for each of the test specimens are shown in Table F-1. Also shown in that table is the ultimate tensile stress carried by these direct tension test specimens.

The relationships between the relative crack length, c/d , and the stress intensity factor ratio, $2K/Eu$, that are used in Table F-2 were determined by finite element analyses of overlays of varying thicknesses elastic moduli, crack openings, and crack lengths. The results of these analyses are reported in detail in reference 39. Two sets of stress intensity factors were calculated, K_i and K_f , corresponding to the two values of elastic modulus. Typical calculations for Fabric G at optimum tack rate are shown in Table F-2. Obviously the stress intensity factor decreases as the crack length increases.

Fracture Mechanics

According to fracture mechanics theory, the size of the stress intensity factor at a given crack length. The correlation between the two is called Paris' Law:

TABLE F-1. Initial and Final Elastic Moduli from the Direct Tension Tests.

Fabric Code	Tack Rate	Initial Elastic Modulus, E_i , psi	Final Elastic Modulus, E_f , psi	Ultimate Tensile Stress σ_m , psi
Control	None	141,000	24,000	77
A	Opt.	300,000	19,700	97
D	Opt.	24,000	20,100	64
E	Opt.	---	12,200	51
F	Opt.	64,000	19,400	67
G	Opt.	360,000	24,700	112
G	Low	268,000	17,000	87
G	High	537,000	27,700	157

TABLE F-2. Calculations of Stress Intensity Factors, K_i and K_f , for Fabric G at Optimum Tack Rate.

Finite Element Analysis Results		"Initial" Stress Intensity Factors, K_i	"Final" Stress Intensity Factors, K_f	Crack Length, inches
Relative Crack Length, $\frac{c}{d}$	$\frac{2K}{Eu}$			
0.06	1.31	12,220	1,130	0.18
0.12	0.69	6,440	600	0.36
0.20	0.55	5,130	400	0.60
0.29	0.46	4,290	400	0.87
0.37	0.42	3,920	360	1.11
0.45	0.38	3,540	330	1.35
0.54	0.36	3,360	310	1.62
0.63	0.34	3,170	290	1.89
0.70	0.33	3,080	285	2.10
0.78	0.32	2,980	280	2.34
0.87	0.31	2,890	270	2.61
0.96	0.27	2,520	230	2.88
1.00	0.00	0	0	3.00

Example:

$$\frac{2K}{Eu} = 1.31 \quad \text{or} \quad K = 1.31 \left(\frac{Eu}{2} \right)$$

$$\frac{E_i u}{2} = 9326 \text{ lb/in.}, \quad \frac{E_f u}{2} = 865 \text{ lb/in.}$$

$$K_i = 1.31 (9326) = 12,217, \quad K_f = 1.31 (865) = 1130$$

$$\frac{dc}{dN} = A[K(c)]^n \quad (1)$$

where K = the stress intensity factor at some crack length, c

$\frac{dc}{dN}$ = the rate of change of crack length per cycle at that same crack length, c

A, n = material properties to be found graphically

N = the number of cycles.

In order to find the two material properties A and n , it is necessary to know the rate of change of crack length per cycle. The overlay test data were plotted on logarithmic paper and equations were found for the measured crack length, c , in terms of the number of cycles, N . Two such plots are shown in Figures F-1 and F-2. Figure F-1 represents the data on crack growth through an overlay with no fabric and Figure F-2 is for Fabric G with optimum tack rate. The equations relating the two variables were of the form:

$$c = a N^b \quad (2)$$

Values of a and b for each material are given in Table F-3. The constants may be interpreted as follows. The constant, a , is the distance, in inches, that the crack travels into the overlay the first time it opens. The constant, b , is a measure of crack retardation. The smaller value of b indicates a slower rate of growth of the crack.

Taking the derivative of c with respect to N gives the rate of crack growth per cycle as a function of number of repetitions. The equation becomes:

$$\frac{dc}{dN} = (ab) N^{b-1} \quad (3)$$

The number of cycles that is required to reach a given crack length can also be found from Equation 2.

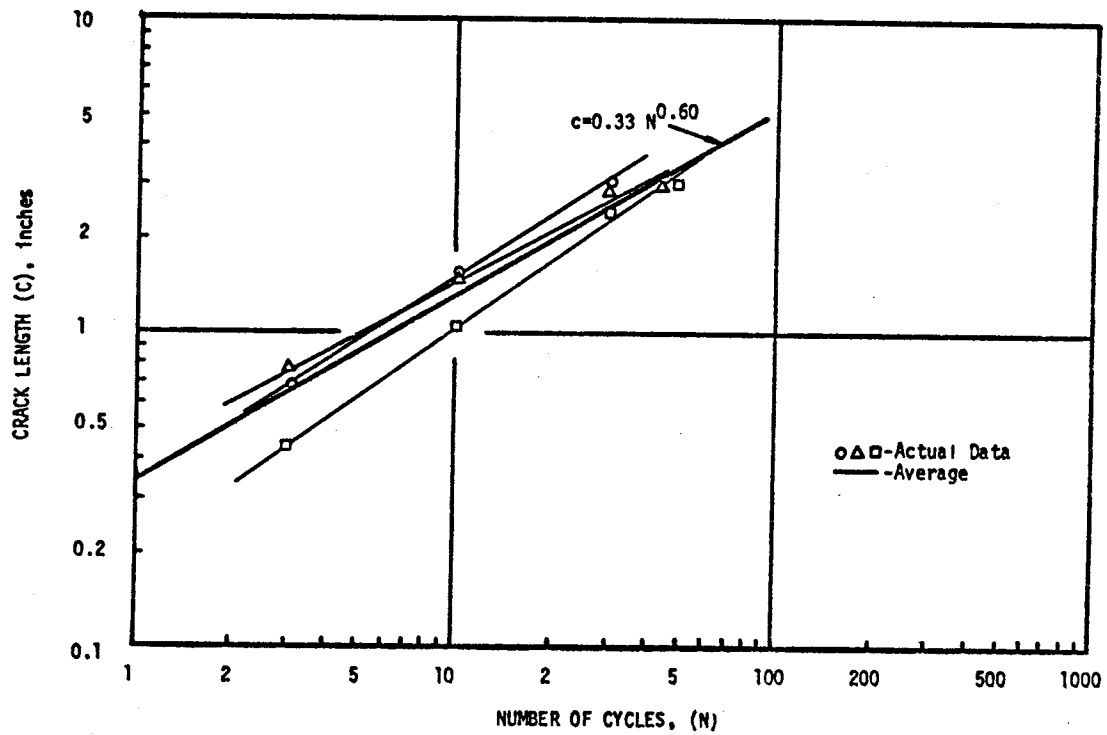


FIGURE F-1. Crack Length as a Function of Number of Tension Cycles for Control Specimens.

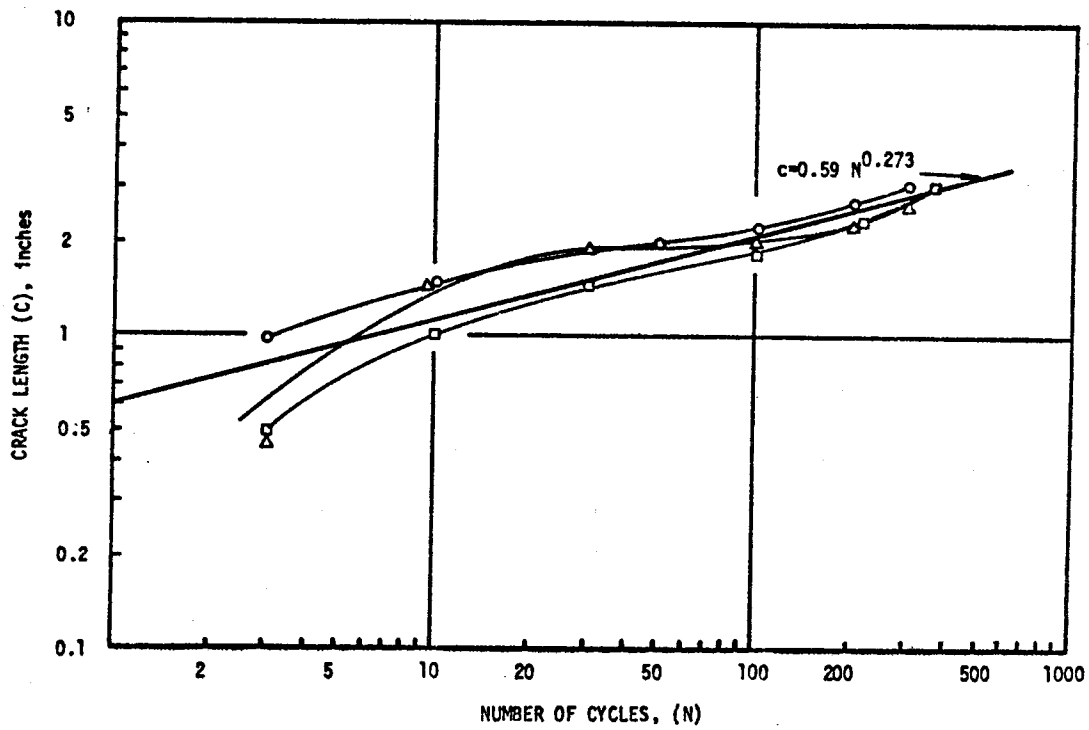


FIGURE F-2. Crack Length as a Function of Number of Tension Cycles for Specimens Containing Fabric G with Optimum Tack.

TABLE F-3. Crack Growth Constants for Different Fabric.

Fabric Code	Tack Rate	a (inches)	b
Control	N.A.	0.33	0.600
A	Opt.	0.68	0.293
D	Opt.	0.75	0.220
E	Opt.	0.86	0.233
F	Opt.	0.73	0.295
G	Opt.	0.59	0.273
G	Low	0.46	0.333
G	High	0.74	0.183

$$N = \left(\frac{c}{a}\right)^{1/b} \quad (4)$$

Equation 3 and 4 are used together to determine the rate of crack growth per cycled for a given crack length:

$$\frac{dc}{dN} = ab \left(\frac{c}{a}\right)^{\frac{b-1}{b}} \quad (5)$$

A typical set of such calculations is shown in Table F-4 for Fabric G with the optimum tack rate.

The experimental values of $\frac{dc}{dN}$ are plotted vertically and the calculated values of K_i and K_f are plotted horizontally on logarithmic graph paper. The plot of $\frac{dc}{dN}$ versus K_i is shown in Figure F-3 and the plot using K_f is shown in Figure F-4.

Several observations may be made about these two graphs.

1. The slope of the control curve is flatter. This means that the growth rate in asphalt concrete without any fabric is less sensitive to changes in stress intensity factor than the same material with fabric.
2. The farther a curve is shifted to the right, the slower a crack will be growing for a given level of stress intensity factor. In both graphs, the curve that is farthest to the right is for Fabric G with high tack rate.

Each of these curves has an equation in the form of Paris' Law (E9. 1), which is repeated here for ready reference.

$$\frac{dc}{dN} = A (K)^n \quad (1)$$

Table F-5 shows the values of A_i and n_i (based upon K_i) and A_f and n_f (based on K_f). These are the fracture properties of the asphalt concrete with and without fabric. It is obvious at a glance that

TABLE F-4. Crack Growth Rate Per Cycle
for Fabric G with Optimum
Tack Rate.

Crack Length, inches	Cycles, N	Crack Growth Rate Per Cycle (in/cycle)
0.18	.013	3.82
0.36	.162	0.60
0.60	1.05	0.16
0.87	4.10	0.058
1.11	10.0	0.030
1.35	20.5	0.018
1.62	39.9	0.011
1.89	70.1	0.007
2.10	103	0.006
2.34	153	0.004
2.61	229	0.003
2.88	328	0.002
3.00	380	0.002

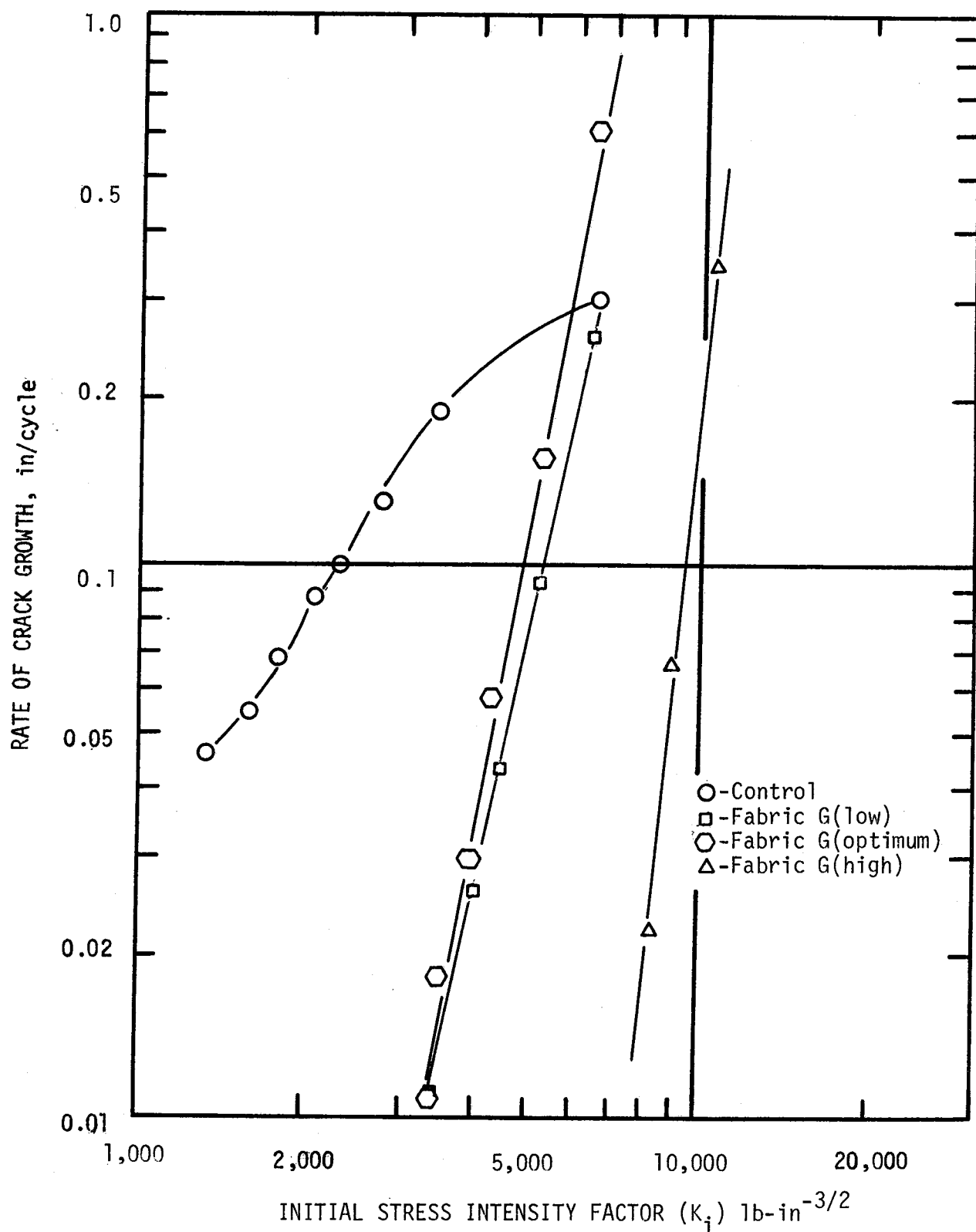


FIGURE F-3. Relationship Between Initial Crack Growth and Initial Stress Intensity Factor .

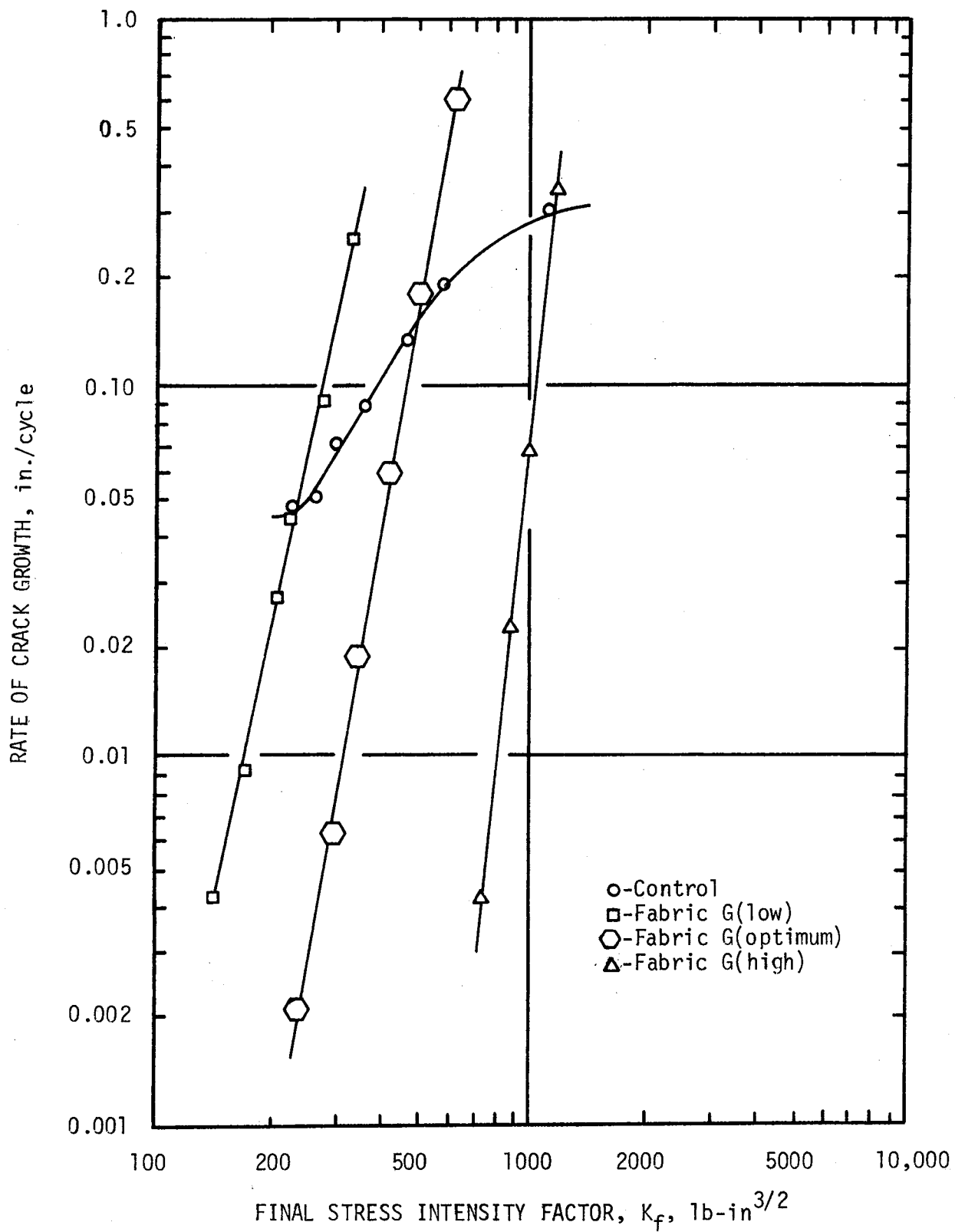


FIGURE F-4. Relationship Between Rate of Crack Growth and Final Stress Intensity Factor.

TABLE F-5. Fracture Properties of Asphalt Concrete With and Without Fabric.

Fabric Code	Tack Rate	A_i	n_i	A_f	n_f
Control	None	2.62×10^{-8}	1.66	1.02×10^{-5}	1.55
A	Opt.	2.05×10^{-23}	5.62	4.74×10^{-15}	5.32
D	Opt.	1.14×10^{-35}	8.50	1.86×10^{-22}	8.15
E	Opt.	--	--	1.41×10^{-18}	7.40
F	Opt.	2.48×10^{-27}	6.20	1.71×10^{-16}	5.65
G	Opt.	2.43×10^{-23}	5.60	9.55×10^{-19}	6.45
G	Low	3.48×10^{-19}	4.70	1.06×10^{-12}	4.50
G	High	3.79×10^{-44}	10.45	9.06×10^{-33}	11.55

fabrics greatly alter the fracture properties of asphalt concrete. A further question that remains to be answered is: What fabric property or direct tension test property is most important in changing these fracture properties?

Before attempting to answer that question several observations can be made on relations between these fracture properties. Firstly, for optimum tack rates, $\log A_i$ may be plotted against n_i as shown in Figure F-5. They form a straight line with equation:

$$n_i = 0.284 \log A_i - 0.5 \quad (6)$$

The same may be done for $\log A_f$ and n_f as shown in Figure F-5 to give an equation:

$$n_f = -0.387 \log A_f - 0.5 \quad (7)$$

The two lines have the same intercept ($n = -0.5$ which is also their point of intersection.

The variation of A_i with tack rate was found to be

$$\log A_i = \log A_{i0} [0.816 - 0.184 \left(\frac{t}{t_0}\right) + 0.368 \left(\frac{t}{t_0}\right)^2] \quad (8)$$

where A_{i0} = the value of A_i at optimum tack rate and

t = tack rate in gallons/square yard

t_0 = the optimum tack rate

Similarly, the variation of A_f with tack rate may be expressed as

$$\log A_f = \log A_{f0} [0.364 + 0.564 \left(\frac{t}{t_0}\right) + 0.072 \left(\frac{t}{t_0}\right)^2] \quad (9)$$

Equations (8) and (9) are valid for tack rates between 50% and 200% of the optimum value. The shift of A-value with tack rate can be calculated with these two equations. The optimum tack rate for Fabric G was 0.20 gal/sq. yd.

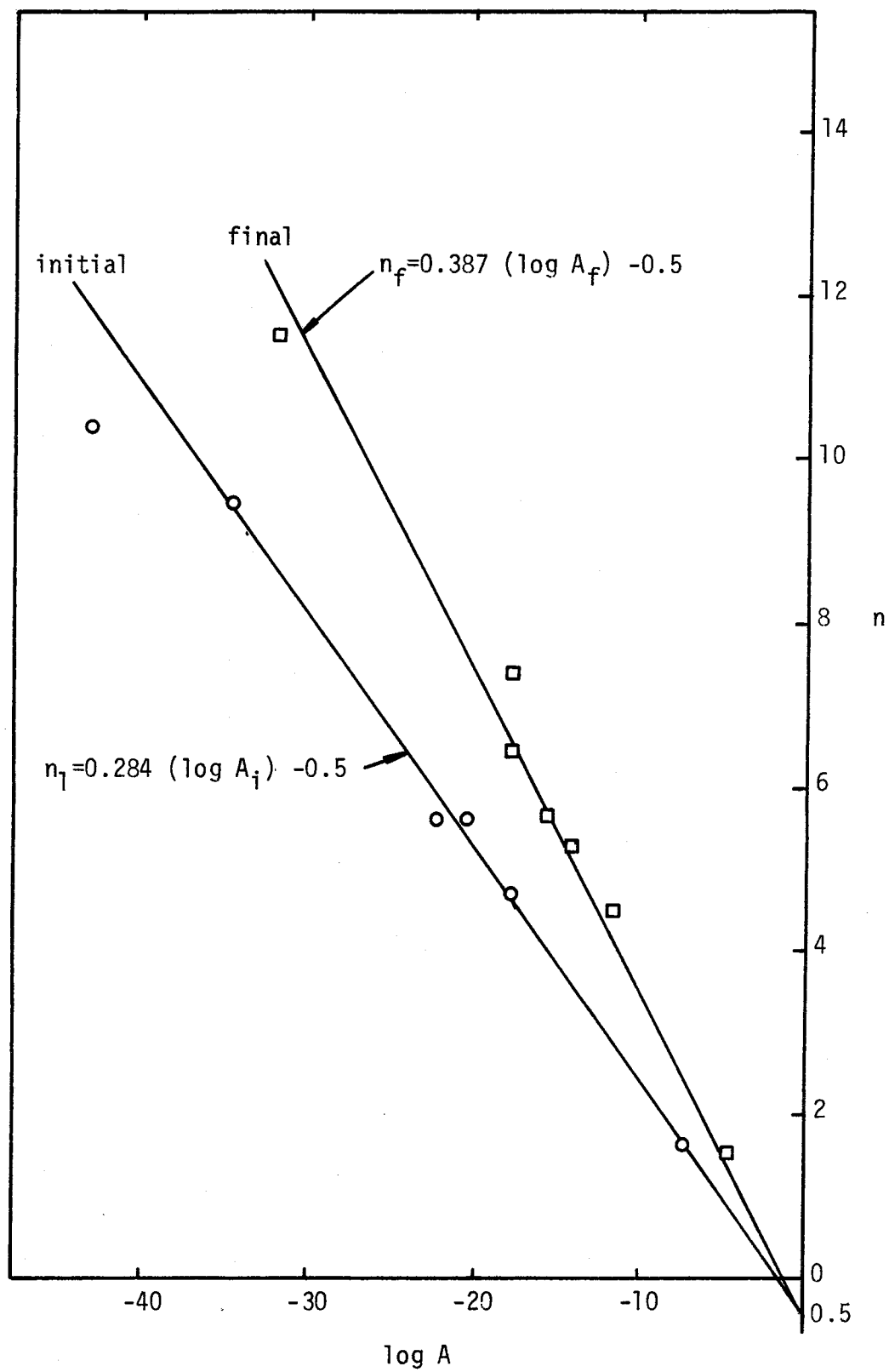


FIGURE F-5. Relationship Between n and $\log A$, Initial and Final.

Computation of Fracture Toughness

Fracture toughness is also called the "crack extension force" in some fracture mechanics applications. Because the term "fracture toughness" indicates an energy density, it will be the preferred term in this discussion. A precise definition of the term will be given in what follows:

The load that is required to open the crack to its full width decreases as the crack length increases. A typical plot of the load, P , against the crack opening, U , for two successive load cycles is shown in Figure F-6. The area under each curve has the units of (lbs x inches) or work. The area was measured using a planimeter for several load cycles during each test on an overlay sample and this successively decreasing sequence of areas was plotted versus number of cycles on logarithmic paper as shown in Figure F-7 for the control specimen and in Figure F-8 for Fabric G at the optimum tack rate. The equations for these curves were of the form

$$E = c N^d \quad (10)$$

where E = the tensile work in one cycle, in-lb and

N = the number of cycles when E was measured.

Table F-6 lists the values of c and d obtained for each of the asphalt concrete specimens with and without fabric. The constant, c , is the initial work that must be done to open the crack. The power, d , indicates the toughness of the specimens. The smaller the number d is, the more resistant is the overlay to further crack extension. The rate of change of work with each cycle is given by taking a derivative of Equation 10 with respect to the number of cycles:

$$\frac{dE}{dN} = cd N^{d-1} \quad (11)$$

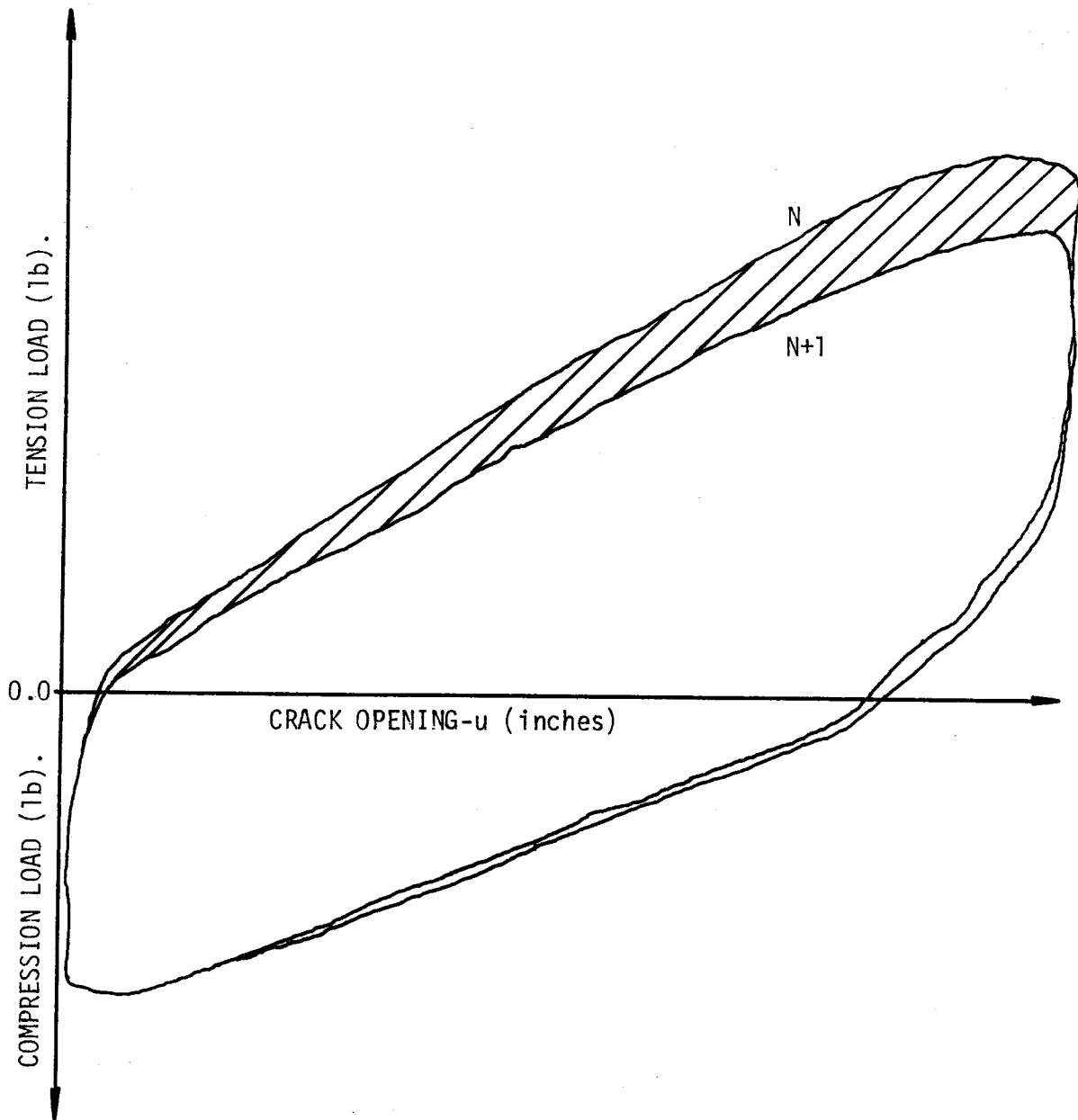


FIGURE F-6. Typical Recording of Load Versus Crack Opening for Two Successive Load Cycles.

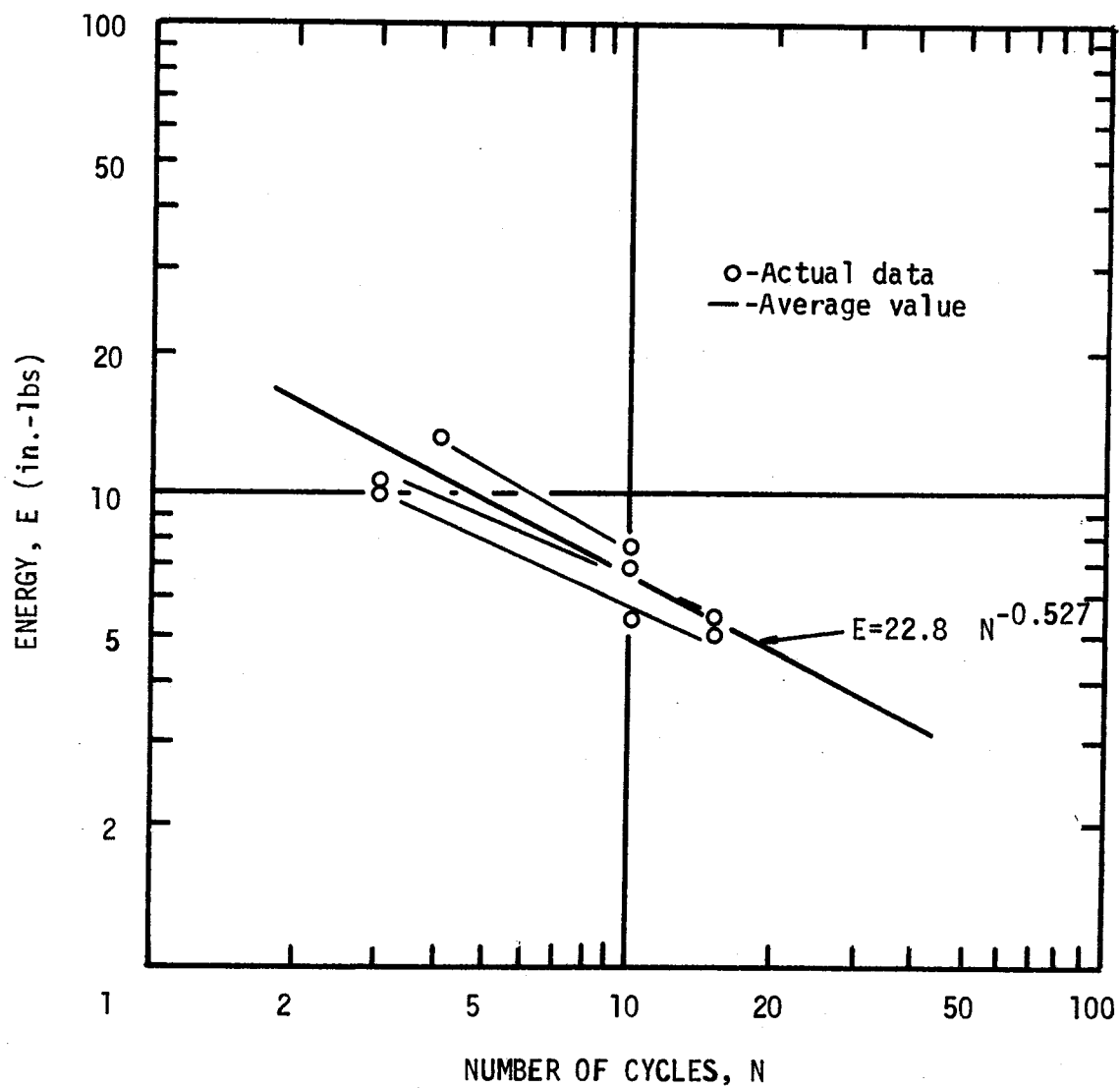


FIGURE F-7. Relationship Between Energy and Number of Tension Cycles for Control Specimens.

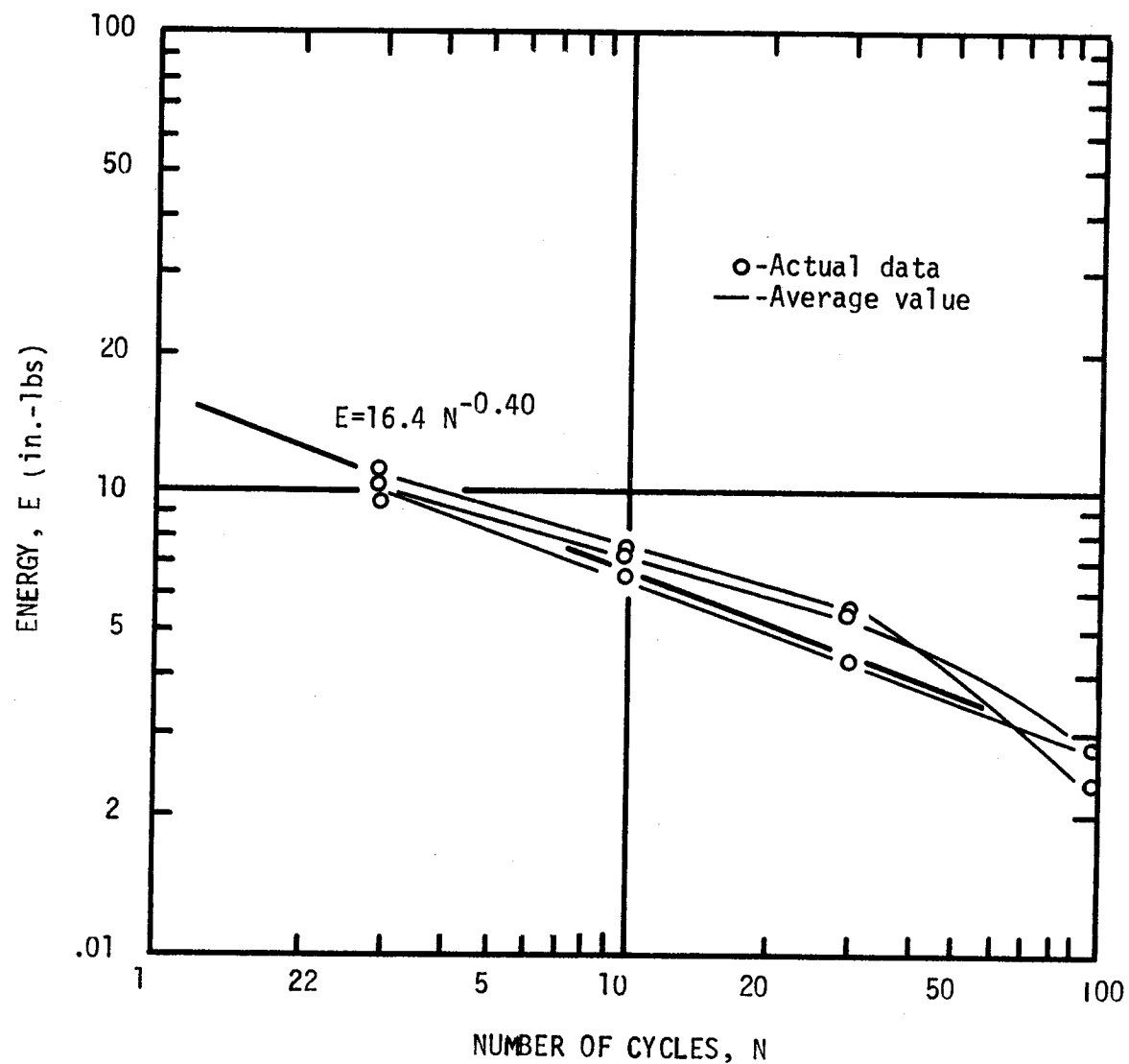


FIGURE F-8. Relationship Between Energy and Number of Tension Cycles for Fabric G-Optimum Tack.

TABLE F-6. Tensile Work Coefficients .

Test Code	Tack Rate	c	d
Control	None	22.8	-0.527
A	Opt.	19.8	-0.500
D	Opt.	14.2	-0.343
E	Opt.	22.7	-0.439
F	Opt.	18.9	-0.349
G	Opt.	16.4	-0.400
G	Low	12.4	-0.440
G	High	12.8	-0.393
G*	Opt.	13.2	-0.291
H	Opt.	21.0	-0.423

*Test Specimens were more than 1-year old.

The rate of change of work with crack length is given by dividing Equation 11 by Equation 3, as follows:

$$\begin{aligned}\frac{dE}{dc} &= \frac{\frac{de}{dN}}{\frac{dc}{dN}} = \frac{cd N^{d-1}}{ab N^{b-1}} \\ &= \frac{cd}{ab} N^{d-b}\end{aligned}\quad (12)$$

The rate of change of work per unit area of the crack is obtained by dividing Equation 12 by twice the width of the overlay specimens, that is, 6-inches.

$$\frac{dE}{dA} = \frac{1}{6} \cdot \frac{dE}{dc} = \frac{1}{6} \frac{cd}{ab} N^{d-b} \quad (13)$$

The quantity

$$G = \frac{1}{6} \frac{cd}{ab} \quad (14)$$

is the initial rate of change of work per unit of increased crack surface area and is defined here as the "fracture toughness," G.

Table F-7 shows the values of fracture toughness derived from each of the overlay specimens tested. (Note: G is a negative number.)

The three major material properties which determine the size of the A-coefficient in Paris' Law are elastic modulus, E, tensile strength, σ_m , and fracture toughness, G. Because most of the overlay specimens included fabrics with different properties, it is reasonable to assume that some fabric properties may be strong determining factors on the size of the A-coefficient.

Summary

The number of thermal cycles which will cause the failure of an overlay is given by integrating Paris' Law.

TABLE F-7. Fracture Toughness Properties.

Test Code	Tack Rate	Fracture Toughness, G, in-lb/in ²
Control	None	-10.12
A	Opt.	- 8.29
D	Opt.	- 4.92
E	Opt.	- 8.29
F	Opt.	- 5.12
G	Opt.	- 6.79
G	Low	- 5.94
G	High	- 6.21
G*	Opt.	- 4.41
H	Opt.	- 9.33

*Test Specimens were more than 1-year old.

$$N_f = \int_a^{t_o} \frac{dc}{A(K)^n} \quad (15)$$

where a = the length of the crack after the first crack opening which is given in Table F-3.

t_o = the thickness of the overlay.

N_f = the number of repetitions to failure.

K = the stress intensity factor which is a function of the elastic modulus, the crack opening, and the crack length.

A, n = the fracture properties which can be predicted by the equations developed in this report

The procedure for determining A would be as follows:

1. With ample data, select regression techniques can be utilized to determine expressions for the A_{i0} and A_{f0} coefficients using basic fabric properties or asphalt requirements as independent variables. Calculations using several models will give confidence in the value of $\log A_0$ that is finally adopted.
2. Use Equation 8 (for A_i) or Equation 9 (for A_f) to determine the value of $\log A$ if some level of tack rate other than optimum is used.
3. Use Equation 6 (for n_i) or Equation 7 (for n_f) to determine the value of n that must be used in the calculation of the number of cycles to failure.

The fracture properties of overlays can be altered substantially by including fabrics in them. As a general rule, it is wise to place the fabric at least the distance, a , (from Table F-3) above the old cracked pavement. This can be done by placing a level-up course

against the old pavement, then placing the fabric, and then laying down a riding course above the fabric. Cracks can be retarded greatly by increasing the tack rate above the optimum, which may be partly a result of increasing asphalt content or decreasing air voids in the surrounding asphalt concrete.

Appendix G

Direct Tension Test Data

TABLE G1. Direct Tension Test Results on Individual Test Specimens.

Fabric	Sample No.	Tensile Stress @ Failure, psi			Tensile Strain @ Failure, in/inx10 ⁻⁶			Secant Modulus of Elasticity, psi x10 ³			Initial Tangent Modulus of Elasticity, psi x10 ³		
		Low	Opt	High	Low	Opt	High	Low	Opt	High	Low	Opt	High
A	1	---	125	113	---	6700	8400	---	18.7	13.5	---	180	113
	2	51	99	125	4300	4800	9400	11.9	20.6	13.3	174	292	116
	3	78	102	139	8300	4800	6800	9.4	21.3	20.4	126	321	284
	4	77	101	112	3100	4200	9900	24.8	24.0	11.3	182	289	103
	5	82	81	144	4600	5200	5800	17.8	15.6	24.8	194	196	351
	6	---	76	---	---	4200	---	---	18.1	---	---	522	---
D	1	---	104	---	---	6800	---	---	15.3	---	---	164	---
	2	---	113	---	---	4500	---	---	25.1	---	---	191	---
	3	---	101	---	---	3700	---	---	27.3	---	---	200	---
	4	---	58	---	---	5500	---	---	10.5	---	---	---	---
	5	---	98	---	---	4800	---	---	20.4	---	---	379	---
	6	---	91	---	---	4100	---	---	22.2	---	---	---	---
E	1	139	62	109	6700	6800	3700	20.7	9.1	29.5	605	---	682
	2	164	51	98	4500	3500	4900	36.4	14.6	20.0	451	---	301
	3	156	43	96	4800	2600	5400	32.5	16.5	17.8	492	---	298
	4	134	56	103	3700	6000	6200	36.2	9.3	16.6	469	---	359
	5	168	42	90	3500	3600	4400	48.0	11.7	20.5	623	---	107
	6	---	---	---	---	---	---	---	---	---	---	---	---
F	1	88	---	127	5100	---	7400	17.3	---	17.2	323	849	171
	2	113	---	135	9900	---	7300	11.4	---	18.5	---	673	204
	3	112	62	117	4300	3400	8800	26.0	18.2	13.3	463	862	149
	4	114	71	113	7100	4300	9900	16.1	16.5	10.3	124	84	142
	5	121	---	129	4700	---	8200	25.7	---	15.7	461	602	223
	6	---	68	---	---	3000	---	---	23.4	---	---	---	---
G	1	102	111	---	5900	3300	---	17.3	33.6	---	169	351	---
	2	52	131	142	3100	5700	6000	16.8	33.9	23.7	269	274	999
	3	62	99	171	4800	4200	---	12.9	23.6	---	261	285	473
	4	102	112	153	5700	5100	6100	17.9	22.0	25.1	215	198	576
	5	117	107	161	5800	5000	4700	20.2	21.4	34.3	428	234	98
	6	---	---	---	---	---	---	---	---	---	---	---	---
Control	1	---	66	---	---	2100	---	---	31.4	---	---	187	---
	2	---	95	---	---	4600	---	---	20.7	---	---	174	---
	3	---	88	---	---	4500	---	---	19.6	---	---	175	---
	4	---	63	---	---	5600	---	---	11.3	---	---	---	---
	5	---	65	---	---	1700	---	---	38.2	---	---	79	---
	6	---	84	---	---	3700	---	---	22.7	---	---	89	---

TABLE G2. Physical Properties of Direct Tension Specimens and Test Results.

Fabric Code	Tack Coat	Specific Gravity*	Air Voids,* percent	Tensile Stress @ Failure, psi	Tensile Strain @ Failure in/in x 10 ⁻⁶
A	Low-	2.34	6.1	72	5100
	Opt-	2.30	11.4	97	5000
	High-	2.36	5.1	127	8100
D	Opt-	2.29	7.7	94	4900
E	Low-	2.30	7.0	152	4600
	Opt-	2.20	11.4	51	4500
	High-	2.34	6.0	99	4900
F	Low-	2.33	6.2	110	6200
	Opt-	2.28	8.3	67	3600
	High-	2.35	5.5	124	8300
G	Low-	2.37	4.9	87	5100
	Opt-	2.27	8.5	112	4700
	High-	2.36	5.1	157	5600
CONTROL	None	2.32	10.3	77	3700

*Properties were measured prior to sawing beams into individual test specimens.

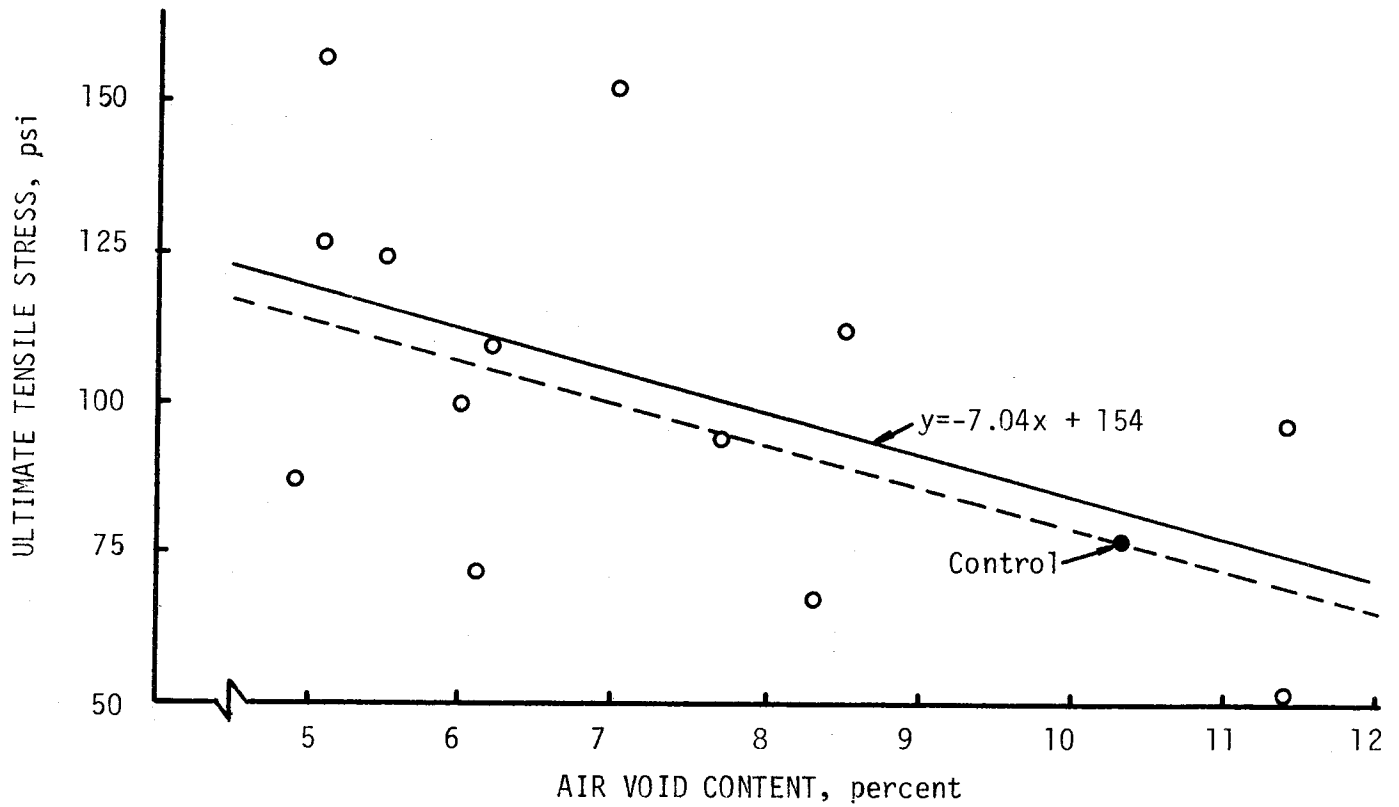


FIGURE G1. Relationship Between Tensile Strength and Air Voids.

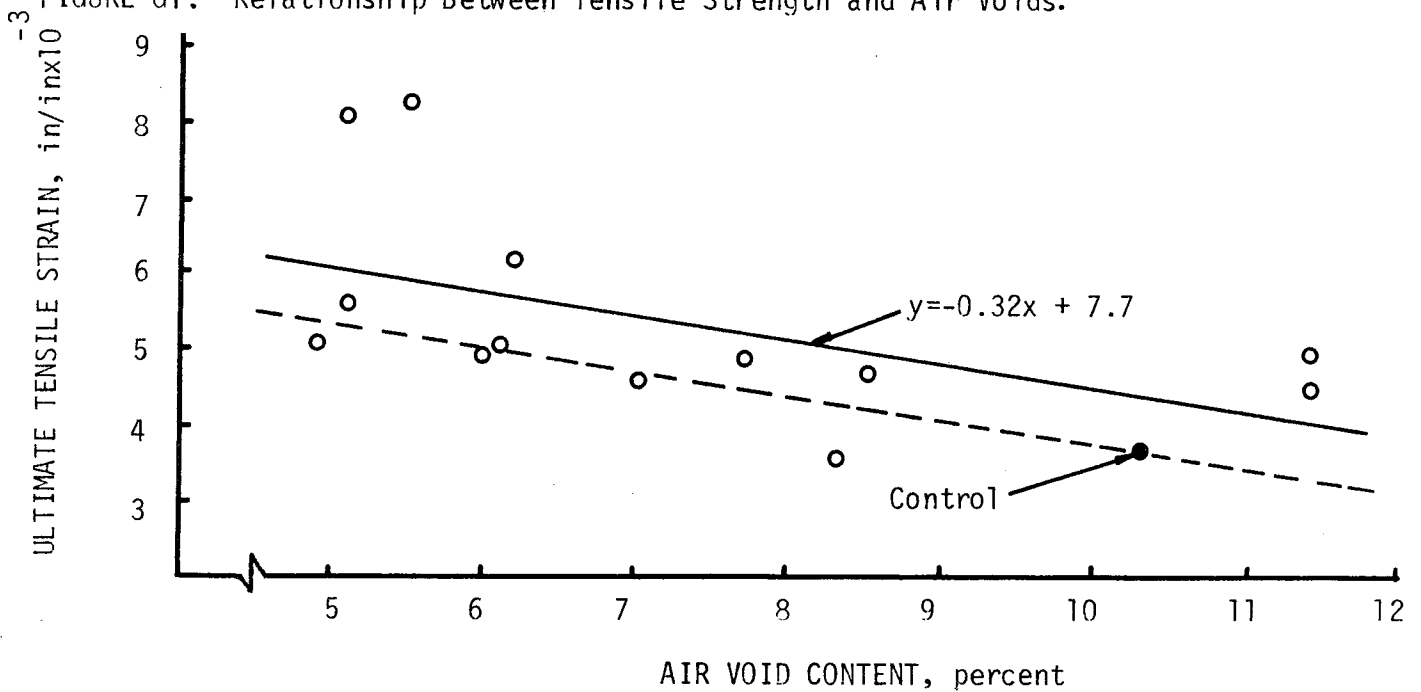


FIGURE G2. Relationship Between Tensile Strain at Failure and Air Voids.

